Aerodynamic Modeling Using Computational Fluid Dynamics and Sensitivity Equations

Alejandro Cesar Limache

Dissertation submitted to the Faculty of the
Virginia Polytechnic Institute and State University
in partial fulfillment of the requirements for the degree of

Doctor of Philosophy
in
Aerospace Engineering

Eugene Cliff, Chair
Bernard Grossman
Frederick Lutze
Mark Anderson
Robert Rogers

April 10, 2000
Blacksburg, Virginia

Keywords: Aerodynamic Forces, Stability Derivatives, CFD, Sensitivity Equation Method

Aerodynamic Modeling Using Computational Fluid Dynamics and Sensitivity Equations

Alejandro Cesar Limache

(ABSTRACT)

A mathematical model for the determination of the aerodynamic forces acting on an aircraft is presented. The mathematical model is based on the generalization of the idea of aerodynamically steady motions. One important use of these results is the determination of steady (time-invariant) aerodynamic forces and moments. Such aerodynamic forces can be determined using computer simulation by determining numerically the associated steady flows around the aircraft when it is moving along such generalized steady trajectories. The method required the extension of standard (inertial) CFD formulations to general non-inertial reference frames. Generalized Navier-Stokes and Euler equations have been derived. The formulation is valid for all ranges of Mach numbers including transonic flow. The method was implemented numerically for the planar case using the generalized Euler equations. The developed computer codes can be used to obtain numerical flow solutions for airfoils moving in general steady motions (i.e. circular motions). From these numerical solutions it is possible to determine the variation of the lift, drag and pitching moment with respect to the pitch rate at different Mach numbers and angles of attack. One of the advantages of the mathematical model developed here is that the aerodynamic forces become well-defined functions of the motion variables (including angular rates). In particular, the stability derivatives are associated with partial derivatives of these functions. These stability derivatives can be computed using finite differences or the sensitivity equation method.

Dedication

This work is dedicated to my parents: Christian and Graciela, to my sisters: Elisabet and Iliana and to my grandmother: “nona” Rita.

Acknowledgments

I thank my advisor Dr. Eugene Cliff for his unyielding and invaluable support. He helped me work through numerous problems during my research. His ideas and suggestions form part of this dissertation. I thank the other members of my committee, for their kindness in answering questions I had for them, and for their very useful suggestions and comments. I thank Dr. Kyle Anderson and Dr. Bernard Grossman for introducing me to the "real" CFD. Without their teaching I would not have been able to obtain the numerical implementations presented here. Finally, I would like to thank Iossif Mugtussidis and Philippe Tetrault for their help as we worked together towards our doctorates.

Contents

List of Tables

List of Figures

Nomenclature

Roman Symbols

a	=	speed of sound
$C_l,\ C_d,\ C_m$	=	lift, drag and pitching moment coefficients
c	=	airfoil's chord or wing's mean chord
$e,\ E$	=	internal energy, total energy per unit mass
$F,\ G,\ H$	=	components of inviscid fluxes
$F_v,\ G_v,\ H_v$	=	components of viscous fluxes
M	=	Mach number
$P,\ T$	=	pressure, temperature
$p,\ q,\ r$	=	body roll rate, pitch rate, yaw rate
Q	=	conservative flow variable
$R,\ R_c$	=	gas constant, radius of circular path
$S_\eta,\ S_p,\ S_q,\ S_r$	=	flow sensitivity with respect to η, p, q and r, respectively.
t	=	time
$u,\ v,\ w$	=	flow velocity components
V	=	speed
W	=	source terms
X	=	generic variable to denote the flow state
$x,\ y,\ z$	=	Cartesian coordinates
$\hat{e}$	=	unit vector of Cartesian axes
$\vec{f}$	=	body force vector
$\overline{F}$	=	steady aerodynamic force function
$\hat{M}$	=	pitching moment
$\hat{n}$	=	unit vector normal to a surface
$\vec{x},\ \vec{V},\ \vec{a}$	=	vector position, velocity and acceleration, respectively

Calligraphic Symbols

$\mathcal{F}$ = generic aerodynamic force

$\mathcal{G}$ = generic function to get the aero forces from a flow solution

$\mathcal{R}$ = general (non-inertial) reference frame

$\mathcal{S}$ = inertial reference frame where the air is still

Greek Symbols

α = angle of attack

β = angle of sideslip

γ = ratio of specific heats

η = generic physical parameter

$\phi,\ \theta,\ \psi$ = Euler angles defining the aircraft attitude

ρ = air density

σ = generic area or segment of a finite-volume element

τ = According to the context: temporal variable or finite-volume

$\overrightarrow{\overrightarrow{\tau}}$ = shear tensor

$\vec{\omega}, \omega$ = angular velocity vector, its magnitude

$\omega_x,\ \omega_y,\ \omega_z$ = components of the angular velocity on a general reference frame

$\vec{\Omega}$ = inertial body force

superscripts

j = denotes the jth finite-volume element of a discretization

n = denotes the flow solution at nth iteration

subscripts

i = denotes the ith segment of the boundary of a finite-volume element

∞ = denotes far-field conditions

c = denotes a predetermined point of the aircraft (usually the center of mass)

m = denotes midpoint (centroid) of a segment (area)

$\mathcal{R},\ \mathcal{S}$ = denote the reference frame ($\mathcal{R}$ or $\mathcal{S}$) in which the variable is measured

$\mathcal{R}/\mathcal{S}$ = denotes the origin of reference frame $\mathcal{R}$ as seen from reference frame $\mathcal{S}$

$x,\ y,\ z$ = denotes Cartesian components

$q,\ \hat{q}$ = denote dimensional and non-dimensional pitch rate stability derivatives

Chapter 1

Introduction

The design of atmospheric vehicles and their control systems is an interesting and challenging area of on-going research. The quality of a design is evaluated by the behavior of the aircraft in performing required tasks and maneuvers. From flight mechanics, one knows that in order to determine this behavior one must be able to calculate the aerodynamic forces and aerodynamic moments acting on the aircraft's surface at any instant of the flight.

The accurate determination of these aerodynamic forces (and aerodynamic moments) is not a trivial problem, since these forces are not independent of the aircraft motion but they are coupled to it. Therefor, at a given time the particular values of the aerodynamic forces will affect the future aircraft motion, and conversely, the particular values of the aerodynamic forces at a given time will depend on the particular maneuver that the aircraft is performing at that time. The problem gets more complex because these forces depend not only on the instantaneous values of the motion variables but also depend on the past history of the motion. As a consequence, even under the assumption that the aerodynamic forces can be evaluated (numerically or experimentally) at any instant for a particular motion of the aircraft, it is obviously materially impossible to evaluate and record all the aerodynamic-force-histories associated to each one of the infinitely many possible histories of motion. From these observations, one can conclude that an analysis of the aircraft behavior is not viable unless a mathematical model for the representation of the aerodynamic forces is introduced.

The formulation of an aerodynamic mathematical model probably started with the work of Bryan [9] at the beginning of the 20th century. Bryan postulated that the aerodynamic forces depend only on the instantaneous values of the motion variables and that this dependence was linear. Since that time the mathematical model has evolved to take into account additional effects such as time lag, dependence on previous history of the motion, non-linearity, aerodynamic hysteris, separation, etc. One of first phenomena that was taken into account was the time lag occuring in the aerodynamic forces responses to changes in the angle of attack. The time lag effect is mainly due to the time it takes the aircraft tail to sense a change in the angle of attack and it was taken into account by adding to the

mathematical models terms proportional to the time-rate of changes of motion variables such as the angle of attack. The use of linear stability analysis in flight mechanics leads naturally to a requirement for the determination of *stability derivatives* (also called stability parameters), which are the coefficients appearing in the linearization of the aerodynamic forces. They basically describe the expected rate of change of the aerodynamic forces with respect to some parameter of the flight motion.

At present, the different techniques used for the determination of the aerodynamic forces are principally based on generalizations of Bryan's work and on the generalization of the idea of linear system responses. In the system response approach, the aerodynamic forces are predicted by calculating time-integrals of the motion variables. For example, the contribution of the angle of attack α to the lift L could be written as,

$$\triangle L(t) = \int_0^t \mathcal{A}(t-\tau)\dot{\overline{\alpha}}(\tau)\, d\tau \tag{1.1}$$

where $\mathcal{A}$ is the indicial (or step-function) response funtion and $\dot{\overline{\alpha}}$ is the time-rate of change of $\overline{\alpha}$. For linear time-invariant systems $\mathcal{A}$ is a function that depends only on time and it is independent of the motion variables. The use of linear-system responses was an important forward step because it generalized the model to allow the dependence of the aerodynamic forces on the past-history of the motion variables.

Etkin [13] presents an equivalent approach by using the idea of Aerodynamic Transfer Functions. So the aerodynamic forces are determined by using transfer functions obtained from studying the aircraft response to appropiate sinusoidal inputs. Finally, Tobak and his colleagues [51], [52], [53] have obtained a very complete aerodynamic mathematical model capable of accounting for non-linearities and other phenomena such as hysteresis. Their idea was to generalize the linear system response approach, by allowing the indicial response functions $\mathcal{A}$ to be functionals of the motion variables.

The choice of a mathematical model eliminates the necessity of determining the aerodynamic forces for the infinitely many aircraft maneuvers and time histories. The underlying idea is that the data to construct the model can be obtained by measuring the aerodynamic forces, the stability derivatives or other appropiate parameters from a smaller class of aircraft motions or maneuvers called *characteristic motions*. Then, as pointed out by Tobak and Schiff [53], the aerodynamic responses to the characteristic motions can be determined once and for all and then can be applied over a wide range of motions.

Once the mathematical model is formulated, the problem consists in the determination of the aerodynamic forces and stability derivatives or aerodynamic responses from the characteristic motions. This determination can be done experimentally using model-scale or full-scale flight tests, using wind tunnel testing or numerically using computational fluid dynamics (CFD). The use of model-scale or full-scale flight tests are probably the most realistic and accurate but very inefficient in the design of a new aircraft because of the cost in time and money of performing the required modifications during a design process. The

use of dynamic experiments on scale-models in wind-tunnel is a standard way to determine the characteristic aerodynamic forces and stability derivatives. However, such testing is still costly because of the equipment and technology necessary to simulate an increasing number of required experiments at different flight conditions. CFD is a promising technique because any required modifications of the prototype during the design proccess can be introduced at low cost and because of its ideal capacity to simulate completely different flight conditions or experiments. However, much progress is needed to reach the ideal capacity of CFD. In the computational hardware area progress is still needed to support memory and speed requirements and in the software area much work still needs to be done in the simulation of turbulence and viscous effects particularly when separation occurs (i.e. at high angles of attack or non-zero angular rates).

In the present work, an aerodynamic mathematical model is presented. The mathematical model is based on the choice of *aerodynamically steady motions* as the set of characteristic motions. The model allows one to formally determine the dependence of the aerodynamic forces (and aerodynamic moments) with respect to all the motion variables including the angular rates of the aircraft. Then, it is shown how the mathematical model can be fitted into a generalized CFD formulation which allows the determination of the aerodynamic forces and the complete set of static and dynamic stability derivatives.

It will be seen that the determination of the stability derivatives can be done by appropiately using finite differences on the obtained flow solutions. In the present work another alternative approach is developed which is potentially better. This approach is based on the continuous sensitivity equation method and consists in developing a linear boundary-value problem (BVP) that directly leads to the required stability derivatives. The approach can be used even in cases where the aircraft is moving with non-zero angular rates.

The work has been completed by the succesful implementation of the two-dimensional application of the theory. The numerical implementation can be used inclusively in the range where other techniques are not applicable, i.e. transonic speeds and non-zero angular rates. The results have been successfully validated against currently used techniques.

In order to carry out the present program the mathematical model will be introduced in Chapter 2. In Chapter 3, a complete generalization of the Navier-Stokes flow equations for non-inertial reference frames [1] will be presented. Then, the mathematical model will be coupled with the non-inertial Navier-Stokes equations. This coupling defines a nonlinear BVP consisting of a nonlinear partial differential equation (PDE) and appropriate boundary conditions. The associated forces and moments on the body can then be computed by certain weighted surface integrals of the local (normal) pressure (and shear forces). It will be seen that the body angular-rates appear as coefficients in the nonlinear BVP. The nonlinear BVP can be solved using a generalized CFD algorithm.

The numerical results for two-dimensional flows around an airfoil will be presented in

[1] An inertial frame is a reference frame where Newton's Laws hold

Chapter 4. In Chapter 5, the sensitivity equation method and its application to aerodynamic modeling will be described. In Chapter 6, the numerical results for the stability derivatives obtained using the sensitivity equation method will be presented.

Chapter 2

Mathematical Modeling

2.1 Preliminary Remarks

In subsequent discussions, it is assumed that the reader is familiar with relations among the various (relative) positions, velocities and accelerations and standard flight mechanics notation. This material may be found in several references, such as Etkin [13] or Miele [35].

Consider a rigid aircraft of arbitrary geometry moving in an arbitrary way in the atmospheric air as shown in Figure (2.1). The air is assumed to be uniform and at rest with respect to an inertial reference frame denoted by $\mathcal{S}$. The unit vectors of the axes of the Cartesian coordinate system associated to $\mathcal{S}$ will be denoted by $\{\hat{e}_{x\mathcal{S}}, \hat{e}_{y\mathcal{S}}, \hat{e}_{z\mathcal{S}}\}$.

Another reference frame is defined to be fixed to the aircraft and is denoted by $\mathcal{R}$. A Cartesian coordinate system associated to $\mathcal{R}$ is defined such that its origin is located at an arbitrary point c of the aircraft and the unit vectors of its axes will be denoted by $\{\hat{e}_{x\mathcal{R}}, \hat{e}_{y\mathcal{R}}, \hat{e}_{z\mathcal{R}}\}$. The subscript $\mathcal{S}$ will be attached to the vector components when the vector is resolved in the inertial coordinate system $\mathcal{S}$. Similarly, the subscripts $\mathcal{R}$ will be attached to the vector components when the vector is resolved in the coordinate system $\mathcal{R}$. For example, the vector position $\vec{x}_c$ of the aircraft with respect to an observer in the reference frame $\mathcal{S}$ will be written as $\vec{x}_c = x_{c\mathcal{S}}\hat{e}_{x\mathcal{S}} + y_{c\mathcal{S}}\hat{e}_{y\mathcal{S}} + z_{c\mathcal{S}}\hat{e}_{z\mathcal{S}}$ when resolved in terms of the Cartesian components of reference frame $\mathcal{S}$.

From the kinematics of rigid bodies it is known that the aircraft motion with respect to the inertial frame $\mathcal{S}$ is completely specified in terms of the linear velocity vector $\vec{V}_c$ of the point c with respect to the air and in terms of the angular velocity vector $\vec{\omega}$ of the aircraft with respect to the inertial coordinate system $\mathcal{S}$.

The vector $\vec{V}_c$ is called the velocity of the aircraft. One can represent this vector in terms of its magnitude V_c which defines the speed of the aircraft, the angle of attack α, and the angle of sideslip β, which define the relative orientation of the velocity vector with respect

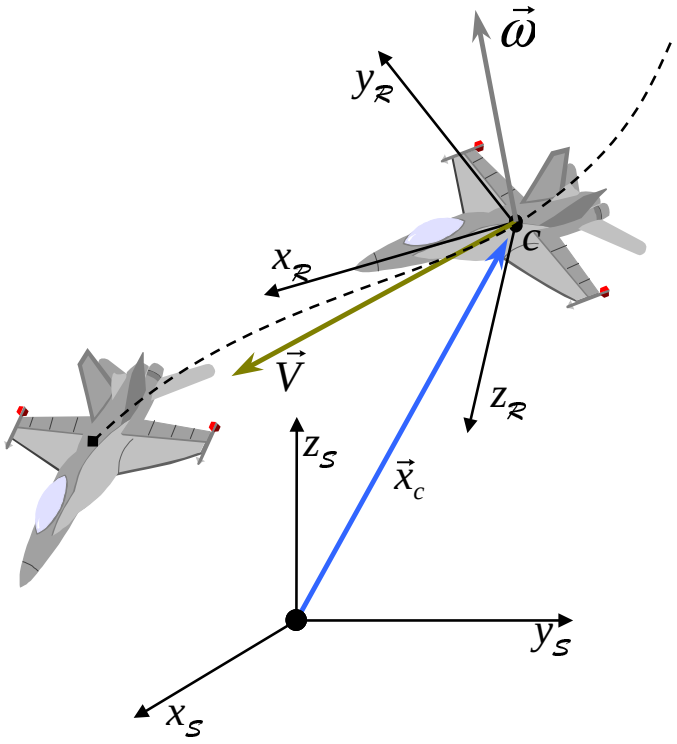

Figure 2.1: Aircraft flying in an arbitrary motion. View of inertial coordinate system $\mathcal{S}$ and body-fixed coordinate system $\mathcal{R}$

to the body-fixed axes of the coordinate system $\mathcal{R}$. Similarly $\vec{\omega}$ can be represented in terms of its three components p, q and r along the body-fixed axes of the coordinate system $\mathcal{R}$. As a consequence, any arbitrary motion U can be defined in terms of the temporal evolution of the six dynamic motion variables:

$$U = \{\overline{V}_c, \overline{\alpha}, \overline{\beta}, \overline{p}, \overline{q}, \overline{r}\} \tag{2.1}$$

Here the motion variables appear with an overline to denote that they are functions (of time).

2.2 Mathematical Modeling of Aerodynamic Forces

As stated in the introduction, the aerodynamic forces (and aerodynamic moments) acting on an aircraft at a given time t depend not only on the instantaneous values of the dynamic motion variables but also depend on the past history of the motion. With this in mind one

can write

$$\overline{\mathcal{F}}(t) = \tilde{\mathcal{F}}\left(\overline{V}_c(\tau), \overline{\alpha}(\tau), \overline{\beta}(\tau), \overline{p}(\tau), \overline{q}(\tau), \overline{r}(\tau), t\right) \qquad t \geq \tau \geq -\infty \tag{2.2}$$

where $\overline{\mathcal{F}}(t)$ represent the value at time t of a typical component of the aerodynamic forces or moments. $\tilde{\mathcal{F}}$ is used to denote the *functional* dependence of the aerodynamic forces on the motion variables. Observe that the temporal parameter τ goes from the time t at which the aerodynamic forces are to be evaluated to all the previous times. The idea that the aerodynamic forces can be described by a functional and depend on the past history of the motion was already recognized by Von Karman and Burgers [57] several decades ago.

Equation (2.2) is not simply an empirical formulation of the aerodynamic forces but it is a formal and exact representation of the physics of the problem. Note that the aerodynamic forces at a given instant t are produced by integration of the pressure and shear forces acting on the aircraft surface at that time. These pressure and shear forces can be determined from the state of the flow surrounding the aircraft. The state of the flow X is completely characterized by the values of the density ρ, the flow velocity components u, v, w and the static pressure P in the flow field [1]. Using these observations, it follows that the aerodynamic forces at any time t can be completely defined by:

$$\overline{\mathcal{F}}(t) = \mathcal{G}(X(t)) \quad \text{where} \quad X = \{\rho, u, v, w, P\}, \tag{2.3}$$

In the above equation, $\mathcal{G}$ represents a generic well-known function whose specific analytic expression depends on the particular aerodynamic force component $\overline{\mathcal{F}}$. For example if the fluid is assumed inviscid and $\overline{\mathcal{F}}$ is chosen to be the pitching-moment $\hat{M}$ we have that:

$$\hat{M} = \mathcal{G}(X) = \mathcal{G}(P) = \int_{\sigma} \left[\vec{x}_{\mathcal{R}} \times -P\hat{n}\right]_{y_{\mathcal{R}}} d\sigma$$

where $\hat{n}$ is the outward-pointing unit normal vector along the aircraft surface σ.

Now, the current state of the flow X is defined by the boundary value problem (BVP) defined by the flow equations (Navier-Stokes). Since the aircraft has been moving in the fluid, its motion influenced the prior flow states and will influence the current flow state [2]. As a consequence, since the aircraft motion can be completely specified in terms of temporal evolution of $\overline{V}_c$, $\overline{\alpha}$, $\overline{\beta}$, $\overline{p}$, $\overline{q}$, $\overline{r}$ we have that:

$$X(t) = \tilde{X}\left(\overline{V}_c(\tau), \overline{\alpha}(\tau), \overline{\beta}(\tau), \overline{p}(\tau), \overline{q}(\tau), \overline{r}(\tau), t\right) \qquad t \geq \tau \geq -\infty \tag{2.4}$$

After, combining equation (2.4) with equation (2.3) one gets equation (2.2) where $\tilde{F} = \mathcal{G}(\tilde{X})$.

Using the reasoning presented above it follows that one can express the problem of the evaluation of the aerodynamic forces using an input/output representation as shown in Figure (2.2). In the case of an aircraft in a free-flight this input/output system is coupled

[1] It is possible to choose another set of physical variables to define the state of the flow

[2] As seen from the inertial reference frame, the aircraft motion affects the flow state through the changes in the boundary conditions of the BVP

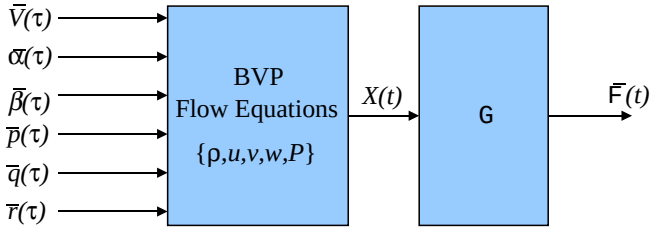

Figure 2.2: Input/Output representation of the Aerodynamic Forces

with the equations of motion and with the addition of the other external forces (gravitational, propulsion forces, etc.) acting on the aircraft.

The evaluation of the functional $\tilde{\mathcal{F}}$ (i.e. of the aerodynamic forces) along specific aircraft motions is certainly possible. For example, Orlik [40] has determined the aerodynamic forces acting on a free aircraft using experimental techniques. It is also possible, within some limitations, to generate numerically time-accurate CFD solutions coupled with the equations of motion. For example, in references [28] and [38]) this type of simulations have been done using flow models based on vortex-lattice methods. Some researchers are currently working on the fully coupled problem: flow equations, body-dynamics and control. For example, Allan et. al. [1] have performed simulations of an airfoil moving with an active control system which modifies the pitching moment of the airfoil. Atwood [5] investigated the separation of a controlled store from a cavity using the Navier-Stokes equations and a pitch attitude control law. Others, like Morton et. al. [37] have extended the problem to include aeroelastic effects.

While PDE-based models (Figure (2.2)) may be useful in some settings, these are far too complex for a standard use. Thus, there is a basic need to obtain a simplified version of the functional (2.2) defining the input/output system of Figure (2.2). Theodorsen [49] and Jones [27] provided approximate representations for this functional in the case of incompressible flow about a thin airfoil. More recently, Herdman and Turi [22] have rigorously studied a representation based on neutral functional differential equations. Several mathematical models are based in the substitution of the exact functional $\tilde{\mathcal{F}}$ by an approximate linear indicial response functional of the type shown in equation (1.1). As mentioned before, Tobak and his colleagues [51], [52], [53] have extended this approach to account for non-linear effects.

The mathematical model usually has incorporated the concept of reusability, i.e. the results obtained from the simulation of a finite number of motions will be reused to predict other motions. For example, if a model of the form (1.1) is used the indicial response function $\mathcal{A}$ will be constructed from a series of experiments. Once $\mathcal{A}$ is obtained, equation (1.1) could

be used to evaluate the lift along an arbitrary motion.

Let's consider another example based on a simplified version of Bryan's model. Assume that the pitching moment coefficient acting on a symmetric aircraft in longitudinal motion can be evaluated from:

$$C_m = C_{m_0} + C_{m_V}\overline{V}_c + C_{m_\alpha}\overline{\alpha} + C_{m_q}\overline{q}. \tag{2.5}$$

The coefficients C_{m_V}, C_{m_α}, C_{m_q} are referred to as stability derivatives. All the coefficients are assumed to be time-invariant. The model is complete when the four coefficients are determined from experimental measurements or numerical calculations of the pitching moment acting on the aircraft as it moves in specified characteristic motions. Once the coefficients are chosen, equation (2.5) can be used to predict the pitching moment for other general motions. The fact that the coefficients in equation (2.5) are time-invariant is one of the main aspects which make the model of practical use.

Notation Issues. The damping-in-pitch stability derivative C_{m_q} shown in equation (2.5) is a dimensional stability derivative. Although many authors use the term C_{m_q} to denote a non-dimensional stability derivative, in this work, C_{m_q} denotes a dimensional stability derivative. Since by convention a non-dimensional pitch rate is denoted by $\hat{q}$, here, the non-dimensional stability derivatives will be denoted by $C_{m_{\hat{q}}}$.

2.3 A Mathematical Model based on Aerodynamically Steady Motions

The mathematical model presented in this dissertation is based on the choice of the set of *aerodynamically steady motions* as the set of characteristic motions. An *aerodynamically steady motion* is defined to be a motion where the flow properties remain steady (time-invariant) as seen from a body-fixed reference frame. From this definition and the discussion that lead to equation (2.3) it follows that an aircraft flying in an aerodynamically steady motion will generate steady (time-invariant) aerodynamic forces. As will be seen, these steadiness properties will make the model of practical use. It will also be seen that the choice of aerodynamically steady motions satisfies the requirement that the set of characteristic motions be small enough to be classified and at the same time big enough to be able to characterize a broad spectrum of general motions.

The most commonly used motion to characterize aerodynamic forces: uniform level rectilinear flight is an aerodynamically steady motion. In this type of rectilinear motion the aircraft is moving in a steady form (shown in Figure (2.3)) at constant values of $\overline{V}_c(t) = V_c$, $\overline{\alpha}(t) = \alpha$ and $\overline{\beta}(t) = \beta$, and with zero angular rates: $\overline{p}(t) = \overline{q}(t) = \overline{r}(t) = 0$. Under the assumption of still, uniform air and neglecting unsteadiness due to separation or turbulence it is obvious that, after a certain transient the aerodynamic forces acting on the aircraft become constant (time-invariant). Then, for these steady motions, the functional of equation

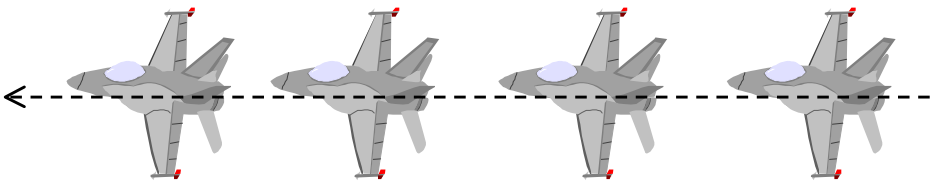

Figure 2.3: Aircraft flying in a rectilinear steady motion with no-angular rates

(2.2) reduces to the simpler form:

$$\overline{\mathcal{F}}(t) \;=\; \tilde{\mathcal{F}}\left(\overline{V}_c(\tau), \overline{\alpha}(\tau), \overline{\beta}(\tau), \overline{p}(\tau), \overline{q}(\tau), \overline{r}(\tau), t\right)$$

$$\Downarrow$$

$$\mathcal{F} \;=\; \overline{F}\left(V_c, \alpha, \beta, 0, 0, 0\right) \tag{2.6}$$

As a consequence, by restricting the motions to the class of rectilinear, steady flights, the mathematical representation of the aerodynamic forces has been simplified from a functional form of six function arguments to a function $\overline{F}$ of three scalar arguments: $\{V_c, \alpha, \beta\}$. Observe that in the representation the Mach number $M_c = \frac{V_c}{a_c}$ could be used instead of the speed V_c, in such a case, equation (2.6) can be rewritten as:

$$\mathcal{F} = \overline{F}\left(M_c, \alpha, \beta, 0, 0, 0\right) \tag{2.7}$$

Now consider a symmetric aircraft moving in rectilinear longitudinal steady motion (i.e. constant speed and angle of attack, $\beta = 0$, no-angular rates) as the one shown in Figure (2.4). Equation (2.6) for the pitching moment coefficient can be written as:

$$C_m = \overline{C}_m\left(V_c, \alpha\right)_{\beta=0, p=0, q=0, r=0} \tag{2.8}$$

If a Taylor Expansion to first order in the motion variables V_c, α is performed in the above equation, then it follows that, except for the rotary contribution due to non-zero q, Bryan's formula (2.5) is the linear approximation to the more general function (2.8). Note that in this case the stability derivatives: C_{m_V} and C_{m_α} have now a clear meaning in terms of the partial derivatives of $\overline{C}_m$. This idea can be extended to the stability derivatives with respect to the sideslip angle β if one considers the general rectilinear steady flight of eq. (2.6).

Figure 2.4: Symmetric aircraft flying in a rectilinear longitudinal steady motion (i.e. $\beta = 0$, no-angular rates)

2.4 Determination of the Function $\overline{F}\left(V_c, \alpha, \beta, 0, 0, 0\right)$

The determination of the function (2.6) or (2.7) can be done numerically, using CFD, or experimentally, using wind-tunnels. The measurement using wind-tunnels is relatively straightforward since it only requires that the model be fixed at the desired orientation with respect to the free-stream. Since the aircraft is moving at a constant rectilinear velocity without angular rotation, the standard CFD formulation for inertial reference frames can be used to determine $\overline{F}\left(V_c, \alpha, \beta, 0, 0, 0\right)$. Also, since the required solution is steady, it is not necessary to get time-accurate solutions.

As an example of the use of CFD attention is restricted to the case of an airfoil moving in rectilinear steady motion with zero angular rates in a inviscid flow as shown in Figure (2.5). In this case the flow will be two-dimensional and a standard two-dimensional CFD

Figure 2.5: Airfoil (wing of infinite span) flying in rectilinear longitudinal steady motion (i.e. $\beta = 0$, no-angular rates)

code for steady flows can be used to determine the aerodynamic forces (*cf.* Equation (2.7)):

$$\mathcal{F} = \overline{F}\left(M_c, \alpha, 0, 0, 0, 0\right) \tag{2.9}$$

Figure (2.6) displays the general streamline pattern and the pressure coefficient contours corresponding to a NACA 0012 airfoil flying at a Mach number $M_c = 0.2$ and at angle of

attack $\alpha = 0.0^o$. The CFD code that was used to obtain the shown flow solutions is called `Class Code`, and it was provided by Dr. Kyle Anderson from NASA Langley. The `Class Code` is based on a finite-volume formulation on unstructured grids and it can be considered as the inviscid version of the `Fun2D Code` [2], [3].

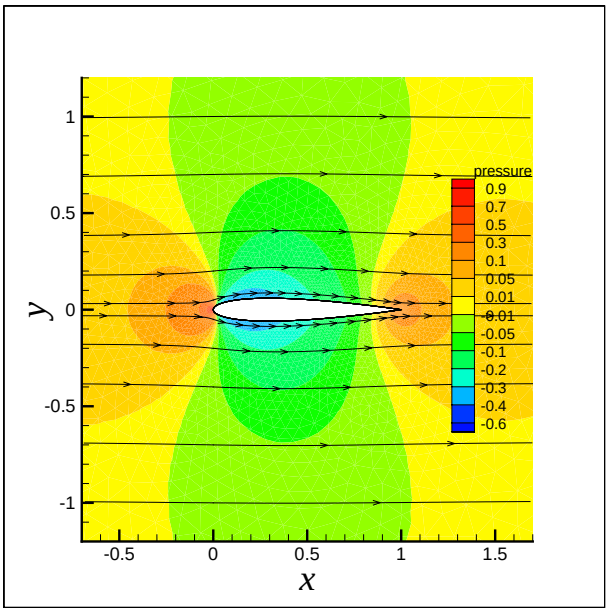

Figure 2.6: Pressure coefficient contours and streamlines of the flow around a NACA 0012 airfoil which is flying at $M_c = 0.2$ and $\alpha = 0.0^o$

The lift C_ℓ, drag C_d and pitching moment C_m coefficients can be calculated by an appropiate integration of the pressure on the airfoil's surface. By running different simulations one can get the behavior of these coefficients at specified speeds (or Mach numbers) and at specified angles of attack. These simulations allow one to determine functions of the form (2.8) or (2.9) for these coefficients.

2.5 Adding Steady Motions with Pitch-Rates into the Mathematical Model: An Illustrative Example

The dependence of the aerodynamic forces with respect to the angular rates $\overline{p}$, $\overline{q}$ and $\overline{r}$ is non-negligible and the aerodynamic model must account for it. According to the previous discussion, the restriction of characteristic motions to the class of rectilinear steady flight provides valuable information about the dependence of the aerodynamic forces with respect to speed, angle of attack and angle of sideslip. However, it is impossible to use these motions to get information about the dependence of the aerodynamic forces with respect to

the angular rates of the aircraft. This problem was clearly seen in the case of rectilinear longitudinal steady motion ($\beta = 0$) discussed previously. There it was impossible to justify the rotary stability derivative C_{m_q} appearing in equation (2.5) in terms of partial derivatives of equation (2.8). As shown below, the problem can be circumvented by extending the model to a broader class of aerodynamically steady motions.

To show how the extension can be done an illustrative example is discussed. Consider again the case of rectilinear, longitudinal, steady flight shown in Figure (2.4). For this case, the aerodynamic forces could be represented as (*cf.* eq. (2.6) with ($\beta = 0$)):

$$\mathcal{F} = \overline{F}\,(V_c, \alpha, 0, 0, 0, 0) \tag{2.10}$$

The objective is to try to get a generalization of the above equation that includes the possibility of non-zero pitch rates q. Since the above equation was obtained under the asumption of steadiness, it follows that a generalization to:

$$\mathcal{F} = \overline{F}\,(V_c, \alpha, 0, q, 0, 0) \tag{2.11}$$

could be obtained only if there exists a planar (longitudinal) aerodynamically steady motion, such that, the aircraft moves with a constant speed, a constant angle of attack and a constant (non-zero) pitch rate q.

The first conjecture, is to try to superimpose on the initial rectilinear flight, a constant pitch rate q of the aircraft. The resulting motion resembles the motion shown in Figure (2.7). However, the approach fails since it is obvious from the figure that the motion is unsteady

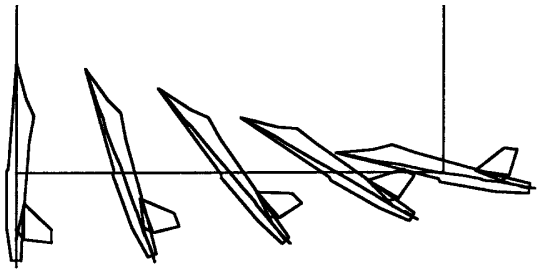

Figure 2.7: Aircraft flying in a uniform, rectilinear path with a constant (non-zero) angular rate q

and that in particular the angle of attack is changing with time. Although this first trial failed, it is possible to see that there exists a correct approach.

The right approach consists in restricting the aircraft to a steady circular trajectory, as shown in Figure (2.8). The main features of the circular motion are:

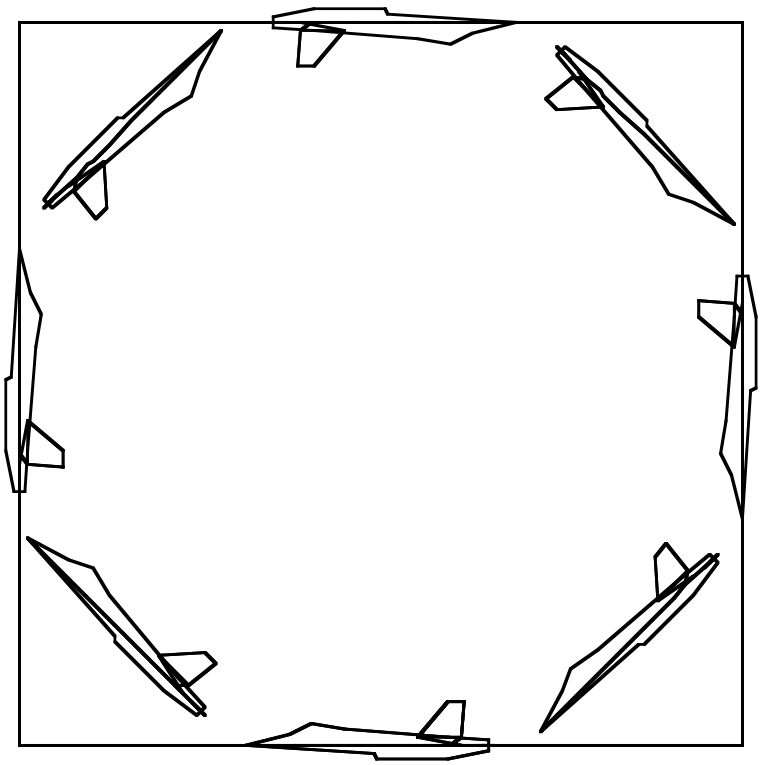

Figure 2.8: Aircraft flying in a steady circular trajectory with constant pitch rate q and constant angle of attack α

1. The radius of the circular trajectory R_c satisfies the condition:

$$R_c = \frac{V_c}{q} \tag{2.12}$$

2. The aircraft can hold a constant speed V_c and it is experiencing a centripetal acceleration:

$$a_c = \frac{V_c^2}{R_c} \tag{2.13}$$

   which is normal to the velocity vector. This result guarantees that the aircraft is not changing its speed.

3. From the pilot's point of view the flow motion is steady, i.e. time-invariant.

The existence of these steady motions, allows one to construct the function $\overline{F}$ of equation (2.11) by determining the aerodynamic forces acting on the aircraft when it is moving in these circular trajectories. In particular, a steady pitching moment function

$$C_m = \overline{C}_m \left(V_c, \alpha, 0, q, 0, 0\right) \tag{2.14}$$

can be defined. Furthermore, the partial derivatives of $\overline{C}_m$ will allow one to determine the pitching moment coefficient C_{m_q} that was missing before.

In the next section, the general aerodynamic model is presented. The generalization will allow one to determine the direct dependence of the aerodynamic forces with respect to the complete set of motion variables (including the dependence on the three components of the angular rates).

2.6 Mathematical Model: General Case

2.6.1 Steps to Get the General Model

In the previous section it was shown how to get the dependence of the aerodynamic forces with respect to the pitch rate q for the particular case of planar longitudinal motions. The extension was possible since there are steady planar motions where the aircraft can have a non-zero pitch rate. The motions turned out to be circular trajectories characterized by the fact that in these motions the aircraft can hold a constant speed V_c, a constant angle of attack α and a constant pitch rate q.

Following the ideas underlying the example, a complete generalization of the mathematical model can be formulated. The generalization will be done in three steps:

1. Determination of the general mathematical conditions for the existence of aerodynamically steady motions.
2. Simplification of the functional representation of the aerodynamic forces for the case of aerodynamically steady motions.
3. Determination of the compatibility of the mathematical conditions with the mechanics of the motion of rigid bodies in the air.

Step 1 refers to the determination of the most general mathematical conditions under which it is possible to generate an aerodynamically steady motion. Step 2 refers to the use of the properties of aerodynamically steady motions and the use of the mathematical conditions in the functional representation of the aerodynamic forces. From Step 2 a simplified mathematical model of practical use will be obtained. Step 3 consists in determining if the imposition of the mathematical conditions still permit the generation of physically meaningful motions, i.e. motions that can exist in the reality. Steps 1 and 2 will be discussed below while Step 3 will be discussed in Section 2.7.

2.6.2 Mathematical Conditions for Aerodynamically Steady Motions

An aerodynamically steady motion was defined to be a motion where, as seen from the pilot's point of view, the flow properties remain steady. Then, in an aerodynamically steady motion the flow state:

$$X = \{\rho, u_{\mathcal{R}}, v_{\mathcal{R}}, w_{\mathcal{R}}, P\} \tag{2.15}$$

does not change with time. From equation (2.3) it follows that an aircraft moving in an aerodynamically steady motion generates steady aerodynamic forces (as seen from the body-fixed reference frame):

$$\left[\textbf{Aero Steady Motions} \Longrightarrow \textbf{constant Aerodynamic Forces:} \quad \overline{\mathcal{F}}(t) \to \mathcal{F}\right] \tag{2.16}$$

The mathematical conditions for the existence of aerodynamically steady motions can be obtained from the following observations.

Observation 1: If an aircraft is flying in an aerodynamically steady motion, then the motion variables $\overline{V}_c$, $\overline{\alpha}$, $\overline{\beta}$, $\overline{p}$, $\overline{q}$ and $\overline{r}$ must remain constant (time-invariant). The above result can be justified by considering the time evolution of the flow as seen from the pilot's point of view. For example, if at a given time the speed of the aircraft $\overline{V}_c$ was increasing then the pilot would see the flow coming towards him with an increasing flow velocity. In such a case, the flow state will not remain constant in time and, as a consequence, the motion will not be an aerodynamically steady motion.

Observation 2: Under the assumption that time-invariant flow equations coupled with time-invariant boundary conditions generates a steady flow, it follows that the converse of Observation 1 is true. That is to say, if in a given motion an aircraft is able to maintain constant values of $\overline{V}_c, \overline{\alpha}, \overline{\beta}, \overline{p}, \overline{q}$ and $\overline{r}$, then the motion is an aerodynamically steady motion.

One can summarize the above results as follows:

$$\left[\begin{array}{c} \textbf{Motions where} \quad \overline{V}_c, \overline{\alpha}, \overline{\beta}, \overline{p}, \overline{q}, \overline{r} \quad \textbf{remain constant} \\ \\ \Updownarrow \\ \\ \textbf{Aero Steady Motions/constant Aerodynamic Forces} \end{array}\right] \tag{2.17}$$

2.6.3 Simplification of the Functional Representation of the Aerodynamic Forces

The results summarized in equation (2.17) are the basis of the mathematical model presented here and are such that it permits to generalize the idea that lead to equation (2.6).

Under the assumption that aerodynamically steady motions are physically meaningful (which will be proved in the next section), if the set of aircraft motions is restricted to the class of aerodynamically steady motions, then the functional of equation (2.2) reduces to:

$$\overline{\mathcal{F}}(t) \;=\; \tilde{\mathcal{F}}\left(\overline{V}_c(\tau), \overline{\alpha}(\tau), \overline{\beta}(\tau), \overline{p}(\tau), \overline{q}(\tau), \overline{r}(\tau), t\right)$$

$$\Downarrow$$

$$\mathcal{F} \;=\; \overline{F}\left(V_c, \alpha, \beta, p, q, r\right) \tag{2.18}$$

In particular, from equation (2.18) the steady pitching moment function $\overline{C}_m$ will look as:

$$C_m = \overline{C}_m\left(V_c, \alpha, \beta, p, q, r\right) \tag{2.19}$$

Observe that once the steady aerodynamic functions $\overline{F}$ are constructed, they can be used to approximate the aerodynamic forces acting on an aircraft flying in an arbitrary motion. For example, if at time t the values of the motion variables are $\overline{V}_c(t)$, $\overline{\alpha}(t)$, $\overline{\beta}(t)$, $\overline{p}(t)$, $\overline{q}(t)$ and $\overline{r}(t)$, the pitching moment coefficient can be estimated by evaluating the steady pitching moment function $\overline{C}_m$ at those instantaneous values:

$$C_m(t) = \overline{C}_m\left(\overline{V}_c(t), \overline{\alpha}(t), \overline{\beta}(t), \overline{p}(t), \overline{q}(t), \overline{r}(t)\right). \tag{2.20}$$

2.7 Aerodynamically Steady Motions

In this Section it will be proved that the aerodynamically steady motions are well-defined and physically meaningful.

Consider the vector $\vec{V}_c$ that describes the translational velocity of a specified point on the aircraft (usually the center-of-mass) with respect to a fixed observer in the inertial reference frame $\mathcal{S}$ where the undisturbed air is assumed to be at rest. Note that the quantities $V_c,\ \alpha,\ \beta$ are scalars so that their rates of change are independent of the reference frame. For vector quantities, such as $\vec{V}_c$, the rates of change in two reference frames are related by the standard Eulerian formula

$$\frac{d_{\mathcal{S}}\,\vec{V}_c}{d_{\mathcal{S}}t} = \frac{d_{\mathcal{R}}\,\vec{V}_c}{d_{\mathcal{R}}t} + \vec{\omega} \times \vec{V}_c, \tag{2.21}$$

where $\vec{\omega}$ is the angular velocity of Frame $\mathcal{R}$ with respect to Frame $\mathcal{S}$.

For an aerodynamically steady motion the speed of the aircraft V_c and the aerodynamic angles $\alpha,\ \beta$ must remain constant. Then, it follows that:

1. The orientation of any body-frame is fixed with respect to the wind-frame, i.e. the body-frame and the wind-frame have the same angular velocity with respect to the inertial frame. Furthermore, in an aerodynamically steady motion, the components of the angular velocity are constant and this implies that:

$$\frac{d_{\mathcal{R}}\vec{\omega}}{d_{\mathcal{R}}t} = 0.$$

2. The velocity of the body-frame with respect to the inertial frame is a fixed vector in the body-frame, so:

$$\frac{d_{\mathcal{R}}\ \vec{V}_c}{d_{\mathcal{R}}t} = \vec{0},$$

This property combined with Equation (2.21) leads to:

$$\frac{d_{\mathcal{S}}\ \vec{V}_c}{d_{\mathcal{S}}t} = \vec{\omega} \times \vec{V}_c. \tag{2.22}$$

Equation (2.22) defines a system of linear, constant-coefficient, ordinary differential equations for the components of $\vec{V}_c$ in the inertial frame $\mathcal{S}$. The system (2.22) can be integrated to yield

$$\begin{bmatrix} u_{c\mathcal{S}}(t) \\ v_{c\mathcal{S}}(t) \\ w_{c\mathcal{S}}(t) \end{bmatrix} = \left(\vec{V}_{c0} \cdot \frac{\vec{\omega}}{\omega}\right)\frac{\vec{\omega}}{\omega} + \left[\vec{V}_{c0} - \left(\vec{V}_{c0} \cdot \frac{\vec{\omega}}{\omega}\right)\frac{\vec{\omega}}{\omega}\right]\cos(\omega t) + \left(\frac{\vec{\omega}}{\omega} \times \vec{V}_{c0}\right)\sin(\omega t). \tag{2.23}$$

A second integration gives the inertial-frame position components as

$$\begin{bmatrix} x_{c\mathcal{S}}(t) \\ y_{c\mathcal{S}}(t) \\ z_{c\mathcal{S}}(t) \end{bmatrix} = \begin{bmatrix} x_{c0} \\ y_{c0} \\ z_{c0} \end{bmatrix} + \left(\vec{V}_{c0} \cdot \frac{\vec{\omega}}{\omega}\right)\left(\frac{\vec{\omega}}{\omega}\right)t + \left[\vec{V}_{c0} - \left(\vec{V}_{c0} \cdot \frac{\vec{\omega}}{\omega}\right)\frac{\vec{\omega}}{\omega}\right]\frac{\sin(\omega t)}{\omega} - \left(\frac{\vec{\omega}}{\omega} \times \vec{V}_{c0}\right)\frac{\cos(\omega t)}{\omega}. \tag{2.24}$$

Equations (2.23-2.24) are a parametric description of a spiral. Note that Equation (2.23) includes a constant component along the direction $\vec{e}_\omega \equiv \left(\frac{\vec{\omega}}{\omega}\right)$ and a harmonic part. The constant vector multiplying $\cos(\omega t)$ in Equation (2.23) is the orthogonal complement of the constant part, while the constant vector multiplying $\sin(\omega t)$ is orthogonal to the plane spanned by $\{\vec{V}_{c0},\ \vec{e}_\omega\}$. The magnitude of the vectors in the harmonic part are, in fact, equal. Such spiral motions are the most general class of motions of an aircraft for which an aerodynamically steady description is possible. For a related discussion see the classical book by von Mises [56, pages 570 - 571].

2.8 Two Well-known Particular Cases

Let's restrict the general steady-motion discussed in the previous section to the case where $\vec{\omega}$ and $\vec{V}_0$ are orthogonal. In this case Equations (2.23) and (2.24) reduce to (modulo the initial position)

$$\begin{bmatrix} u_{c\mathcal{S}}(t) \\ v_{c\mathcal{S}}(t) \\ w_{c\mathcal{S}}(t) \end{bmatrix} = \vec{V}_{c0}\cos(\omega t) + \left(\frac{\vec{\omega}}{\omega} \times \vec{V}_{c0}\right)\sin(\omega t). \tag{2.25}$$

$$\begin{bmatrix} x_{c\mathcal{S}}(t) \\ y_{c\mathcal{S}}(t) \\ z_{c\mathcal{S}}(t) \end{bmatrix} = \frac{\vec{V}_{c0}}{\omega}\sin(\omega t) - \left(\frac{\vec{\omega}}{\omega} \times \frac{\vec{V}_{c0}}{\omega}\right)\cos(\omega t)\ . \tag{2.26}$$

Moreover, in equation (2.26) the constant vector multiplying $\sin(\omega t)$ has the same magnitude as that multiplying $\cos(\omega t)$ and is orthogonal to it. Then, it follows that, the motion is planar, and, that in fact it is a circular path.

This result can be seen more clearly if, the coordinate system is chosen in such a way that $\vec{\omega}$ points in the direction of the y-axis and $\vec{V}_{c0}$ in the direction of the x -axis:

$$\vec{\omega} = q\hat{e}_y \qquad \text{and} \qquad \vec{V}_{c0} = V_{c0}\hat{e}_x\ .$$

Then, equations (2.25) and (2.26) simplify to:

$$\begin{bmatrix} u_{c\mathcal{S}}(t) \\ v_{c\mathcal{S}}(t) \\ w_{c\mathcal{S}}(t) \end{bmatrix} = \begin{bmatrix} V_{c0}\cos(qt) \\ 0 \\ -V_{c0}\sin(qt) \end{bmatrix} \tag{2.27}$$

$$\begin{bmatrix} x_{c\mathcal{S}}(t) \\ y_{c\mathcal{S}}(t) \\ z_{c\mathcal{S}}(t) \end{bmatrix} = \begin{bmatrix} \frac{V_{c0}}{q}\cos(qt) \\ 0 \\ \frac{V_{c0}}{q}\cos(qt) \end{bmatrix}. \tag{2.28}$$

It is obvious from the above expressions that the motion is a circular motion in the plane x, z. This circular motion is exactly the circular aerodynamically steady motion described previously in Section 2.1 and shown in Figure (2.8). Note in particular that the radius of the circular path satisfies the relationship:

$$R_c = \frac{V_{c0}}{q},$$

which is the same as equation (2.12).

Finally note that in the limit where $\vec{\omega} \longrightarrow 0$ the general motion (cf equation (2.23)) reduces to the condition

$$\vec{V}_c(t) = \vec{V}_{c0}$$

which is the well-known uniform, rectilinear, steady motion (constant speed, no-angular rates) shown in Figure (2.3).

2.9 Interpretation of the Mathematical Model

We conclude the chapter by presenting a series of useful interpretations of the mathematical model presented here.

Interpretation 1

Under the assumption that the aerodynamic forces depend uniquely on the instantaneous values of the motion variables, equation (2.18) and its particular case equation (2.19) can be considered as the complete generalization to the non-linear case of Bryan's formulation.

Interpretation 2

Following Tobak and Schiff's formulation (reference [53]) in which they are able to decouple the aerodynamic forces in two parts: one part containing an "steady contribution" and other part containing the "unsteady contribution", one can consider that the function $\overline{F}\left(V_a, \alpha, \beta, p, q, r\right)$ is the complete generalization of the "steady contribution" to the aerodynamic forces. Observe for example that according to eq. (42) of reference [53], the pitching moment can be written as

$$C_m(t) = C_m(\infty, \overline{\alpha}(t), \overline{\beta}(t)) + \overline{p}(t) C_{m_p}(\infty, \overline{\alpha}(t), \overline{\beta}(t)) + \overline{q}(t) C_{m_q}(\infty, \overline{\alpha}(t), \overline{\beta}(t)) +$$

$$\overline{r}(t) C_{m_r}(\infty, \overline{\alpha}(t), \overline{\beta}(t)) + \dot{\alpha} C_{m_{\dot{\alpha}}}(\overline{\alpha}(t), \overline{\beta}(t)) + \dot{\beta} C_{m_{\dot{\beta}}}(\overline{\alpha}(t), \overline{\beta}(t))$$

where the first four terms represent the "steady contribution" which can be recognized by the infinite symbol (∞) while the last two terms represent the "unsteady contribution" to the pitching moment. Then a more general formulation will follow by replacing the "steady contribution" by the steady pitching moment function, so as to get:

$$C_m(t) = \overline{C}_m\left(\overline{V}_c(t), \overline{\alpha}(t), \overline{\beta}(t), \overline{p}(t), \overline{q}(t), \overline{r}(t)\right) +$$

$$+ \dot{\alpha} C_{m_{\dot{\alpha}}}(\overline{\alpha}(t), \overline{\beta}(t)) + \dot{\beta} C_{m_{\dot{\beta}}}(\overline{\alpha}(t), \overline{\beta}(t))$$

Interpretation 3: Geometrical interpretation

The flow state X is infinite-dimensional and can be represented by the five functions

$$X = \{\rho, u_{\mathcal{R}}, v_{\mathcal{R}}, w_{\mathcal{R}}, P\}$$

between the braces. The flow state $X(t)$ at time t is determined by the input motion profile:

$$U = \{\overline{V}_c(\tau), \overline{\alpha}(\tau), \overline{\beta}(\tau), \overline{p}(\tau), \overline{q}(\tau), \overline{r}(\tau)\} \qquad t \geq \tau \geq -\infty$$

defining a particular history of motion of the aircraft. To visualize these observations consider Figure (2.9) where, with obvious limitations, the state X is represented along a single axis

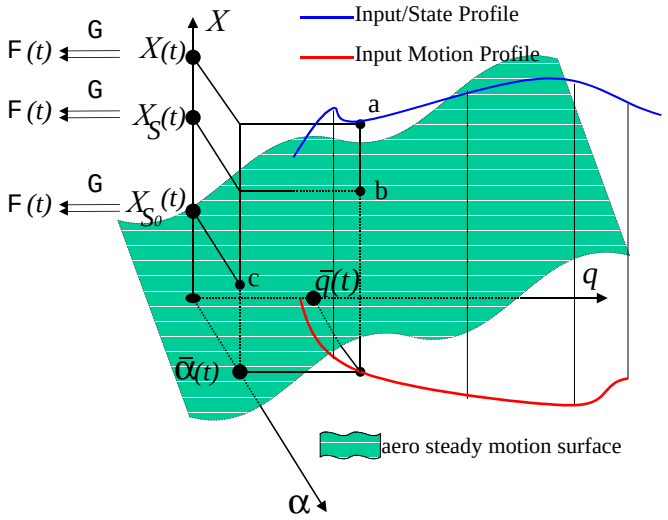

Figure 2.9: Geometric Representation of the Mathematical Model

and the input motion profile U is represented using α and q only. The red curve in the α-q plane shows a prescribed history of the (input) motion. Time is a parameter of the curve. The blue curve shows the corresponding path in the input/state space. At a particular time t the input variables have values $(\overline{\alpha}(t), \overline{q}(t))$ and point labeled 'a' along the blue curve defines the corresponding actual unsteady state $X(t)$. Using equation (2.3), the exact aerodynamic forces $\overline{\mathcal{F}}(t)$ can be evaluated from the current flow state $X(t)$ as $\overline{\mathcal{F}}(t) = \mathcal{G}(X(t))$

The mathematical model developed here allows one to associate a unique steady flow $X = X_S$ with each set of constant input variables $\{V_c, \alpha, \beta, p, q, r\}$. The association defines a surface in the input/state space. Using our geometrical representation the surface will appear as in Figure (2.9). For the aerodynamically steady motion defined by the input values $(\alpha, q) = (\overline{\alpha}(t), \overline{q}(t))$ the input/state point is labeled 'b' and the state coordinate is X_S. Again, using equation (2.3), one can evaluate the aerodynamic forces at this state as: $\mathcal{F}(t) = \mathcal{G}(X_S(t))$.

On the other hand, in the classical steady flow model (rectilinear motion, $\overline{q}(t) = 0$) , the input motion profile is projected onto the α (only) axis and the aerodynamic forces are evaluated from the associated steady flow (labeled X_{S_0} in Figure (2.9)) defined by the steady motion surface.

The distance $\|X(t) - X_S(t)\|$ is a measure of the unsteadiness in the flow, and the distance $|\mathcal{G}(X(t)) - \mathcal{G}(X_S(t))|$ is the 'error' between the steady force prediction and the true unsteady forces. Similarly the difference $|\mathcal{G}(X_S(t)) - \mathcal{G}(X_{S_0}(t))|$ is the error between the generalized steady flow forces developed here and the classical steady prediction.

Chapter 3

Flow Equations for Aerodynamically Steady Motions.

3.1 Some Remarks

In Section 2.7 the kinematics of general aerodynamically steady motions was determined. It was shown there that these motions belong to a set of helical trajectories. The next point that has to be addressed is how to calculate the aerodynamic forces along these steady trajectories. Those calculations will enable one to determine the form of the steady aerodynamic functions $F = \overline{F}(V_c, \alpha, \beta, p, q, r)$ defining the aerodynamic model.

The complexity of the motion (the aircraft is rotating and moving in an accelerated trajectory) seems to preclude the use of wind-tunnel measurements. However, it is useful to point out here that several groups have worked on wind-tunnel experiments for determining the aerodynamic forces in simulations that have a strong analogy with the aerodynamically steady motions defined here. Tobak [53] already pointed out that the experiment of the circular trajectory of Figure (2.8) can be generated by fixing the model to the end of an arm which is caused to rotate at a constant rate around a fixed point. The experiment is called the whirling-arm experiment and the main difficulties arise from the interference betweem the model, the arm and their own wake. In reference [16], the NASA Langley forced-oscillation apparatus was used to determine the stability derivatives for a model of a fighter. The apparatus can be used for pitching, yawing and rolling experiments in a fashion similar to the whirling arm. Also, noteworthy are the experiments (references [30] and [31]) performed in the Stability Wind Tunnel of the Virginia Polytechnic Institute and State University. There curved flow tests were performed to determine dynamic stability derivatives. Those curved flows simulate in part the flows that a non-inertial observer fixed to the aircraft will see when the aircraft moves with non-zero angular rates.

Another alternative is to calculate the aerodynamic forces along aerodynamically steady

motions using CFD. The results obtained in the present work show that the CFD approach is indeed a very promising one. To start using CFD, a reference frame must be chosen. The choice of the inertial reference frame $\mathcal{S}$ where the air is still implies the need of a CFD formulation that allows moving boundaries. This type of CFD formulation exists and has been used to simulate several types of problems. The favorite approach seems to be the one based on the use of overset grid methods. In these methods one grid is attached to the moving body and a basic grid is fixed in an inertial frame. The method have been used for example in the simulation of controlled [5] or uncontrolled [29], [60] store separation. Noack and Bishop [39] have used a Delaunay unstructured grid generator and a flow solver to simulate the problem of bodies in relative motion.

The complication of the CFD formulation based on an inertial reference frame is that from such a reference frame the problem we are considering is unsteady. On the other hand, if a body-fixed reference frame $\mathcal{R}$ fixed to the aircraft is chosen, the flow to be simulated will be steady. Furthermore, the specification of the fluid/solid interface is staightforward. For these reasons the body-fixed reference frame $\mathcal{R}$ will be our chosen reference frame. However, since the simulations are to be performed along motions where the aircraft is accelerated and rotating, the body-fixed reference frame $\mathcal{R}$ becomes a non-inertial reference frame. This observation introduces the problem that the well-known standard (inertial) Navier-Stokes equations can not be used. It is necessary to determine flow equations that be valid in non-inertial references frames.

3.2 Non-inertial Navier-Stokes Equations

The flow equations as seen from a general non-inertial reference frame, i.e. the non-inertial Navier-Stokes equations, can be obtained after careful, tedious work by starting from the standard (inertial) Navier-Stokes equations (defined in an inertial reference frame). The idea is to put into the standard Navier-Stokes equations the relationships between scalar, vector and tensor quantities as seen from the two different reference frames. The above process is outlined in [41] for inviscid compressible flows.

As shown in Figure (3.1), $\mathcal{S}$ will denote the inertial reference frame and $\mathcal{R}$ will denote the completely arbitrary non-inertial reference frame. $\mathcal{R}$ is assumed to be moving with an arbitrary translational velocity $\vec{V}_{\mathcal{R}/\mathcal{S}}$ and an arbitrary translational acceleration $\vec{a}_{\mathcal{R}/\mathcal{S}}$. $\mathcal{R}$ is also assumed to be rotating with an arbitrary angular velocity $\vec{\omega}_{\mathcal{R}/\mathcal{S}} = \vec{\omega}$ with respect to $\mathcal{S}$. Using these definitions and assuming there are no heat sources, it can be seen that the non-inertial Navier-Stokes equations as seen from an observer in the non-inertial reference frame $\mathcal{R}$ are:

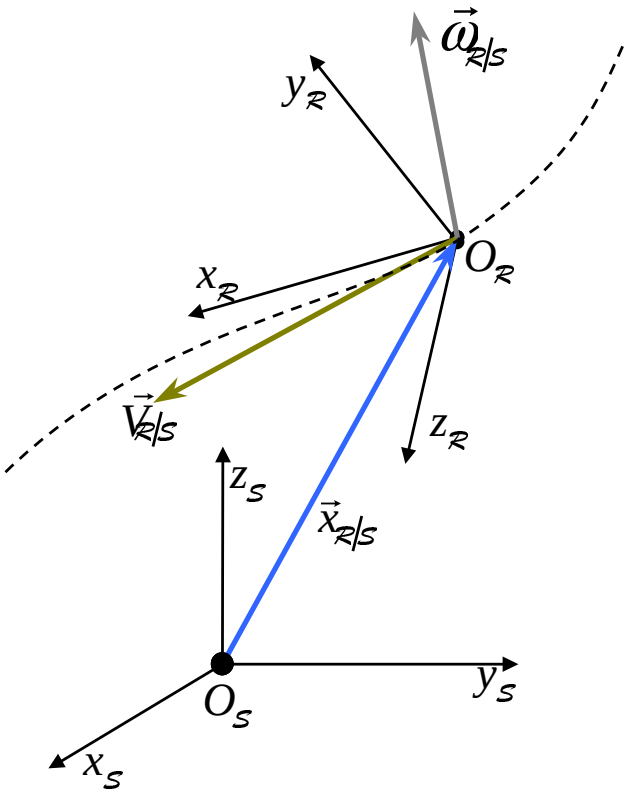

Figure 3.1: View of inertial coordinate system $\mathcal{S}$ and general non-inertial coordinate system $\mathcal{R}$

1. The Equation of Conservation of Mass or Continuity Equation:

$$\frac{\partial \rho}{\partial t} + \nabla \cdot \left(\rho \vec{V_{\mathcal{R}}} \right) = 0 \tag{3.1}$$

2. The equation of Conservation of Momentum

$$\frac{\partial \rho \vec{V_{\mathcal{R}}}}{\partial t} + \nabla \cdot \left[\rho \vec{V_{\mathcal{R}}} \otimes \vec{V_{\mathcal{R}}} + P \overrightarrow{\overrightarrow{I}} - \overrightarrow{\overrightarrow{\tau}} \right] = \rho \left[\vec{f} + \vec{\Omega} - 2\vec{\omega} \times \vec{V_{\mathcal{R}}} \right] \tag{3.2}$$

3. The Equation of Conservation of Energy

$$\frac{\partial \rho E_{\mathcal{R}}}{\partial t} + \nabla \cdot \left[\left(\rho E_{\mathcal{R}} + P \right) \vec{V_{\mathcal{R}}} - \overrightarrow{\overrightarrow{\tau}} \cdot \vec{V_{\mathcal{R}}} - k_T \nabla T \right] = \rho \left[\vec{f} + \vec{\Omega} \right] \cdot \vec{V_{\mathcal{R}}} \tag{3.3}$$

In equations (3.1)-(3.3) the variables are expressed in a Eulerian (local) way as seen from the non-inertial rotating frame $\mathcal{R}$. In this sense, $\vec{V_{\mathcal{R}}}$ is the local velocity of the

flow as seen from the rotating reference frame; ρ, P , T and e are the density, the static pressure, the temperature and the internal energy of the flow, respectively; $E_{\mathcal{R}}$ is the total energy (per unit of mass) as seen from the rotating frame:

$$E_{\mathcal{R}} = e + \frac{1}{2}\vec{V_{\mathcal{R}}} \cdot \vec{V_{\mathcal{R}}}. \tag{3.4}$$

$\vec{f}$ is net body force; $\vec{\Omega}$ is the "pseudo force vector":

$$\vec{\Omega} = -\vec{\omega} \times (\vec{\omega} \times \vec{x_{\mathcal{R}}}) - \frac{d_{\mathcal{R}}\vec{\omega}}{d_{\mathcal{R}}t} \times \vec{x_{\mathcal{R}}} - \vec{a}_{\mathcal{R}/\mathcal{S}}. \tag{3.5}$$

and contains the effect of the non-inertial motion (except for the Coriolis term $-2\vec{\omega} \times \vec{V_{\mathcal{R}}}$). $\vec{V} \otimes \vec{V}$ is a second order tensor defined in terms of its components in Cartesian coordinates as $\left[\vec{V} \otimes \vec{V}\right]_{ij} = \left[\vec{V}\right]_i \left[\vec{V}\right]_j$ where $\left[\vec{V}\right]_i$ is the i-th component of the velocity vector. $\overrightarrow{\overrightarrow{I}}$ is the identity tensor and $\overrightarrow{\overrightarrow{\tau}}$ is the stress tensor; each of these is a second order tensor. Equations (3.1)-(3.3) are a generalization of the equations presented in [23].

3.3 Notation Issues

From now on, unless otherwise specified, the subindex $\mathcal{R}$ will be dropped from all the physical quantities refered to the non-inertial frame $\mathcal{R}$. The convention also includes the geometric vectors such as the position vector $\vec{x}_{\mathcal{R}}$ and the unit vectors $\hat{e}_{x\mathcal{R}}, \hat{e}_{y\mathcal{R}}, \hat{e}_{z\mathcal{R}}$. So the vectors $\vec{x}_{\mathcal{R}}, \vec{V}_{\mathcal{R}}, \vec{\omega}$, and $\vec{\Omega}$, when resolved in terms of their components in the non-inertial frame $\mathcal{R}$ will be written simply as

$$\begin{aligned}
\vec{x} &= x\hat{e}_x + y\hat{e}_y + z\hat{e}_z, && (3.6)\\
\vec{V} &= u\hat{e}_x + v\hat{e}_y + w\hat{e}_z, && (3.7)\\
\vec{\omega} &= \omega_x\hat{e}_x + \omega_y\hat{e}_y + \omega_z\hat{e}_z, \quad \text{and} && (3.8)\\
\vec{\Omega} &= \Omega_x\hat{e}_x + \Omega_y\hat{e}_y + \Omega_z\hat{e}_z, && (3.9)
\end{aligned}$$

Following this convention, the non-inertial Navier-Stokes equations can be rewritten as:

1. The Equation of Conservation of Mass or Continuity Equation:

$$\frac{\partial \rho}{\partial t} + \nabla \cdot \left(\rho \vec{V}\right) = 0 \tag{3.10}$$

2. The equation of Conservation of Momentum

$$\frac{\partial \rho \vec{V}}{\partial t} + \nabla \cdot \left[\rho \vec{V} \otimes \vec{V} + P\overrightarrow{\overrightarrow{I}} - \overrightarrow{\overrightarrow{\tau}}\right] = \rho\left[\vec{f} + \vec{\Omega} - 2\vec{\omega} \times \vec{V}\right] \tag{3.11}$$

3. The Equation of Conservation of Energy

$$\frac{\partial \rho E}{\partial t} + \nabla \cdot \left[(\rho E + P)\, \vec{V} - \vec{\vec{\tau}} \cdot \vec{V} - k_T \nabla T \right] = \rho \left[\vec{f} + \vec{\Omega} \right] \cdot \vec{V} \tag{3.12}$$

with

$$E = e + \frac{1}{2} \vec{V} \cdot \vec{V} \tag{3.13}$$

$$\vec{\Omega} = -\vec{\omega} \times (\vec{\omega} \times \vec{x}) - \frac{d\vec{\omega}}{dt} \times \vec{x} - \vec{a}_{\mathcal{R}/\mathcal{S}} \tag{3.14}$$

3.4 Non-Dimensional Form of the Non-Inertial Navier-Stokes Equations

The form of the above equations remains unchanged if an appropiate non-dimensionalization is performed. As a consequence, equations (3.10)-(3.14) can also be considered as the non-dimensional non-inertial Navier-Stokes equations. For example, if the non-dimensional variables (denoted with an asterix: *) are defined in terms of reference (far-field) conditions (denoted with the "∞" symbol) and a reference length ℓ as:

$$\vec{V} = V_\infty \vec{V}^* \quad ; \quad \vec{x} = \ell \vec{x}^* \quad ; \quad t = \frac{\ell}{V_\infty} t^* \quad ; \quad \vec{\omega} = \frac{V_\infty}{\ell} \vec{\omega}^*$$

$$\rho = \rho_\infty \rho^* \quad ; \quad P = \rho_\infty V_\infty^2 P^* \quad ; \quad T = T_\infty T^* \quad ; \quad e = V_\infty^2 e^* \quad ; \quad \vec{f} = \frac{V_\infty^2}{\ell} \vec{f}^* \quad ; \quad \mu = \mu_\infty \mu^*$$

The non-dimensional equations are obtained simply by replacing each variable by its corresponding non-dimensional variable. Parameters including the viscosity coefficient μ, the thermal conduction coefficient k_T and the specific heat at constant volume c_v should be replaced by:

$$\mu \longrightarrow \frac{\mu^*}{Re_\infty}$$

$$k_T \longrightarrow \frac{k_T T_\infty}{\ell^2} \frac{1}{\rho_\infty V_\infty^2} \frac{\ell}{V_\infty} = \frac{\mu^*}{Re_\infty \,\mathrm{Pr}\, M_\infty^2 [\gamma - 1]}$$

$$c_v \longrightarrow \frac{c_v T_\infty}{V_\infty^2} = \frac{c_v \gamma R T_\infty}{\gamma [c_p - c_v] V_\infty^2} = \frac{c_v}{\gamma [c_p - c_v] M_\infty^2} = \frac{1}{\gamma [\gamma - 1] M_\infty^2}$$

where $Re_\infty = \frac{\rho_\infty V_\infty \ell}{\mu_\infty}$ is the Reynolds number, $\mathrm{Pr} = \frac{\mu c_p}{k_T}$ is the Prandtl number and $M_\infty = \frac{V_\infty}{a_\infty}$ is the Mach number.

3.5 Conservative Form of Non-Inertial Navier Stokes Equations

The non-inertial Navier Stokes equations (3.10)-(3.14) can be written in the Cartesian coordinate system x, y, z of the non-inertial reference frame $\mathcal{R}$ in the following compact form:

$$\frac{\partial Q}{\partial t} + \frac{\partial F}{\partial x} + \frac{\partial G}{\partial y} + \frac{\partial H}{\partial z} = W + \frac{\partial F_v}{\partial x} + \frac{\partial G_v}{\partial y} + \frac{\partial H_v}{\partial z} \tag{3.15}$$

where Q is defined as,

$$Q = \begin{bmatrix} Q_1 \\ Q_2 \\ Q_3 \\ Q_4 \\ Q_5 \end{bmatrix} = \begin{bmatrix} \rho \\ \rho u \\ \rho v \\ \rho w \\ \rho E \end{bmatrix}. \tag{3.16}$$

Here

$$F = \begin{bmatrix} \rho u \\ \rho u u + P \\ \rho u v \\ \rho u w \\ u\left(\rho E + P\right) \end{bmatrix} \quad ; \quad F_v = \begin{bmatrix} 0 \\ \tau_{xx} \\ \tau_{xy} \\ \tau_{xz} \\ \tau_{xx}u + \tau_{xy}v + \tau_{xz}w + k\frac{\partial T}{\partial x} \end{bmatrix} \tag{3.17}$$

$$G = \begin{bmatrix} \rho v \\ \rho v u \\ \rho v v + P \\ \rho v w \\ v\left(\rho E + P\right) \end{bmatrix} \quad ; \quad G_v = \begin{bmatrix} 0 \\ \tau_{yx} \\ \tau_{yy} \\ \tau_{yz} \\ \tau_{yx}u + \tau_{yy}v + \tau_{yz}w + k\frac{\partial T}{\partial y} \end{bmatrix} \tag{3.18}$$

$$H = \begin{bmatrix} \rho w \\ \rho w u \\ \rho w v \\ \rho w w + P \\ w\left(\rho E + P\right) \end{bmatrix} \quad ; \quad H_v = \begin{bmatrix} 0 \\ \tau_{zx} \\ \tau_{zy} \\ \tau_{zz} \\ \tau_{zx}u + \tau_{zy}v + \tau_{zz}w + k\frac{\partial T}{\partial z} \end{bmatrix} \tag{3.19}$$

are the components of the conservative and viscous fluxes; and W is given by:

$$W = \begin{bmatrix} 0 \\ \rho\left[f_x + \Omega_x\right] - 2\rho(\omega_y w - \omega_z v) \\ \rho\left[f_y + \Omega_y\right] - 2\rho(\omega_z u - \omega_x w) \\ \rho\left[f_z + \Omega_z\right] - 2\rho(\omega_x v - \omega_y u) \\ \rho\left[f_x + \Omega_x\right]u + \rho\left[f_y + \Omega_y\right]v + \rho\left[f_z + \Omega_z\right]w \end{bmatrix}. \tag{3.20}$$

In equation (3.20) the cross vector product $-2\rho\left(\vec{\omega}\times\vec{V}\right)$ and the vector $\vec{\Omega}$ have been expanded in their components using equations (3.6)-(3.9).

It is noteworthy to mention that the Navier-Stokes equations (3.15)-(3.20) are more general than the Navier-Stokes equations commonly used in turbomachinery [4] or rotor simulations [45]. In the Navier-Stokes equations (3.15)-(3.20) the non-inertial reference frame $\mathcal{R}$ is not only allowed to rotate at a (non-constant) angular velocity but it is also allowed to have a translational velocity and a translational acceleration.

An important thing to be noted here is that, except for the source term W, the functional form of the non-inertial Navier-Stokes equations (3.15)-(3.20) is the same as the functional form of the standard conservative equations defined for inertial reference frames. In particular, it is possible to develop a conservative formulation in terms of the conservative variables Q defined in equation (3.16).

Let's start by showing that all the physical variables and fluxes can be re-written in terms of the conservative variables Q. From equation (3.16) one gets that

$$\rho = Q_1 \tag{3.21}$$

$$u = Q_2/Q_1 \quad ; \quad v = Q_3/Q_1 \quad ; \quad w = Q_4/Q_1 \tag{3.22}$$

$$E = Q_5/Q_1 \tag{3.23}$$

$$e = \frac{Q_5}{Q_1} - \frac{1}{2}\left[\left(\frac{Q_2}{Q_1}\right)^2 + \left(\frac{Q_3}{Q_1}\right)^2 + \left(\frac{Q_4}{Q_1}\right)^2\right]. \tag{3.24}$$

According to the principles of thermodynamics the temperature can be given in terms of the internal energy and density, and as a consequence for any fluid, the temperature can also be written in terms of the conserved quantities Q_i. A similar fact is true for the static pressure P and the speed of sound a [1] since by the state equation, they are functions of the temperature and density only. In particular if the fluid is given by a (calorically perfect) gas one can write

$$e = c_v T \quad ; \quad P = (\gamma - 1)\,\rho e \quad ; \quad a = \sqrt{\gamma R T}, \tag{3.25}$$

$$V = \sqrt{u^2 + v^2 + w^2} \quad ; \quad M = \frac{V}{a}, \tag{3.26}$$

[1] The speed of sound $a = \sqrt{\left(\frac{\partial P}{\partial \rho}\right)_s}$ is also a thermodynamic property of the state of fluid.

and as a consequence:

$$T = \frac{Q_5}{c_v Q_1} - \frac{1}{2c_v}\left[\left(\frac{Q_2}{Q_1}\right)^2 + \left(\frac{Q_3}{Q_1}\right)^2 + \left(\frac{Q_4}{Q_1}\right)^2\right] \tag{3.27}$$

$$P = (\gamma - 1)\, Q_1 \left(\frac{Q_5}{Q_1} - \frac{1}{2}\left[\left(\frac{Q_2}{Q_1}\right)^2 + \left(\frac{Q_3}{Q_1}\right)^2 + \left(\frac{Q_4}{Q_1}\right)^2\right]\right) \tag{3.28}$$

$$E + \frac{P}{\rho} = \frac{\gamma Q_5}{Q_1} - \frac{(\gamma - 1)}{2}\left[\left(\frac{Q_2}{Q_1}\right)^2 + \left(\frac{Q_3}{Q_1}\right)^2 + \left(\frac{Q_4}{Q_1}\right)^2\right] \tag{3.29}$$

Using equations (3.21)-(3.29) one can write the conservative flux vectors as

$$F = \begin{bmatrix} Q_2 \\ Q_2 Q_2/Q_1 + (\gamma - 1)\left(Q_5 - \frac{1}{2Q_1}\left[Q_2^2 + Q_3^2 + Q_4^2\right]\right) \\ Q_2 Q_3/Q_1 \\ Q_2 Q_4/Q_1 \\ \frac{Q_2}{Q_1}\left(\gamma Q_5 - \frac{(\gamma-1)}{2Q_1}\left[Q_2^2 + Q_3^2 + Q_4^2\right]\right) \end{bmatrix} \tag{3.30}$$

$$G = \begin{bmatrix} Q_3 \\ Q_3 Q_2/Q_1 \\ Q_3 Q_3/Q_1 + (\gamma - 1)\left(Q_5 - \frac{1}{2Q_1}\left[Q_2^2 + Q_3^2 + Q_4^2\right]\right) \\ Q_3 Q_4/Q_1 \\ \frac{Q_3}{Q_1}\left(\gamma Q_5 - \frac{(\gamma-1)}{2Q_1}\left[Q_2^2 + Q_3^2 + Q_4^2\right]\right) \end{bmatrix} \tag{3.31}$$

$$H = \begin{bmatrix} Q_4 \\ Q_4 Q_2/Q_1 \\ Q_4 Q_3/Q_1 \\ Q_4 Q_4/Q_1 + (\gamma - 1)\left(Q_5 - \frac{1}{2Q_1}\left[Q_2^2 + Q_3^2 + Q_4^2\right]\right) \\ \frac{Q_2}{Q_1}\left(\gamma Q_5 - \frac{(\gamma-1)}{2Q_1}\left[Q_2^2 + Q_3^2 + Q_4^2\right]\right) \end{bmatrix} \tag{3.32}$$

In a similar way, the viscous fluxes F_v, G_v and H_v can be expressed as functions of the conservative quantities.

Equations (3.21)-(3.32) are identical to the functional relations of the thermodynamic variables and fluxes in terms of conservative varibles in inertial frames.

What happens with the source term W? Using equations (3.21)- (3.22) in (3.20), W can also be expressed in terms of the conservative variables (and the components of $\vec{f}$, Ω and $\vec{\omega}$) as:

$$W = \begin{bmatrix} 0 \\ Q_1 \left[f_x + \Omega_x \right] - 2(\omega_y Q_4 - \omega_z Q_3) \\ Q_1 \left[f_y + \Omega_y \right] - 2(\omega_z Q_2 - \omega_x Q_4) \\ Q_1 \left[f_z + \Omega_z \right] - 2(\omega_x Q_3 - \omega_y Q_2) \\ \left[f_x + \Omega_x \right] Q_2 + \left[f_y + \Omega_y \right] Q_3 + \left[f_z + \Omega_z \right] Q_4 \end{bmatrix} \tag{3.33}$$

3.6 Non-Inertial Euler Equations: Conservative Form

Under the assumption of inviscid flows ($\mu = 0$), the conservative form of the non-inertial Navier-Stokes equations (3.15) reduces to the conservative form of the non-inertial Euler equations:

$$\frac{\partial Q}{\partial t} + \frac{\partial F}{\partial x} + \frac{\partial G}{\partial y} + \frac{\partial H}{\partial z} = W \tag{3.34}$$

where Q, F, G, H and W remain unchanged:

$$Q = \begin{bmatrix} Q_1 \\ Q_2 \\ Q_3 \\ Q_4 \\ Q_5 \end{bmatrix} = \begin{bmatrix} \rho \\ \rho u \\ \rho v \\ \rho w \\ \rho E \end{bmatrix}, \tag{3.35}$$

$$F = \begin{bmatrix} \rho u \\ \rho u u + P \\ \rho u v \\ \rho u w \\ u \left(\rho E + P \right) \end{bmatrix} \quad ; \quad G = \begin{bmatrix} \rho v \\ \rho v u \\ \rho v v + P \\ \rho v w \\ v \left(\rho E + P \right) \end{bmatrix} \quad ; \quad H = \begin{bmatrix} \rho w \\ \rho w u \\ \rho w v \\ \rho w w + P \\ w \left(\rho E + P \right) \end{bmatrix} \tag{3.36}$$

$$W = \begin{bmatrix} 0 \\ \rho \left[f_x + \Omega_x \right] - 2\rho(\omega_y w - \omega_z v) \\ \rho \left[f_y + \Omega_y \right] - 2\rho(\omega_z u - \omega_x w) \\ \rho \left[f_z + \Omega_z \right] - 2\rho(\omega_x v - \omega_y u) \\ \rho \left[f_x + \Omega_x \right] u + \rho \left[f_y + \Omega_y \right] v + \rho \left[f_z + \Omega_z \right] w \end{bmatrix} \tag{3.37}$$

The relationships (3.21)-(3.29) between the physical variables and the conservative variables remain also unchanged.

3.7 Boundary Conditions for the Navier-Stokes or Euler Equations in Non-Inertial Reference Frames

The boundary conditions along solid walls for Navier-Stokes (viscous) flows are different from those for Euler flows. In the case of viscous flows, the velocity of the flow must vanish at the walls, while in the case of Euler flows, it is only required that the flow does not go through the wall, i.e.:

$$\vec{V} \cdot \hat{n} = 0. \tag{3.38}$$

In general, the boundary conditions applied at the far-field boundary are the same for Navier-Stokes and Euler flows. Many of the physical boundary conditions in external flows are a type of matching with given uniform far-field conditions Q_∞, i.e.:

$$\lim_{\|\vec{x}\| \to \infty} Q_{\mathcal{S}} = Q_{\mathcal{S}\infty}.$$

Here the subscript $\mathcal{S}$ indicates that the values of the flow variables at the far-field are defined as seen from the inertial frame $\mathcal{S}$.

Certain thermodynamic variables: density ρ, pressure P, temperature T, entropy s, internal energy e, and the speed of sound a are scalar quantities, they are independent of the reference frame. For these quantities one has that:

$$\lim_{\|\vec{x}\| \to \infty} f(\vec{x}) = f_\infty, \tag{3.39}$$

where f is replaced by any of the symbols $\{\rho, P, T, s, e, a\}$.

The only variables that require special care are the ones related to the flow velocity. The velocity of the flow depends on the reference frame, since it is a vector quantity. We are interested in the velocity of the flow as seen from the non-inertial reference frame $\mathcal{R}$:

$$\lim_{\|\vec{x}\| \to \infty} \vec{V}(\vec{x}) = \lim_{\|\vec{x}\| \to \infty} \left[\vec{V}_{\mathcal{S}}(\vec{x}) - \vec{V}_{\mathcal{R}/\mathcal{S}} - \vec{\omega} \times \vec{x} \right]$$

In the case where the unperturbed air is at rest in the inertial frame $\mathcal{S}$ the above equation simplifies to

$$\lim_{\|\vec{x}\| \to \infty} \vec{V}(\vec{x}) = \lim_{\|\vec{x}\| \to \infty} \left[-\vec{V}_{\mathcal{R}/\mathcal{S}} - \vec{\omega} \times \vec{x} \right], \tag{3.40}$$

which written in components reads:

$$\lim_{\|\vec{x}\| \to \infty} \begin{bmatrix} u \\ v \\ w \end{bmatrix} = \lim_{\|\vec{x}\| \to \infty} \begin{bmatrix} -u_{\mathcal{R}/\mathcal{S}} - (\omega_y z - \omega_z y) \\ -v_{\mathcal{R}/\mathcal{S}} - (\omega_z x - \omega_x z) \\ -w_{\mathcal{R}/\mathcal{S}} - (\omega_x y - \omega_y x) \end{bmatrix}. \tag{3.41}$$

From equations (3.39)-(3.41) and the definition (3.16) one can get the far-field conditions for the conservative variables:

$$\lim_{\|\vec{x}\|\to\infty} \begin{bmatrix} Q_1 \\ Q_2 \\ Q_3 \\ Q_4 \\ Q_5 \end{bmatrix} = \begin{bmatrix} \rho_\infty \\ \rho_\infty \left[-u_{\mathcal{R}/\mathcal{S}} - (\omega_y z - \omega_z y)\right] \\ \rho_\infty \left[-v_{\mathcal{R}/\mathcal{S}} - (\omega_z x - \omega_x z)\right] \\ \rho_\infty \left[-w_{\mathcal{R}/\mathcal{S}} - (\omega_x y - \omega_y x)\right] \\ \rho_\infty \left(c_v T_\infty + \frac{1}{2} \lim_{\|\vec{x}\|\to\infty} (u^2 + v^2 + w^2)\right) \end{bmatrix}$$

It must pointed out that in actual numerical calculations the matching with the far-field boundary conditions is done by using an appropiate combination of internal information of the current values of the flow state variables and external information obtained from the far-field values of the flow state variables. The far-field conditions are applied computationally at "large" $\|\vec{x}\|$ (e.g., when $\|\vec{x}\|$ equals 30 chord lengths).

3.8 Integral Equations of Flow Motion

Integrating the conservative form of the non-inertial Navier-Stokes equations around a finite volume τ enclosed by a surface σ one gets

$$\frac{\partial}{\partial t} \int_\tau Q \; d\tau + \int_\sigma \vec{F} \cdot \hat{n} \; d\sigma = \int_\tau W \; d\tau + \int_\sigma \vec{F}_v \cdot \hat{n} \; d\sigma \tag{3.42}$$

where $\hat{n}$ is the outward-pointing unit vector normal to the surface σ and where the vectors $\vec{F}$ and $\vec{F}_v$ are defined as:

$$\vec{F} = F\hat{e}_x + G\hat{e}_y + H\hat{e}_z \tag{3.43}$$

$$\vec{F}_v = F_v\hat{e}_x + G_v\hat{e}_y + H_v\hat{e}_z \tag{3.44}$$

Equation (3.42) is the integral form of the non-inertial Navier-Stokes equations and it is valid for general reference frames (inertial or non-inertial). The source term W contains the effects of non-inertial reference frames. In this sense W is identically zero for inertial reference frames.

In general, for practical applications the volumes τ are chosen to be polyhedrons, that is to say they are volumes enclosed by a closed union of planar surfaces σ_i. In such cases, the unit normal vectors are constant on each surface σ_i and equation (3.42) can be written as:

$$\frac{\partial}{\partial t} \int_\tau Q \; d\tau + \sum_{i=1}^{k} \int_{\sigma_i} \vec{F} \; d\sigma \cdot \hat{n}_i = \int_\tau W \; d\tau + \sum_{i=1}^{k} \int_{\sigma_i} \vec{F}_v \; d\sigma \cdot \hat{n}_i \tag{3.45}$$

where $\hat{n}_i$ is the unit vector normal to the surface σ_i and k is the total number of surfaces σ_i.

Defining the flux averages over the surfaces σ_i:

$$\vec{F}^{\sigma_i} = \frac{1}{\sigma_i}\int_{\sigma_i} \vec{F}\ d\sigma \quad \text{and} \quad \vec{F}_v^{\sigma_i} = \frac{1}{\sigma_i}\int_{\sigma_i} \vec{F}_v\ d\sigma$$

and defining the volume averages of Q and W as:

$$Q^\tau = \frac{1}{\tau}\int_\tau Q\ d\tau$$

$$W^\tau = \frac{1}{\tau}\int_\tau W\ d\tau,$$

it follows that equation (3.45) can be re-written simply as

$$\tau\frac{\partial Q^\tau}{\partial t} + \sigma_i \sum_{i=1}^{k} \vec{F}^{\sigma_i}\cdot\hat{n}_i = \tau W^\tau + \sigma_i \sum_{i=1}^{k} \vec{F}_v^{\sigma_i}\cdot\hat{n}_i\ . \tag{3.46}$$

If the flow variables are assumed to be constant over each surface σ_i then one can write:

$$\vec{F}^{\sigma_i} = \vec{F}(\vec{x}_{im}) \quad \text{and} \quad \vec{F}_v^{\sigma_i} = \vec{F}_v(\vec{x}_{im})$$

where $\vec{x}_{im}$ denotes the centroid of the surface σ_i. Using this assumption, equation (3.46) can be further simplified to

$$\tau\frac{\partial Q^\tau}{\partial t} + \sigma_i \sum_{i=1}^{k} \vec{F}(\vec{x}_{im})\cdot\hat{n}_i = \tau W^\tau + \sigma_i \sum_{i=1}^{k} \vec{F}_v(\vec{x}_{im})\cdot\hat{n}_i\ . \tag{3.47}$$

3.9 Flow Equations for Aerodynamically Steady Motions

In the previous sections the boundary value problem (flow equations+boundary conditions) which defines the flow properties as seen from a non-inertial reference frame $\mathcal{R}$ was determined. The reference frame $\mathcal{R}$ was assumed to be moving with an arbitrary translational acceleration $\vec{a}_{R/S}$ and rotating with an arbitrary angular velocity $\vec{\omega}$ with respect to an inertial reference frame $\mathcal{S}$. In this section, the flow equations for aerodynamically steady motions will be determined by imposing the associated mathematical conditions into the non-inertial flow equations.

3.9.1 Summary of Needed Relationships

First, the reference frames $\mathcal{R}$ will be restricted to the one fixed to the aircraft. This restriction implies that we can identify the vector position $\vec{x}_{\mathcal{R}/\mathcal{S}}$ of the origin of reference frame $\mathcal{R}$ with the vector position $\vec{x}_c$ of the aircraft. Then:

$$\vec{x}_{\mathcal{R}/\mathcal{S}} = \vec{x}_c \tag{3.48}$$

$$\vec{V}_{\mathcal{R}/\mathcal{S}} = \vec{V}_c \tag{3.49}$$

$$\vec{a}_{\mathcal{R}/\mathcal{S}} = \vec{a}_c = \frac{d_{\mathcal{S}}\vec{V}_c}{d_{\mathcal{S}}t} \tag{3.50}$$

Also, the angular velocity components ω_x, ω_y and ω_z can be identified with the standard flight mechanics angular velocity components p, q and r of the aircraft:

$$\omega_x = p \qquad \omega_y = q \qquad \omega_z = r \tag{3.51}$$

Now, since the aircraft will be forced to move in an aerodymically steady motion, the following conditions apply:

$$\frac{d\vec{\omega}}{dt} = \vec{0} \tag{3.52}$$

and

$$\frac{d_{\mathcal{S}}\vec{V}_c}{d_{\mathcal{S}}t} = \vec{\omega} \times \vec{V}_c \tag{3.53}$$

3.9.2 Euler Equations for Aerodynamically Steady Motions

Imposing equations (3.48)-(3.53) into the non-inertial Euler Equations defined in Section 3.6, it follows that the conservative form of the aerodynamically steady Euler Equations are given by

$$\frac{\partial Q}{\partial t} + \frac{\partial F}{\partial x} + \frac{\partial G}{\partial y} + \frac{\partial H}{\partial z} = W \tag{3.54}$$

with Q, F, G , H unchanged:

$$Q = \begin{bmatrix} Q_1 \\ Q_2 \\ Q_3 \\ Q_4 \\ Q_5 \end{bmatrix} = \begin{bmatrix} \rho \\ \rho u \\ \rho v \\ \rho w \\ \rho E \end{bmatrix}, \tag{3.55}$$

$$F = \begin{bmatrix} \rho u \\ \rho uu + P \\ \rho uv \\ \rho uw \\ u\left(\rho E + P\right) \end{bmatrix} \quad ; \quad G = \begin{bmatrix} \rho v \\ \rho vu \\ \rho vv + P \\ \rho vw \\ v\left(\rho E + P\right) \end{bmatrix} \quad ; \quad H = \begin{bmatrix} \rho w \\ \rho wu \\ \rho wv \\ \rho ww + P \\ w\left(\rho E + P\right) \end{bmatrix} \tag{3.56}$$

Except that $\vec{\Omega}$ and W are now given by:

$$\vec{\Omega} = -\vec{\omega} \times \left(\vec{\omega} \times \vec{x}\right) - \vec{\omega} \times \vec{V}_c \tag{3.57}$$

$$W = \begin{bmatrix} 0 \\ \rho\left[f_x + \Omega_x\right] - 2\rho(qw - rv) \\ \rho\left[f_y + \Omega_y\right] - 2\rho(ru - pw) \\ \rho\left[f_z + \Omega_z\right] - 2\rho(pv - qu) \\ \rho\left[f_x + \Omega_x\right] u + \rho\left[f_y + \Omega_y\right] v + \rho\left[f_z + \Omega_z\right] w \end{bmatrix} \tag{3.58}$$

From the definition (3.55) of the conservative variables Q and the definitions of the conservative fluxes (3.56), it follows that is still possible to write all the fluxes components as explicit functions of Q. In particular the expressions (3.30)-(3.32) are still valid for flows corresponding to aerodynamically steady motions. The same is true for the source term which can be written as:

$$W = \begin{bmatrix} 0 \\ Q_1\left[f_x + \Omega_x\right] - 2(qQ_4 - rQ_3) \\ Q_1\left[f_y + \Omega_y\right] - 2(rQ_2 - pQ_4) \\ Q_1\left[f_z + \Omega_z\right] - 2(pQ_3 - qQ_2) \\ \left[f_x + \Omega_x\right] Q_2 + \left[f_y + \Omega_y\right] Q_3 + \left[f_z + \Omega_z\right] Q_4 \end{bmatrix} \tag{3.59}$$

Note: Observe that the pseudo force vector $\vec{\Omega}$ can be expanded in its components as:

$$\begin{bmatrix} \Omega_x \\ \Omega_y \\ \Omega_z \end{bmatrix} = \begin{bmatrix} -p\left(px + qy + rz\right) + x\left(p^2 + q^2 + r^2\right) - \left(qw_c - rv_c\right) \\ -q\left(px + qy + rz\right) + y\left(p^2 + q^2 + r^2\right) - \left(ru_c - pw_c\right) \\ -r\left(px + qy + rz\right) + z\left(p^2 + q^2 + r^2\right) - \left(pv_c - qu_c\right) \end{bmatrix} \tag{3.60}$$

or as:

$$\begin{bmatrix} \Omega_x \\ \Omega_y \\ \Omega_z \end{bmatrix} = \begin{bmatrix} -p\left(qy + rz\right) + x\left(q^2 + r^2\right) - \left(qw_c - rv_c\right) \\ -q\left(px + rz\right) + y\left(p^2 + r^2\right) - \left(ru_c - pw_c\right) \\ -r\left(px + qy\right) + z\left(p^2 + q^2\right) - \left(pv_c - qu_c\right) \end{bmatrix} \tag{3.61}$$

3.9.3 Navier-Stokes Equations for Aerodynamically Steady Motions

The Navier-Stokes equations for the determination of flows around an aircraft moving in a general aerodynamically steady motion can be obtained by imposing equations (3.48)-(3.53) into the non-inertial Navier-Stokes equations defined in Section 3.5. The resulting aerodynamically steady Navier-Stokes equations are still given by:

$$\frac{\partial Q}{\partial t}+\frac{\partial F}{\partial x}+\frac{\partial G}{\partial y}+\frac{\partial H}{\partial z}=W+\frac{\partial F_v}{\partial x}+\frac{\partial G_v}{\partial y}+\frac{\partial H_v}{\partial z}$$

with the expressions for the conservative variables, the inviscid fluxes and the viscous fluxes unchanged. The only difference being that W and the components of $\vec{\Omega}$ are now given by:

$$W=\begin{bmatrix} 0 \\ \rho\left[f_x+\Omega_x\right]-2\rho(qw-rv) \\ \rho\left[f_y+\Omega_y\right]-2\rho(ru-pw) \\ \rho\left[f_z+\Omega_z\right]-2\rho(pv-qu) \\ \rho\left[f_x+\Omega_x\right]u+\rho\left[f_y+\Omega_y\right]v+\rho\left[f_z+\Omega_z\right]w \end{bmatrix}$$

and

$$\begin{bmatrix} \Omega_x \\ \Omega_y \\ \Omega_z \end{bmatrix}=\begin{bmatrix} -p\left(qy+rz\right)+x\left(q^2+r^2\right)-\left(qw_c-rv_c\right) \\ -q\left(px+rz\right)+y\left(p^2+r^2\right)-\left(ru_c-pw_c\right) \\ -r\left(px+qy\right)+z\left(p^2+q^2\right)-\left(pv_c-qu_c\right) \end{bmatrix},$$

respectively.

3.9.4 Boundary Conditions for Aerodynamically Steady Flows

Using again equations (3.48)-(3.53) the far-field boundary conditions can be written as:

$$\lim_{\|\vec{x}\|\to\infty} f(\vec{x})=f_\infty, \tag{3.62}$$

for scalar quantities such as $f=\{\rho,P,T,s,e,a\}$. The boundary condition for the components of the flow velocity can be written as

$$\lim_{\|\vec{x}\|\to\infty}\begin{bmatrix} u \\ v \\ w \end{bmatrix}=\lim_{\|\vec{x}\|\to\infty}\begin{bmatrix} -u_c-(qz-ry) \\ -v_c-(rx-pz) \\ -w_c-(py-qx) \end{bmatrix}. \tag{3.63}$$

For viscous flows, the velocity must vanish at solid walls. On the other hand, if the flow is inviscid (Euler equations) the flow velocity must satisfy the non-penetration condition:

$$\vec{V}\cdot\hat{n}=0\Longrightarrow un_x+vn_y+wn_z=0 \tag{3.64}$$

Chapter 4

Two-Dimensional Aerodynamically Steady Flows

In this chapter the two-dimensional numerical implementation of the aerodynamic mathematical model will be presented.

4.1 Airfoils in Rectilinear Steady Motion

4.1.1 Two-Dimensional Euler Equations

Consider an airfoil (wing of infinite span) moving in a rectilinear motion through the air at constant speed V_c and at constant angle of attack α, (with no sideslip angle and no angular rates) as shown in Figure (2.5).

Following the usual convention and as shown in Figure (4.1), the body-fixed coordinate system $\mathcal{R}$ is chosen such that the $z_{\mathcal{R}}$-axis points in the direction of the span and the $x_{\mathcal{R}}, y_{\mathcal{R}}$ axes form the plane of the airfoil. The $x_{\mathcal{R}}$-axis is chosen to be along the chord of the airfoil. As seen from $\mathcal{R}$, this rectilinear motion corresponds to a two-dimensional uniform steady flow passing around the airfoil.

Since the problem is two-dimensional the only aerodynamic forces and moments that have to be considered are the lift L, the drag D and the pitching moment $\hat{M}$. For the class of rectilinear motions defined above these three aerodynamic forces and their corresponding non-dimensional coefficients C_ℓ, C_d and C_m can be represented in terms of the steady aerodynamic function $\overline{F}$ of equation (2.18) as:

$$\mathcal{F} = \overline{F}\,(V_c, \alpha, 0, 0, 0, 0) \tag{4.1}$$

Assuming the flow is inviscid, these aerodynamic forces can be determined by an ap-

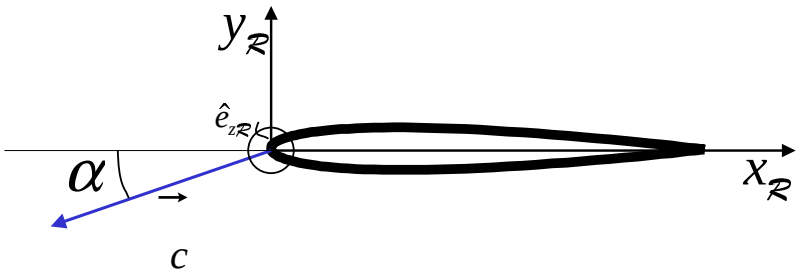

Figure 4.1: Body-fixed coordinate system $\mathcal{R}$ for an airfoil flying at constant velocity $\vec{V}_c$ and at constant angle of attack α

propiate integration of the static pressure P along the airfoil's surface σ_a:

$$L = -\left(\int_{\sigma_a} P\hat{n}\, d\sigma\right) \cdot \hat{e}_L \tag{4.2}$$

$$D = -\left(\int_{\sigma_a} P\hat{n}\, d\sigma\right) \cdot \hat{e}_D \tag{4.3}$$

$$\hat{M} = -\left(\int_{\sigma_a} \vec{x} \times P\hat{n}\, d\sigma\right) \cdot \hat{e}_z \tag{4.4}$$

where $\hat{e}_L = -\sin\alpha\hat{e}_x + \cos\hat{e}_y$ and $\hat{e}_D = \cos\alpha\hat{e}_x + \sin\alpha\hat{e}_y$.

The static pressure can be determined by solving the standard (inertial) 2D-Euler Equations:

$$\frac{\partial Q}{\partial t} + \frac{\partial F}{\partial x} + \frac{\partial G}{\partial y} = 0 \tag{4.5}$$

where the matrix vector of conservative variables Q and the flux components F and G are given by:

$$Q = \begin{bmatrix} Q_1 \\ Q_2 \\ Q_3 \\ Q_4 \end{bmatrix} = \begin{bmatrix} \rho \\ \rho u \\ \rho v \\ \rho E \end{bmatrix}; \quad F = \begin{bmatrix} \rho u \\ \rho uu + P \\ \rho uv \\ u\left(\rho E + P\right) \end{bmatrix}; \quad G = \begin{bmatrix} \rho v \\ \rho vu \\ \rho vv + P \\ v\left(\rho E + P\right) \end{bmatrix} \tag{4.6}$$

Assuming the air behaves as a perfect gas the total energy E and P are related to the internal energy e, the temperature T, the speed of sound a, the flow velocity V and the Mach number M through:

$$a^2 = \gamma RT; \quad M = \frac{V}{a}; \quad P = \rho RT = \frac{1}{\gamma}\rho a^2 \tag{4.7}$$

$$e = \frac{P}{(\gamma - 1)\,\rho} = \frac{1}{(\gamma - 1)\,\gamma} a^2; \quad E = e + \frac{1}{2}\left(u^2 + v^2\right) \tag{4.8}$$

4.1.2 Boundary Conditions

Equation (4.5) must be solved with appropriate boundary conditions. At the airfoil, the condition of non-penetration ($\vec{V} \cdot \hat{n} = 0 \Longrightarrow u n_x + v n_y = 0$) must be imposed.

The far-field conditions for the flow velocity can be determined from the fact that the airfoil is moving with a velocity $\vec{V_c}$ with respect to the air. Then, the flow velocity $\vec{V_\infty}$ at the far-field as seen from the body-fixed reference frame $\mathcal{R}$ is:

$$\vec{V_\infty} = \lim_{\|\vec{x}\| \longrightarrow \infty} \vec{V}(\vec{x}) = -\vec{V_c}$$

From Figure (4.1), the components of $\vec{V_c}$ in the body-fixed axis are given by:

$$\vec{V_c} = -V_c \cos\alpha \hat{e}_x - V_c \sin\alpha \hat{e}_y$$

or in matrix-form:

$$\begin{bmatrix} u_c \\ v_c \end{bmatrix} = \begin{bmatrix} -V_c \cos\alpha \\ -V_c \sin\alpha \end{bmatrix} \tag{4.9}$$

As a consequence, it follows that the far-field conditions for the flow velocity components are:

$$\begin{bmatrix} u_\infty(x,y) \\ v_\infty(x,y) \end{bmatrix} = \lim_{\|\vec{x}\| \longrightarrow \infty} \begin{bmatrix} u(x,y) \\ v(x,y) \end{bmatrix} = \begin{bmatrix} V_c \cos\alpha \\ V_c \sin\alpha \end{bmatrix} \tag{4.10}$$

The other far-field boundary conditions are applied to all the scalar flow quantities and simply consist in the matching with the free-stream conditions: $\lim_{\|\vec{x}\| \longrightarrow \infty} f(x,y) = f_\infty$ where $f = \{\rho, P, T, s, e, a\}$.

4.1.3 Numerical Results

A standard 2D-CFD code for external flows can be used to solve the above flow equations. Examples of the numerical solutions obtained using CFD are shown in Figures (2.6), (4.2) and (4.3) for a NACA 0012 airfoil. The general streamlines pattern and the pressure coefficient contours corresponding to a Mach number of flight $M_c = 0.2$ and at angle of attack $\alpha = 0^o$ are shown in Figure (2.6). In Figures (4.2) and (4.3) are shown the flow solutions for the same airfoil and the same angle of attack but at other Mach numbers (i.e speeds). Figure (4.2) corresponds to $M_c = 0.5$ and Figure (4.3) corresponds to $M_c = 0.8$.

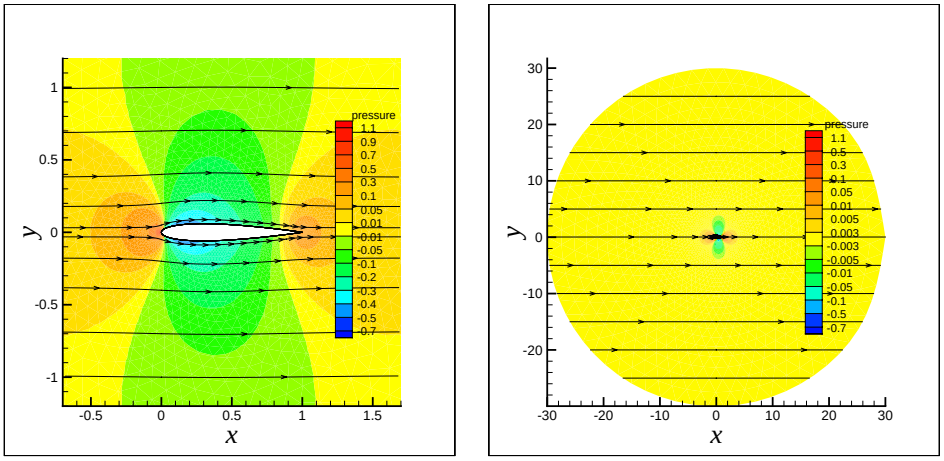

(a) Close-view, Mach $M_c = 0.5$ (b) Wide-view, Mach $M_c = 0.5$

Figure 4.2: Pressure contours and velocity streamlines for the air passing around an airfoil which is in a steady rectilinear uniform flight at Mach $M_c = 0.5$, $\alpha = 0^o$.

The flow solutions were obtained using the `Class Code` provided by Dr. Kyle Anderson. The `Class Code` solves the inviscid flow equations using a finite-volume formulation [55]. The formulation uses an implicit, time-marching, iterative, node-centered scheme [24], [48]. The fluxes can be evaluated at the faces using Van Leer flux splitting [54] or the Roe difference scheme [44]. The method is second order, since it uses a second-order approximation of the flow variables at the faces.

Something that must be noted from the obtained solutions is the behavior of the flow variables at the far field. The far-field behavior is shown in Figure (4.2)-(b) for the $M_c = 0.5$ case and in Figure (4.3)-(b) for the $M_c = 0.8$ case. From these Figures it can be seen that the pressure coefficient

$$C_p = \frac{P - P_\infty}{\frac{1}{2}\rho_\infty V_\infty^2} = \frac{P - P_\infty}{\frac{1}{2}\gamma P_\infty M_c^2} \tag{4.11}$$

goes to zero at the far-field, i.e. the pressure P matches with the free-stream condition P_∞. Also, as expected, it can be seen that the streamlines tend to be straight lines since in the simulation the airfoil is flying in a rectilinear motion.

Finally, observe that the aerodynamic forces can be determined from the obtained pressure distributions by using equations (4.2)-(4.4). From the symmetry, it follows that for the cases shown in Figures (2.6), (4.2) and (4.3): $C_\ell = 0.0$ and $C_m = 0.0$. By running the CFD code at different Mach numbers M and different angles of attack α the three set of functions

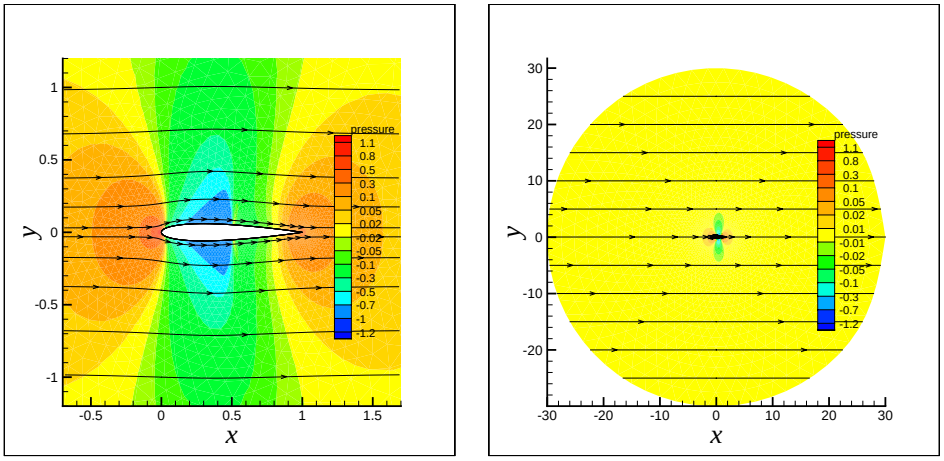

(a) Close-view, Mach $M_c = 0.8$ (b) Wide-view, Mach $M_c = 0.8$

Figure 4.3: Pressure contours and velocity streamlines for the air passing around an airfoil which is in a steady rectilinear uniform flight at Mach $M_c = 0.8$, $\alpha = 0^o$.

can be constructed:

$$\begin{aligned} C_\ell &= \overline{C}_\ell(M, \alpha) \\ C_d &= \overline{C}_d(M, \alpha) \\ C_m &= \overline{C}_m(M, \alpha) \end{aligned} \tag{4.12}$$

4.2 Airfoils in Planar Aerodynamically Steady Motion

4.2.1 Two-Dimensional Aerodynamically Steady Euler Equations

In a general planar motion, the three functions that describe the airfoil motion are $\overline{V}_c(t), \overline{\alpha}(t)$ and the pitch-rate $\overline{q}(t)$. The dependence of the aerodynamic forces on the pitch rate can not be obtained from the equations (4.12). As discussed in Chapters 2 and 3, this dependence can only be determined by calculating the aerodynamic forces acting on a more general class of aerodynamically steady motions: circular motions as the one shown in Figure (4.4). For the present case of the airfoil problem, the body-fixed coordinate system $\mathcal{R}$ is chosen such that the z_R-axis is perpendicular to the plane of the airfoil (see Figure (4.4)). This choice implies that the angular velocity vector $\vec{\omega}$ can be written as

$$\vec{\omega} = q\hat{e}_z \tag{4.13}$$

where q defines the pitch-rate (positive nose-down). In Figure (4.4) it can also be observed how the coordinate system $\mathcal{R}$ moves with respect to the inertial reference frame. It is clear

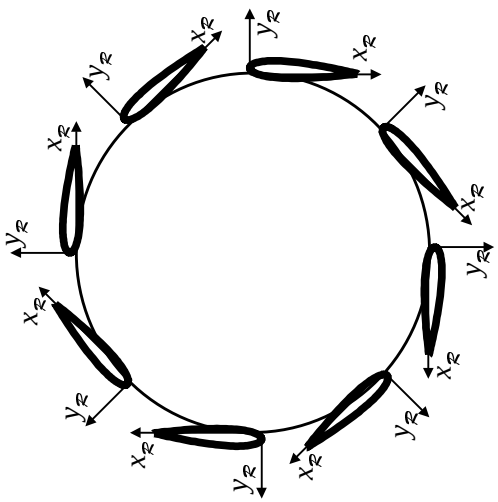

Figure 4.4: Airfoil flying in a steady circular motion. Also shown is the motion of the body-fixed reference frame $\mathcal{R}$

from the figure that $\mathcal{R}$ is rotating and has a translational acceleration which implies that it is a non-inertial reference frame.

For the numerical determination of the aerodynamic forces along these planar aerodynamically steady motions, the flow equations derived in Section 3.9 must be used. The aerodynamically steady Euler equations (3.54) for the two-dimensional case reduce to:

$$\frac{\partial Q}{\partial t} + \frac{\partial F}{\partial x} + \frac{\partial G}{\partial y} = W \tag{4.14}$$

where Q is the matrix vector of conservative variables:

$$Q = \begin{bmatrix} Q_1 \\ Q_2 \\ Q_3 \\ Q_4 \end{bmatrix} = \begin{bmatrix} \rho \\ \rho u \\ \rho v \\ \rho E \end{bmatrix}, \tag{4.15}$$

F and G are the components of the conservative fluxes:

$$F = \begin{bmatrix} \rho u \\ \rho u u + P \\ \rho u v \\ u\left(\rho E + P\right) \end{bmatrix}; \quad G = \begin{bmatrix} \rho v \\ \rho v u \\ \rho v v + P \\ v\left(\rho E + P\right) \end{bmatrix}. \tag{4.16}$$

E is the total energy as seen from the rotating body-fixed reference frame and the source

term W is given by[1]:

$$W = \begin{bmatrix} 0 \\ \rho\Omega_x - 2\rho(\vec{\omega} \times \vec{V})_x \\ \rho\Omega_y - 2\rho(\vec{\omega} \times \vec{V})_y \\ \rho\Omega_x u + \rho\Omega_y v \end{bmatrix} = \begin{bmatrix} 0 \\ \rho\Omega_x + 2\rho q v \\ \rho\Omega_y - 2\rho q u \\ \rho\Omega_x u + \rho\Omega_y v \end{bmatrix} \tag{4.17}$$

where

$$\begin{bmatrix} \Omega_x \\ \Omega_y \\ \Omega_z \end{bmatrix} = -\vec{\omega} \times (\vec{\omega} \times \vec{x}) - \vec{\omega} \times \vec{V_c} = \begin{bmatrix} q^2 x - q V_c \sin\alpha \\ q^2 y + q V_c \cos\alpha \\ 0 \end{bmatrix} \tag{4.18}$$

Equations (4.14)-(4.18) have been derived from equations (3.54)-(3.61) after the following steps:

1. Setting $w = 0$
2. Zeroing any dependence with respect to z, in particular $\frac{\partial H}{\partial z} = 0$
3. Setting $p = q = 0$ and using q instead of r.
4. Making note that for this case

$$\begin{bmatrix} u_c \\ v_c \\ w_c \end{bmatrix} = \begin{bmatrix} -V_c \cos\alpha \\ -V_c \sin\alpha \\ 0 \end{bmatrix} \tag{4.19}$$

Inserting equations (4.15)-(4.17) into the 2D aerodynamically steady Euler equations (4.14), one gets that:

$$\frac{\partial}{\partial t}\begin{bmatrix} \rho \\ \rho u \\ \rho v \\ \rho E \end{bmatrix} + \frac{\partial}{\partial x}\begin{bmatrix} \rho u \\ \rho u u + P \\ \rho u v \\ u\left(\rho E + P\right) \end{bmatrix} + \frac{\partial}{\partial y}\begin{bmatrix} \rho v \\ \rho v u \\ \rho v v + P \\ v\left(\rho E + P\right) \end{bmatrix} = \begin{bmatrix} 0 \\ \rho\Omega_x + 2\rho q v \\ \rho\Omega_y - 2\rho q u \\ \rho\Omega_x u + \rho\Omega_y v \end{bmatrix} \tag{4.20}$$

which is the expanded form of the 2D aerodynamically steady Euler equations.

4.2.2 Relationships between physical variables

The relationships between the static pressure P, the internal energy e, the temperature T , the speed of sound a, the flow velocity V and the Mach number M are the same as in the 3D case:

$$a^2 = \gamma R T \tag{4.21}$$

[1] assuming there are no external forces

$$M = \frac{V}{a} \tag{4.22}$$

$$P = \rho RT = \frac{1}{\gamma}\rho a^2 \tag{4.23}$$

$$e = \frac{P}{(\gamma - 1)\,\rho} = \frac{1}{(\gamma - 1)\,\gamma}a^2 \tag{4.24}$$

The expression for the total energy simplifies to:

$$E = e + \frac{1}{2}\left(u^2 + v^2\right) \tag{4.25}$$

because of the fact that $w = 0$. Observe that expressions (4.21)-(4.25) are exactly the same as the ones corresponding to the standard (inertial) relationships defined in equations (4.7)-(4.8).

4.2.3 Boundary Conditions

At the airfoil the non-penetration condition must be imposed:

$$\vec{V} \cdot \hat{n} = 0 \Longrightarrow un_x + vn_y = 0 \tag{4.26}$$

The far-field boundary conditions for the scalar quantities are simply the matching with the unperturbed air:

$$\lim_{\|\vec{x}\| \longrightarrow \infty} f(x, y) = f_\infty \tag{4.27}$$

where $f = \{\rho, P, T, s, e, a\}$.

The far-field conditions for the velocity vector $\vec{V}$ of the flow as seen from the rotating non-inertial body-fixed reference frame $\mathcal{R}$ can be obtained from the relationship between the velocity vector $\vec{V}$ and the velocity vector $\vec{V}_\mathcal{S}$ of the flow as seen from the inertial frame $\mathcal{S}$.

$$\vec{V}_\mathcal{S}(\vec{x}) = \vec{V}(\vec{x}) + \vec{V}_c + \vec{\omega} \times \vec{x}$$

Using that the unperturbed air is at rest at the inertial reference frame $\mathcal{S}$ ($\lim_{\|\vec{x}\| \to \infty} \vec{V}_\mathcal{S}(\vec{x}) = 0$), it follows that:

$$\lim_{\|\vec{x}\| \longrightarrow \infty} \vec{V}(\vec{x}) = -\vec{V}_c - \lim_{\|\vec{x}\| \longrightarrow \infty} \vec{\omega} \times \vec{x} = V_c \cos\alpha \hat{e}_x + V_c \sin\alpha \hat{e}_y - \lim_{\|\vec{x}\| \longrightarrow \infty} (qx\hat{e}_y - qy\hat{e}_x)$$

which can be writen in components as:

$$\begin{bmatrix} u_\infty(x, y) \\ v_\infty(x, y) \end{bmatrix} = \lim_{\|\vec{x}\| \longrightarrow \infty} \begin{bmatrix} u(x, y) \\ v(x, y) \end{bmatrix} = \begin{bmatrix} V_c \cos\alpha \\ V_c \sin\alpha \end{bmatrix} + \lim_{\|\vec{x}\| \longrightarrow \infty} \begin{bmatrix} qy \\ -qx \end{bmatrix}. \tag{4.28}$$

Note that equation (4.28) could also have been obtained by restricting equation (3.63) to the two-dimensional case.

Using equations (4.27) and (4.28) into relationships (4.21)-(4.25) it follows that at the far-field one must have that

$$a_\infty^2 = \gamma R T_\infty \tag{4.29}$$

$$M_\infty(x,y) = \frac{V_\infty(x,y)}{a_\infty} \tag{4.30}$$

$$P_\infty = \frac{1}{\gamma}\rho_\infty a_\infty^2 \tag{4.31}$$

$$e_\infty = \frac{P_\infty}{(\gamma-1)\,\rho_\infty} = \frac{1}{(\gamma-1)\,\gamma}a_\infty^2 \tag{4.32}$$

$$E_\infty(x,y) = e_\infty + \frac{1}{2}\left(u_\infty^2(x,y) + v_\infty^2(x,y)\right) = e_\infty + \frac{1}{2}\left(-u_c + qy\right)^2 + \frac{1}{2}\left(-v_c - qx\right)^2 \tag{4.33}$$

4.3 A Consistency Check

One expects that the "unperturbed flow":

$$\rho = \rho_\infty, P = P_\infty, u = -u_c + qy, v = -v_c - qx, e = e_\infty,$$

$$E = e_\infty + \frac{1}{2}\left(-u_c + qy\right)^2 + \frac{1}{2}\left(-v_c - qx\right)^2$$

defined when there are no internal obstacles must be solution of the 2D aerodynamically steady Euler equations:

$$\frac{\partial}{\partial t}\begin{bmatrix}\rho\\ \rho u\\ \rho v\\ \rho E\end{bmatrix} + \frac{\partial}{\partial x}\begin{bmatrix}\rho u\\ \rho u u + P\\ \rho u v\\ u\left(\rho E + P\right)\end{bmatrix} + \frac{\partial}{\partial y}\begin{bmatrix}\rho v\\ \rho v u\\ \rho v v + P\\ v\left(\rho E + P\right)\end{bmatrix} = \begin{bmatrix}0\\ \rho\Omega_x + 2\rho q v\\ \rho\Omega_y - 2\rho q u\\ \rho\Omega_x u + \rho\Omega_y v\end{bmatrix}. \tag{4.34}$$

That the "unperturbed flow" is in fact a solution of equation (4.34) can be proved as follows. Using that in this case ρ, u, v and E are time-invariant and that ρ and P are constants the LHS of equation (4.34) reduces to

$$\begin{bmatrix}\rho\left(\partial u/\partial x\right) + \rho\left(\partial v/\partial y\right)\\ \rho\left(\partial u^2/\partial x\right) + \rho\left(\partial uv/\partial y\right)\\ \rho\left(\partial uv/\partial x\right) + \rho\left(\partial v^2/\partial y\right)\\ \left(\rho E + P\right)\left(\partial u/\partial x\right) + u\rho\left(\partial E/\partial x\right) + \left(\rho E + P\right)\left(\partial v/\partial y\right) + v\rho\left(\partial E/\partial y\right)\end{bmatrix}.$$

So after some simplification one can rewrite equation (4.34) as

$$\begin{bmatrix} (\partial u/\partial x + \partial v/\partial y) \\ (\partial u^2/\partial x + \partial uv/\partial y) \\ (\partial uv/\partial x + \partial v^2/\partial y) \\ (E + P/\rho)(\partial u/\partial x + \partial v/\partial y) + u(\partial E/\partial x) + v(\partial E/\partial y) \end{bmatrix} = \begin{bmatrix} 0 \\ \Omega_x + 2qv \\ \Omega_y - 2qu \\ \Omega_x u + \Omega_y v \end{bmatrix}. \quad (4.35)$$

Since

$$\frac{\partial u}{\partial x} + \frac{\partial v}{\partial y} = \frac{\partial (qy)}{\partial x} + \frac{\partial (-qx)}{\partial y} = 0$$

The equation in the first row of (4.35) holds. Let's consider the LHS of the equation in the second row:

$$\frac{\partial u^2}{\partial x} + \frac{\partial uv}{\partial y} = 2u\frac{\partial u}{\partial x} + u\frac{\partial v}{\partial y} + v\frac{\partial u}{\partial y} = v\frac{\partial qy}{\partial y} = vq = -v_c q - q^2 x.$$

On the other hand the corresponding RHS can be written as:

$$\Omega_x + 2qv = q^2 x + qv_c + 2q(-v_c - qx) = -qv_c - q^2 x$$

so the equation in the second row holds. The same result can be proved for the equation in the third row. Finally, consider the equation in the fourth row. Its LHS can be written as:

$$(E + P/\rho)\left(\frac{\partial u}{\partial x} + \frac{\partial v}{\partial y}\right) + u\frac{\partial E}{\partial x} + v\frac{\partial E}{\partial y} =$$

$$u\frac{\partial \left(e_\infty + \frac{1}{2}u^2 + \frac{1}{2}v^2\right)}{\partial x} + v\frac{\partial \left(e_\infty + \frac{1}{2}u^2 + \frac{1}{2}v^2\right)}{\partial y} = u\frac{\partial \left(\frac{1}{2}u^2 + \frac{1}{2}v^2\right)}{\partial x} + v\frac{\partial \left(\frac{1}{2}u^2 + \frac{1}{2}v^2\right)}{\partial y}$$

where we have used that $\frac{\partial u}{\partial x} + \frac{\partial v}{\partial y} = 0$ (which was already proved to be true) and that e_∞ is constant.

Differentiating one gets that:

$$u\frac{\partial \left(\frac{1}{2}u^2 + \frac{1}{2}v^2\right)}{\partial x} + v\frac{\partial \left(\frac{1}{2}u^2 + \frac{1}{2}v^2\right)}{\partial y} = u\left(u\frac{\partial u}{\partial x} + v\frac{\partial v}{\partial x}\right) + v\left(u\frac{\partial u}{\partial y} + v\frac{\partial v}{\partial y}\right) = uv\frac{\partial v}{\partial x} + vu\frac{\partial u}{\partial y}$$

So the LHS of the fourth row equation in (4.35) can be written as:

$$uv\frac{\partial v}{\partial x} + vu\frac{\partial u}{\partial y} = -quv + qvu = 0$$

Now the RHS of the fourth equation can be written as:

$$\Omega_x u + \Omega_y v = q(qx + v_c)(-u_c + qy) + q(qy - u_c)(-v_c - qx) = 0$$

So the fourth row equation is satisfied. This result completes the check for consistency.

4.4 Planar Aerodynamically Steady Flows: CFD Formulation

4.4.1 Preliminary Remarks

The BVP which allows one to get the flow properties for the case of aerodynamically steady motions has been completely defined. For the two-dimensional case (airfoils in planar steady motions) the BVP is defined through the non-linear partial differential equation (PDE) given by equation (4.14) plus its corresponding boundary conditions at the far-field and at the airfoil's surface.

Note the similitude between the standard (inertial) flow equations and the non-inertial flow equations corresponding to aerodynamically steady motions. This similitude can be clearly seen by comparing the inertial 2D Euler equations (4.5) with the 2D aerodynamically steady Euler equations (4.14). Observe that the functional dependence between the conservative variables Q and the physical flow variables is exactly the same for both cases. The same is true for the functional dependence between the flux components F, G and the physical flow variables. Then, it follows that, at the PDE level the only difference between the two cases is the presence of a source term W in the 2D aerodynamically steady Euler equation (4.14).

If one compares the boundary conditions of the two BVP, one sees that the condition of non-penetration is the same for both. On the other hand, the far-field conditions for the non-inertial motion case are altered from the inertial motion case.

1. The far-field boundary conditions for the flow velocity components are different. In the case of (inertial) rectilinear motion, one has:

$$\begin{bmatrix} u_\infty(x,y) \\ v_\infty(x,y) \end{bmatrix} = \begin{bmatrix} V_c \cos\alpha \\ V_c \sin\alpha \end{bmatrix},$$

   i.e. a "uniform" boundary condition independent of the position (x, y). While in the case of the general 2D aerodynamically steady motions one has:

$$\begin{bmatrix} u_\infty(x,y) \\ v_\infty(x,y) \end{bmatrix} = \begin{bmatrix} V_c \cos\alpha + qy \\ V_c \sin\alpha - qx \end{bmatrix},$$

   i.e. a "non-uniform" boundary condition which depends on the particular position (x, y) in the far-field.

2. The far-field boundary conditions for the Mach number M are different. In the case of inertial rectilinear motion one has:

$$M_\infty(x,y) = \frac{V_\infty}{a_\infty} = \frac{\sqrt{u_c^2 + v_c^2}}{a_\infty}$$

i.e. a "uniform" boundary condition independent of the position (x, y). While in the case of the general 2D aerodynamically steady motion one gets:

$$M_\infty(x,y) = \frac{V_\infty(x,y)}{a_\infty} = \frac{\sqrt{(-u_c + qy)^2 + (-v_c - qx)^2}}{a_\infty}$$

i.e. a "non-uniform" boundary condition which depends on the particular position (x, y) in the far-field.

3. The far-field boundary conditions for "E" are also different. In the case of rectilinear flight one has:

$$E_\infty(x,y) = e_\infty + \frac{1}{2}u_c^2 + \frac{1}{2}v_c^2$$

i.e. a "uniform" boundary condition independent of the position (x, y) in the far-field. On the other hand, in the case of the general 2D aerodynamically steady motion one has:

$$E_\infty(x,y) = e_\infty + \frac{1}{2}(-u_c + qy)^2 + \frac{1}{2}(-v_c - qx)^2$$

i.e. a "non-uniform" boundary condition which depends on the particular position (x, y) in the far-field.

4.5 Conservative Form of the Flow Equations

The two-dimensional aerodynamically steady Euler equations (4.14) can be written in terms of the conservative quantities:

$$Q = \begin{bmatrix} Q_1 \\ Q_2 \\ Q_3 \\ Q_4 \end{bmatrix} = \begin{bmatrix} \rho \\ \rho u \\ \rho v \\ \rho E \end{bmatrix}. \tag{4.36}$$

First, observe that the flow variables can be expressed in terms of the conservative variables Q_i:

$$\rho = Q_1 \tag{4.37}$$

$$u = \frac{Q_2}{Q_1} \tag{4.38}$$

$$v = \frac{Q_3}{Q_1} \tag{4.39}$$

$$E = \frac{Q_4}{Q_1} \tag{4.40}$$

$$P = (\gamma - 1)\left[Q_4 - \frac{1}{2}\rho\left(u^2 + v^2\right)\right] = (\gamma - 1)\left[Q_4 - \frac{1}{2}\frac{1}{Q_1}\left(Q_2^2 + Q_3^2\right)\right] \tag{4.41}$$

From the above relationships and equation (4.16) it follows that:

$$F = F(Q) = \begin{bmatrix} Q_2 \\ \frac{Q_2^2}{Q_1} + (\gamma - 1)\left(Q_4 - \frac{1}{2Q_1}\left[Q_2^2 + Q_3^2\right]\right) \\ \frac{Q_2 Q_3}{Q_1} \\ \frac{Q_2}{Q_1}\left(\gamma Q_4 - \frac{(\gamma-1)}{2Q_1}\left[Q_2^2 + Q_3^2\right]\right) \end{bmatrix}$$

$$G = G(Q) = \begin{bmatrix} Q_3 \\ \frac{Q_3 Q_2}{Q_1} \\ \frac{Q_3^2}{Q_1} + (\gamma - 1)\left(Q_4 - \frac{1}{2Q_1}\left[Q_2^2 + Q_3^2\right]\right) \\ \frac{Q_3}{Q_1}\left(\gamma Q_4 - \frac{(\gamma-1)}{2Q_1}\left[Q_2^2 + Q_3^2\right]\right) \end{bmatrix}.$$

Then, as in the inertial case, the components of the fluxes are exclusive functions of the conservative variables Q_i , i.e. $F = F(Q)$ and $G = G(Q)$. The source term W (4.17) can also be written in terms of the conservative variables:

$$W = W(Q) = \begin{bmatrix} 0 \\ Q_1\Omega_x + 2Q_3 q \\ Q_1\Omega_y - 2Q_2 q \\ Q_2\Omega_x + \Omega_y Q_3 \end{bmatrix}. \tag{4.42}$$

As a consequence one can rewrite the 2D aerodynamically steady Euler Equations as:

$$\frac{\partial Q}{\partial t} + \frac{\partial F(Q)}{\partial x} + \frac{\partial G(Q)}{\partial y} = W(Q)$$

Note. W is also spatially dependent because Ω_x and Ω_y are functions which depend on the position coordinates $\vec{x} = (x, y)$. Also, W depends explicitly on the constant parameters V_c, α and q characterizing the particular aerodynamically steady motion. So rigorously one should write:

$$W = W(Q, \vec{x}\,;\, V_c, \alpha, q)$$

4.6 Aerodynamically Steady Finite-Volume Equations

The similitude between the inertial PDE and the non-inertial PDE descriptions is crucial for the development of numerical techniques for solving the BVP associated with generalized aerodynamically steady motions. In particular, this similitude leads to an equivalent similitude between the finite-volume formulations for these cases. To this end, observe that one can express equation (4.14) in the following integral form:

$$\frac{\partial}{\partial t}\int_{\tau} Q \; d\tau + \int_{\sigma} \vec{F}\cdot\hat{n} \; d\sigma = \int_{\tau} W \; d\tau \tag{4.43}$$

where $\hat{n}$ is the unit outward vector normal to the surface σ and $\vec{F}$ is defined as:

$$\vec{F} = F\hat{e}_x + G\hat{e}_y \tag{4.44}$$

Equation (4.43) is valid for any finite volume τ enclosed by a surface σ. This equation can be obtained also from equation (3.42) by restricting to the particular case of a two-dimensional inviscid flow.

For getting actual finite-volume numerical implementations the following comments are useful:

1. From the expressions for F and G and the definition of $\vec{F}$ one can write $\vec{F}\cdot\hat{n}$ explicitly as:

$$\vec{F}\cdot\hat{n} = \begin{bmatrix} \rho\left[\vec{V}\cdot\hat{n}\right] \\ \rho u\left[\vec{V}\cdot\hat{n}\right] + Pn_x \\ \rho v\left[\vec{V}\cdot\hat{n}\right] + Pn_y \\ (\rho E + P)\left[\vec{V}\cdot\hat{n}\right] \end{bmatrix} \tag{4.45}$$

   where n_x and n_y are the Cartesian components of the unit vector $\hat{n}$.

2. The volumes τ are usually chosen to be areas enclosed by the union of rectilinear segments σ_i. A typical 2D finite-volume τ is shown in Figure (4.5). In this case, the unit normal vectors are constant along each point of the segments σ_i and equation (4.43) can be rewritten as:

$$\frac{\partial}{\partial t}\int_{\tau} Q \; d\tau + \sum_{i=1}^{k}\int_{\sigma_i} \vec{F}\cdot\hat{n}_i \; d\sigma = \int_{\tau} W \; d\tau. \tag{4.46}$$

   Here $\hat{n}_i$ is the unit vector normal to the segment σ_i and k is the total number of segments σ_i.

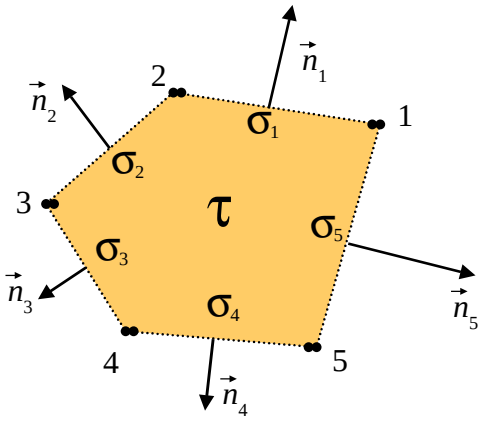

Figure 4.5: Typical finite volume formed by the union of a finite number of straight segments

3. Equation (4.46) is exact, no approximations have been done. Numerical solutions are obtained after an appropriate discretization of this equation.

4. The typical approximations used in standard (inertial) finite-volume formulations can also be used here. The flux $\vec{F} \cdot \hat{n}_i$ along each segment σ_i can be approximated by its value at the midpoint of such segment. As a consequence, using equation (4.45) one can write:

$$\int_{\sigma_i} \vec{F} \cdot \hat{n}_i \; d\sigma = \sigma_i \vec{F}_{im} \cdot \hat{n}_i = \sigma_i \begin{bmatrix} \rho_{im} \left[\vec{V}_{im} \cdot \hat{n}_i \right] \\ \rho_{im} u_{im} \left[\vec{V}_{im} \cdot \hat{n}_i \right] + P_{im} n_{ix} \\ \rho_{im} v_{im} \left[\vec{V}_{im} \cdot \hat{n}_i \right] + P_{im} n_{iy} \\ (\rho_{im} E_{im} + P_{im}) \left[\vec{V}_{im} \cdot \hat{n}_i \right] \end{bmatrix} \tag{4.47}$$

where $\{\rho_{im}, u_{im}, v_{im}, E_{im}, P_{im}, \vec{V}_{im}\}$ are the values of the physical variables $\{\rho$, u, v, E, P, $\vec{V}\}$ at the midpoint m of the straight segment σ_i .

4.7 Spatial Discretization and Variable Discretization

To solve numerically the aerodynamically steady flow equations one must proceed to the discretization of the flow region in a similar way as it is done in solving the inertial flow equations. Accordingly, one has to discretize the space defined by the coordinate system $\mathcal{R}$. Since $\mathcal{R}$ is a body-fixed reference frame, as seen from $\mathcal{R}$, the position of the airfoil (or the aircraft) remains fixed. Only one discretization of the space is needed for all times.

The discretization of the space is made by partitioning the space in small simple volumes (or areas), usually triangles or quadrilaterals. The vertices of these small volumes are usually called "grid nodes". In Figure (4.6) one can see an example of the discretization of the region around a NACA 0012 airfoil into small triangles. In Figure (4.6)-(a) is shown a wide view of the discretization and in Figure (4.6)-(b) is shown a close view of discretization around the airfoil. Since the actual space is infinite the discretization is usually done up to a distance far enough from the object(s) of concern. In this case the object of concern is the airfoil, so the space was discretized using a circular outer boundary which is located approximately a distance of 30 times the length of the airfoil's chord. This outer boundary defines the "far-field" location.

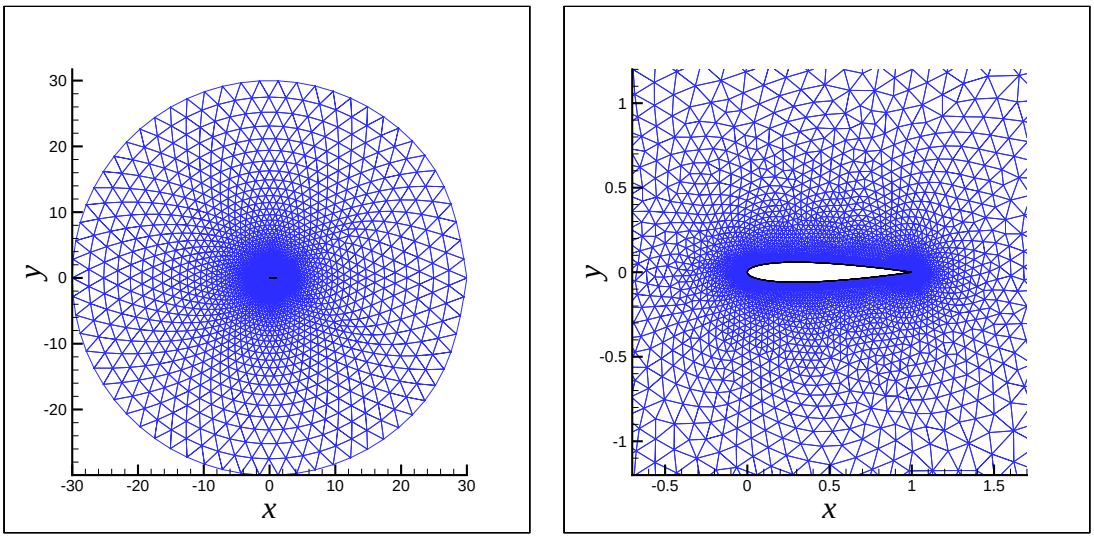

(a) Wide-view

(b) Close-view

Figure 4.6: Typical grid

The numerical discretization of the space is usually done using structured grid generators or unstructured grid generators. Unstructured grid generators are becoming increasingly more popular. In our case we have used two unstructured grid generators: `Double9` which is a research code developed by Dr. Kyle Anderson and it is based on Delaunay's triangulation, and `AFLR2` [32], [33] which was developed by D.L Marcum at Missisippi State University. Since `AFLR2` generates a more "uniform" mesh we have used it to generate the results shown in this work. In particular, the grid shown in Figure (4.6) was obtained using `AFLR2` and it will be the grid used for the numerical calculations. For a complete discussion about the theory and methods of grid-generation see references [50], [34].

The finite nature of numerical calculations implies that the values of the flow state variables can be determined only in a discrete number of locations in the space. These

locations are usually called "state nodes". The discretization of the space defines more or less automatically the position of the states nodes. Usually, the location of the states nodes coincide with the position of the grid nodes or their location corresponds to the position of the centroid of the small volumes defined by the grid. In our case we will use a node-centered schemed so the state nodes coincide with the grid nodes. In what follows we will use N to generically denote the total number of grid nodes and state nodes in the space[2] and we will use Q^j to denote the values of the four conservative variables at state node j.

In Figure (4.7) is shown a partial view of the discretization of the space into finite triangles (defined by the dotted-lines). The "grid nodes" and the "state nodes" are the vertices of

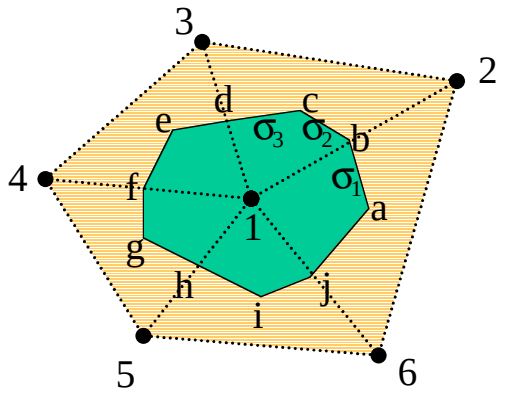

Figure 4.7: Typical finite-volume formed by the union of a finite number of triangles sharing a common node (node 1). This type of finite-volume is the one used for the numerical calculations shown in this work.

the triangles and they have been numbered from 1 to 6. The location of the state nodes is then given by $\{\vec{x}^1, \vec{x}^2, ..., \vec{x}^6, ..., \vec{x}^N\}$ and at these nodes the corresponding state variables $\{Q^1, Q^2, ..., Q^6, ..., Q^N\}$ are defined. It is useful to arrange the values Q^j of all the N state nodes by using a global vector array. So we define:

$$\hat{Q} = \begin{bmatrix} Q^1 \\ Q^2 \\ \vdots \\ Q^j \\ \vdots \\ Q^N \end{bmatrix}. \tag{4.48}$$

[2]For the numerical simulations presented here $N \approx 6000$ nodes

4.8 Discretized Finite-Volume Equations

The two-dimensional aerodynamically steady flow equations will be solved using a finite-volume formulation. The chosen geometry of the finite volumes τ is as the generic volume defined by the dark colored area surrounding node 1 in Figure (4.7). The boundary σ of the finite-volume τ is formed by the union of straight segments "ab", "bc",... and "ja". Each of these segments is formed by joining the centroid of a triangle with the mid-point of one of its sides. For example the segment "ab" is formed by joining the centroid of triangle "1-2-6" and the midpoint of segment "1-2". Observe that each finite volume contains one-and-only one state node.

The discretized flow equations are obtained by applying the integral form of the flow equations to each finite volume τ and by using the discretized information of the "state nodes". For a finite volume τ^j as the one shown in Figure (4.7) one has:

$$\frac{\partial}{\partial t}\int_{\tau^j} Q\ d\tau + \sum_{i=1}^{k^j}\int_{\sigma_i^j} \vec{F}\cdot\hat{n}_i^j\ d\sigma = \int_{\tau^j} W\ d\tau \tag{4.49}$$

where $\hat{n}_i^j$ is the outward unit vector normal to the boundary segment σ_i^j and k^j is the total number of boundary segments σ_i^j of volume τ^j. Equation (4.49) is exact, no approximations have been done yet.

The numerical calculation of equation (4.49) imposes the necessity of calculating the quantities $\int_{\tau^j} Q\ d\tau$, $\int_{\sigma_i^j} \vec{F}\cdot\hat{n}_i^j\ d\sigma$ and $\int_{\tau^j} W\ d\tau$ in an approximate way using only the information of the discrete values of Q at each of the N state nodes. Using a generalized mean value theorem we can approximate $\int_{\tau^j} Q\ d\tau$:

$$\int_{\tau^j} Q\ d\tau = \int_{\tau^j} Q(\vec{x})\ d\tau \approx \tau^j Q(\vec{x}^j) = \tau^j Q(\vec{x}^j) = \tau^j Q^j \tag{4.50}$$

where $\vec{x}^j$ is the position of the state node enclosed by τ^j. Similarly we can approximate $\int_{\sigma_i^j} \vec{F}\cdot\hat{n}_i^j\ d\sigma$ and $\int_{\tau^j} W\ d\tau$ as follows:

$$\int_{\tau^j} W\ d\tau = \int_{\tau^j} W(Q(\vec{x}),\vec{x})\ d\tau \approx \tau^j W(Q(\vec{x}^j),\vec{x}^j) = \tau^j W(Q^j,\vec{x}^j) = \tau^j W^j \tag{4.51}$$

$$\int_{\sigma_i^j} \vec{F}\ d\sigma = \int_{\sigma_i^j} \vec{F}(Q(\vec{x}))\ d\sigma \approx \sigma_i^j \vec{F}(Q(\vec{x}_{im}^j)) = \sigma_i^j \vec{F}(Q_{im}^j) \tag{4.52}$$

where $\vec{x}_{im}^j$ is the position of the midpoint m of segment σ_i^j and Q_{im}^j is the approximate value of Q at such midpoint. Using equations (4.50)-(4.52) in equation (4.49) we get:

$$\tau^j \frac{\partial Q^j}{\partial t} = \tau^j W^j - \sum_{i=1}^{k^j} \sigma_i^j \vec{F}(Q_{im}^j)\cdot\hat{n}_i^j. \tag{4.53}$$

For stability purposes the numerical fluxes at the midpoints are calculated using the van Leer scheme [3]. In these numerical schemes the fluxes $\vec{F}(Q^j_{im}) \cdot \hat{n}^j_i$ at the face σ^j_i are given by analytical expressions that depend on two arguments: the values of the conservative variables at the left of the face, which we denote by Q^{j+}_{im}, and the values of conservative variables at the right of the face, which we denote by Q^{j-}_{im}. For first-order accuracy the values of Q^{j+}_{im} and Q^{j-}_{im} are set equal to the values of Q at the nodes lying at each side of the segment σ^j_i. For example, in Figure (4.7) for the face "ac" formed by the segments "ab" and "bc" we set:

$$Q^{1+}_{\mathrm{ac}m} = Q^1 \quad \text{and} \quad Q^{1-}_{\mathrm{ac}m} = Q^2$$

For second-order accuracy the variables are extrapolated from the nodes to the midpoints of the faces using a Taylor series expansion. For example, in Figure (4.7) for the face "ac" whose midpoint is "b" we set:

$$Q^{1+}_{\mathrm{ac}m} = Q^1 + \nabla_1 Q \cdot \vec{r}_{1,\mathrm{ac}} \quad \text{and} \quad Q^{1-}_{\mathrm{ac}m} = Q^2 + \nabla_2 Q \cdot \vec{r}_{2,\mathrm{ac}} \tag{4.54}$$

where $\nabla_1 Q$ and $\nabla_2 Q$ are approximate gradients obtained using the nodes surrounding node 1 and the nodes surrounding node 2, respectively. $\vec{r}_{1,\mathrm{ac}}$ is the vector position joining node 1 with the midpoint of face "ac" and $\vec{r}_{2,\mathrm{ac}}$ is the vector position joining node 2 with the midpoint of face "ac". For more details see [2]. The extrapolation method discussed here is based on the same ideas used in the MUSCL approach (see reference [48], pp. 204-209, 395-396).

Equation (4.53) must be applied at each one of the N finite-volumes τ^j. As a consequence, for each discretized conservative variable Q^j we have an equation of the type:

$$\tau^j \frac{\partial Q^j}{\partial t} = R^j(\hat{Q}) \tag{4.55}$$

where

$$R^j(\hat{Q}) = \tau^j W(Q^j, \vec{x}^j) - \sum_{i=1}^{k^j} \sigma^j_i \vec{F}(Q^j_{im}) \cdot \hat{n}^j_i \tag{4.56}$$

Observe that we use $\hat{Q}$ in the notation of the residual R^j because R^j depends not only on the value Q^j at node j but also on other components of $\hat{Q}$.

4.9 Time discretization

Equation (4.55) is a differential equation that is time-dependent. This equation will be time-discretized using an Euler implicit, iterative scheme. We will use the superscript n to denote

[3] We can use the numerical schemes (such as van Leer or Roe) used in standard CFD in our formulation, because, we have written the non-inertial flow equations in such a way that the analytical expressions of the non-inertial fluxes are exactly the same as the analytical expressions of the inertial fluxes used in standard (inertial) CFD

time $t^n = n\,(\triangle t)$ and $\triangle Q^n$ to denote the change in Q with respect to two consecutives times

$$\triangle Q^n = Q^{n+1} - Q^n = Q(t^n + \triangle t) - Q(t^n).$$

An implicit, first order expansion in time is used to get the following approximations:

$$\frac{\partial Q^{n,j}}{\partial t} \approx \frac{\triangle Q^{n,j}}{\triangle t} \tag{4.57}$$

$$R^j(\hat{Q}^{n+1}) \approx R^j(\hat{Q}^n) + \frac{\partial R^j(\hat{Q}^n)}{\partial \hat{Q}} \triangle \hat{Q}^n. \tag{4.58}$$

Replacing equations (4.57)-(4.58) into equation (4.55) we get that:

$$\left[\frac{1}{\triangle t}\hat{I}^\tau + \frac{\partial \hat{R}(\hat{Q}^n)}{\partial \hat{Q}}\right] \triangle \hat{Q}^n = \hat{R}(\hat{Q}^n) \tag{4.59}$$

where $\hat{I}^\tau$ is an N by N diagonal matrix whose diagonal elements $\hat{I}^\tau_{j,j}$ are the volumes τ^j and where $\hat{R}$ denotes the N-dimensional vector array containing all the values of the finite-volume residuals R^j at the N state nodes:

$$\hat{R} = \begin{bmatrix} R^1 \\ R^2 \\ \vdots \\ R^j \\ \vdots \\ R^N \end{bmatrix}. \tag{4.60}$$

Starting with an initial guess $\hat{Q}^0$ at time $t = 0$, equation (4.59) defines a time marching algorithm. At each time station a linear-equation for the unknowns $\triangle \hat{Q}^n$ must be solved. So if the solution $\hat{Q}^n$ is known up to time $t^n = n\triangle t$ then after solving equation (4.59) for $\triangle \hat{Q}^n$ we can obtain the values for $\hat{Q}$ at time $t = t^n + \triangle t$ from:

$$\hat{Q}^{n+1} = \hat{Q}^n + \triangle \hat{Q}^n.$$

4.10 Numerical Solutions

We have developed a computational code called `NISFLOW` (non-inertial-steady-flow) which is based on the iterative technique described in the previous Section. `NISFLOW` can be used to determine the flows around airfoils moving in generalized aerodynamically steady motions.

We note the following about the code implementation of `NISFLOW`.

1. Observe that we do not need time-accurate solutions since we are looking for the steady state solution, i.e.

$$\hat{R}(\hat{Q}) = 0. \tag{4.61}$$

The numerical solution $\hat{Q}$ of this equation defines the steady flow that an observer in the the body-fixed reference frame $\mathcal{R}$ sees when the airfoil (or the aircraft) is moving in an aerodynamically steady motion.

2. Note that equation (4.59) defines the well-known Euler implicit scheme used to solve equations of the form $\partial\hat{Q}/\partial t = \hat{R}(\hat{Q})$

3. In particular, this scheme is used to solve the inertial flow equations in the `Class Code`. The difference now lies in the fact that, for the case of generalized aerodynamically steady motions, the residual $\hat{R}(\hat{Q}^n)$ and the Jacobian $\frac{\partial\hat{R}(\hat{Q})}{\partial\hat{Q}}$ contain additional terms due to the presence of the source term W.

4. It may seem that the additional term W may change some stability properties ([11]), and this is the case indeed. For stability purposes the Jacobian $\frac{\partial\hat{R}(\hat{Q})}{\partial\hat{Q}}$ must contain terms involving the Jacobians of the source term $\frac{\partial W(\hat{Q})}{\partial\hat{Q}}$. It must be pointed out that we did not get convergence when these terms were neglected.

5. Following Tobak and Schiff we will define the non-dimensional pitch rate as:

$$\hat{q} = \frac{qc}{V_c} \tag{4.62}$$

where c is the chord of the airfoil. **Note.** Others authors (such as Etkin) define the non-dimensional pitch-rate as $\hat{q} = (qc)/(2V_c)$. The reader should be aware of this difference.

6. From the condition (Equation (2.12)) for the radius R_c of the circular trajectory it follows that the non-dimensional pitch rate $\hat{q}$ is related to R_c through:

$$\hat{q} = \frac{c}{R_c} \tag{4.63}$$

7. The numerical scheme will allow us to evaluate the aerodynamic forces and moments and its non-dimensional coefficients. As a consequence, equations (4.12) can be generalized to include the dependence on the pitch-rate q:

$$\begin{aligned} C_\ell &= \overline{C}_\ell(M, \alpha, \hat{q}) \\ C_d &= \overline{C}_d(M, \alpha, \hat{q}) \\ C_m &= \overline{C}_m(M, \alpha, \hat{q}) \end{aligned} \tag{4.64}$$

In the following figures we show some numerical solutions obtained using `NISFLOW`. The van Leer Flux Splitting scheme was used for the evaluation of the fluxes. The flow variables were extrapolated at the faces using equation (4.54). The cases to be considered here are the ones where the airfoil is moving in generalized 2D aerodynamically steady trajectories at a Mach number $M_c = 0.2$ and at an angle of attack $\alpha = 0^o$. In Figures (4.8)(a)-(b) is shown the case where the pitch-rate q is $\hat{q} = 0$. If we compare this solution with the solution shown in Figure (2.6) (which was obtained using the `Class Code`), we see that the flow solutions are the same. This result is what we expected since the 2D aerodynamically steady motion with $q = 0$ is the one corresponding to a uniform rectilinear steady motion. As a consequence, all the solutions obtained by the `Class Code` can be obtained by the `NISFLOW Code` with $\hat{q} = 0$.

In Figures (4.8)(c)-(d) and (4.9) the resulting flow solutions for cases where the pitch-rate is set to different non-zero values are shown. As we mentioned, these flow solutions correspond to cases where the airfoil is flying in circular trajectories as in Figure (4.4). Figures (4.8)(c)-(d) show the pressure coefficient contours and the velocity streamlines for the case where the airfoil has a non-dimensional pitch-rate of $\hat{q} = 0.01$. According to equation (4.63) this value corresponds to a circular trajectory of radius R_c equal to 100 times the airfoil chord.

In Figures (4.9)(a)-(b) we see the flow solutions for the case where the pitch rate has been set to $\hat{q} = 0.03$. This value corresponds to a circular trajectory of radius R_c equal to 33 times the airfoil chord. In Figures (4.9)(c)-(d) we see the flow solutions for the case where the pitch rate has been increased to $\hat{q} = 0.05$. This value corresponds to a circular trajectory of radius R_c equal to 20 times the airfoil chord.

From the close-view of the Figures (4.8)-(4.9) an interesting phenomenon can be seen: as the pitch rate increases nose-down the pressure in the upper surface of the airfoil tends to increase while in the lower surface tends to decrease. Then, it follows that an increasing negative lift is produced as q increases nose-down. This behavior is also clear from the Table (4.1) where the results corresponding to the use of `NISFLOW Code` are shown between parentheses. From these numerical simulations, it follows that C_ℓ is a decreasing function of the (nose-down) pitch-rate q. Conversely, C_ℓ is a increasing function of a (nose-up) pitch-rate q. Similarly, from the results shown in Table (4.1), it follows that a restoring pitching moment (nose-up) is produced when the airfoil is pitching (nose-down). The magnitude of this restoring moment increases with the magnitude of the pitch rate. These results are in agreement with what is observed in reality and, as discussed in the last section of this chapter, they have been validated with other methods.

If we look at the far-field behavior of the flow solutions, we see that the streamlines tend to be circular curves. This result is in complete agreement with the physics of the problem since that is the behavior an observer in the body-fixed reference frame will see when the airfoil is flying in a steady circular trajectory. The result is also in agreement with the mathematics, since the flow defined in equation (4.28) corresponds to circular streamlines.

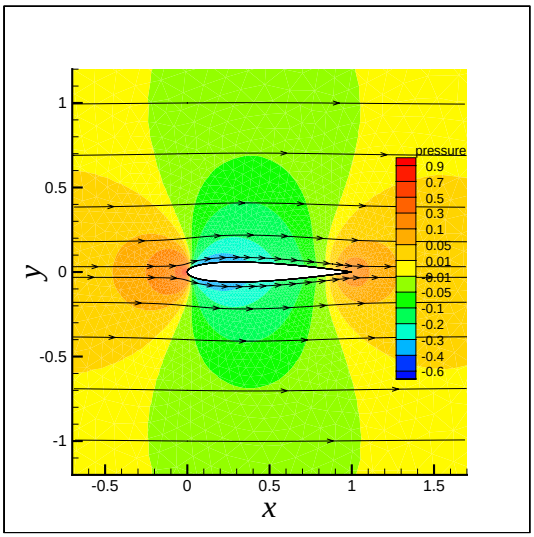

(a) Close-view, $M_c = 0.2$, $\hat{q} = 0.0$

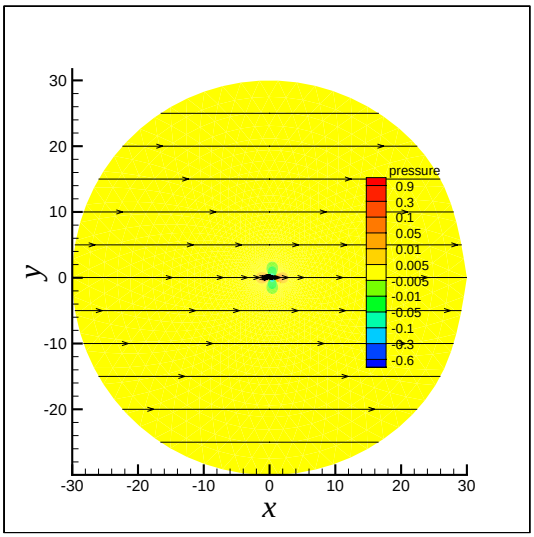

(b) Wide-view, $M_c = 0.2$, $\hat{q} = 0.0$

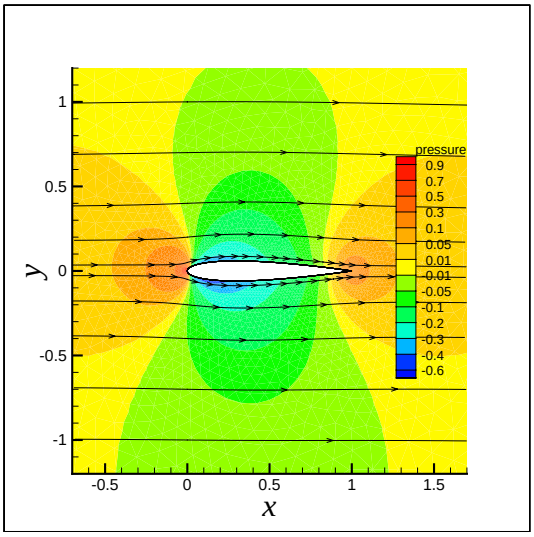

(c) Close-view, $M_c = 0.2$, $\hat{q} = 0.01$

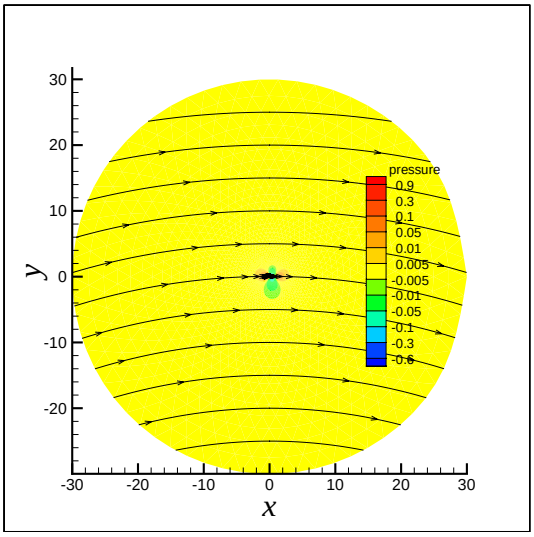

(d) Wide-view, Mach $M_c = 0.2$, $\hat{q} = 0.01$

Figure 4.8: Pressure coefficient contours and velocity streamlines, obtained using the `NISFLOW Code`, for the air around a NACA 0012 airfoil which is moving in aerodynamically steady motions at Mach $M_c = 0.2$, $\alpha = 0^o$ and with pitch-rates $\hat{q} = 0.0$ and $\hat{q} = 0.01$.

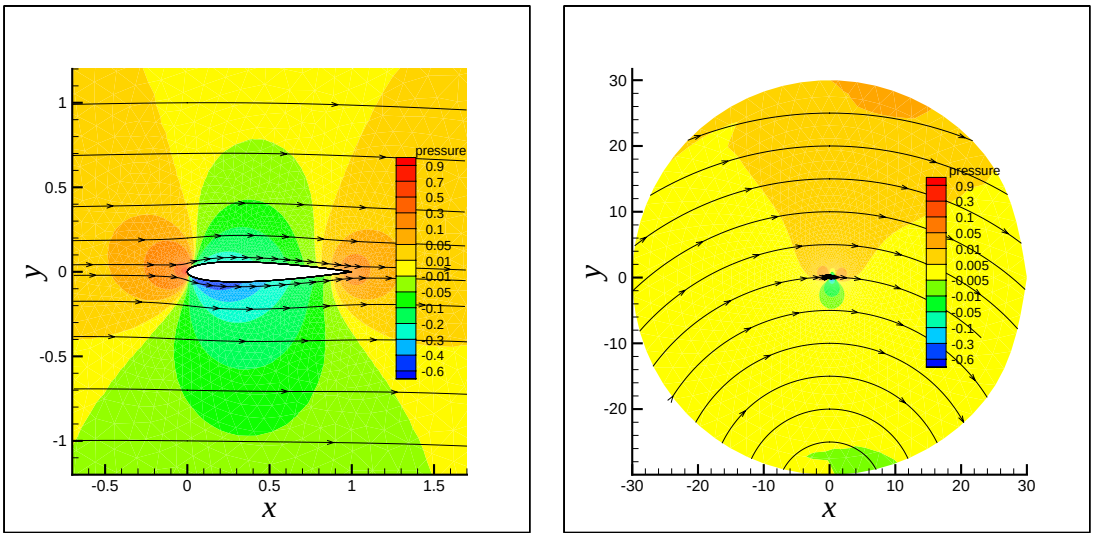

(a) Close-view, $M_c = 0.2$, $\hat{q} = 0.03$

(b) Wide-view, Mach $M_c = 0.2$, $\hat{q} = 0.03$

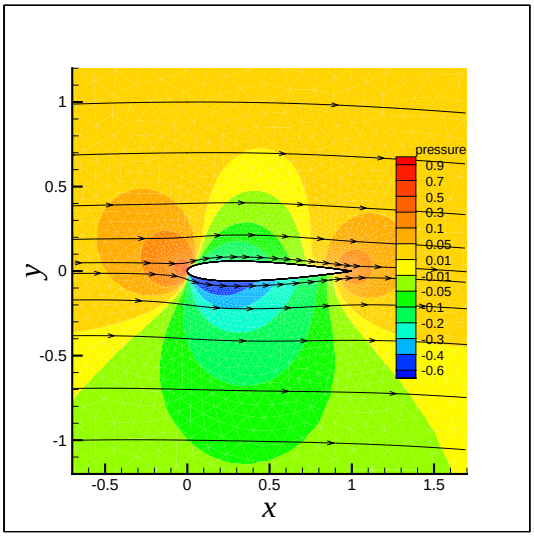

(c) Close-view, $M_c = 0.2$, $\hat{q} = 0.05$

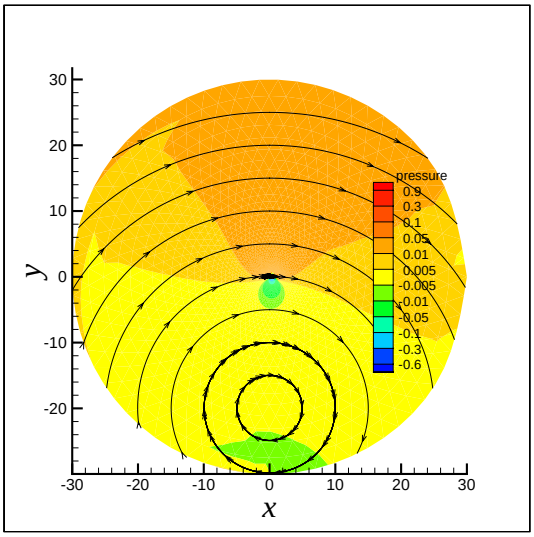

(d) Wide-view, $M_c = 0.2$, $\hat{q} = 0.05$

Figure 4.9: Pressure coefficient contours and velocity streamlines, obtained using the `NISFLOW Code`, for the air around an airfoil which is moving with a in aerodynamically steady motions at Mach $M_c = 0.2$ and $\alpha = 0^o$ with non-zero pitch-rates $\hat{q} = 0.03$ and $\hat{q} = 0.05$.

$M_c = 0.2$				
$\hat{q}$	0	0.01	0.03	0.05
C_ℓ	0.000 (0.000)	-0.053 (-0.052)	-0.157 (-0.155)	-0.262 (-0.259)
C_m	0.000 (0.000)	-0.018 (-0.018)	-0.053 (-0.052)	-0.088 (-0.087)
$M_c = 0.5$				
$\hat{q}$	0	0.01	0.03	0.05
C_ℓ	0.000 (0.000)	-0.060 (-0.059)	-0.180 (-0.177)	-0.299 (-0.293)
C_m	0.000 (0.000)	-0.020 (-0.020)	-0.060 (-0.059)	-0.100 (-0.099)
$M_c = 0.8$				
$\hat{q}$	0	0.01	0.03	0.05
C_ℓ	0.000 (0.000)	-0.108 (-0.108)	-0.316 (-0.308)	-0.498 (-0.483)
C_m	0.000 (0.000)	-0.042 (-0.042)	-0.124 (-0.121)	-0.201 (-0.195)

Table 4.1: Dependence of the lift and the pitching-moment coefficients with respect to the pitch-rate q for a NACA 0012 airfoil for different Mach numbers and angle of attack $\alpha = 0^o$. The numbers between parentheses were obtained using the `NISFLOW Code`. The numbers without parentheses correspond to the values obtained using `A-NISFLOW Code`.

Finally, observe that in all the solutions the center of the circular streamlines is located at a distance equal to the radius R_c. This phenomenon can be seen clearly for the case $\hat{q} = 0.05$ (corresponding to $R_c = 20c$) shown in Figure (4.9)-(d). It is important to mention that this phenomenon appears naturally from the flow solution and has not been imposed explicitly.

The other condition that we can check at the far-field is if the pressure coefficient tends to zero as $\|\vec{x}\| \longrightarrow \infty$. This property seems to be true for the small $\hat{q}$'s but it seems to deteriorate as $\hat{q}$ increases. In particular for the cases $\hat{q} = 0.03$ and $\hat{q} = 0.05$ there is a wide zone near the upper-part of the far-field where this condition is not met. The cause of this phenomenon is that the evaluation of the residuals $R^j(\hat{Q})$ with the approximations of equations (4.51)-(4.52) is not accurate. The problem appears due to the fact that the unperturbed velocity is no longer uniform. It has a rotational component that increases proportionally to q and $\|\vec{x}\|$ as $\|\vec{x}\| \longrightarrow \infty$. As $\|\vec{x}\| \longrightarrow \infty$ the finite volumes defined by the grid generator become much bigger (of the order of the chord length) than the ones very close to the airfoil. For these reasons the approximations (4.51)-(4.52) are relatively poor and some errors are produced. In the next section we discuss a way to take into account this phenomenon in order to get more accuracy in the evaluation of the residuals, i.e improved solutions.

4.11 Increasing the Accuracy of Numerical Solutions

As noted in equation (4.61), the condition

$$\hat{R}(\hat{Q}) = 0.$$

defines the solution $\hat{Q}$ of the discretized flow equations. The expression used for the calculation of the residual components $R^j(\hat{Q})$ is given in equation (4.56) and was based on the approximations defined in equations (4.51)-(4.52). These approximations basically assumed that

1. The variation of $W(Q(\vec{x}), \vec{x})$ within the control volume τ^j is negligible and its value is equal to $W(Q^j, \vec{x}^j)$. As a consequence:

$$\int_{\tau^j} W(Q(\vec{x}), \vec{x})\ d\tau \approx \tau^j W(Q^j, \vec{x}^j) \tag{4.65}$$

2. The flux $\int_\sigma \vec{F}(Q)\ d\sigma$ through a straight face σ of the boundary of the control volume is equal to the value of $\vec{F}$ at the midpoint $\vec{x}_m$ multiplied by the area σ of the segment. That is to say:

$$\int_\sigma \vec{F}(Q(\vec{x}))\ d\sigma = \sigma \vec{F}(Q(\vec{x}_m)) = \sigma \vec{F}(Q_m) \tag{4.66}$$

The above approximations are valid as long as the control volumes are small and as long as the flow variables Q do not vary rapidly with the position $\vec{x}$.

In the case of uniform flows around a fixed airfoil the variation of Q occurs mainly in the neigborhood of the airfoil, while at the far-field (say at a distance equal to 20 times the chord of the airfoil) the values of Q tend to be constant and their variation is almost negligible. For this reason, grid generators generate grids with small volumes near the airfoil and relatively large volumes at the far-field.

On the contrary, in the case of the simulation of the generalized aerodynamically steady motions the flow velocities do not tend to a constant value at the far-field. Actually their values change with position and their magnitude increase proportionally with the distance to the airfoil. This tendency can be clearly seen from equation (1):

$$\begin{bmatrix} u_\infty(x,y) \\ v_\infty(x,y) \end{bmatrix} = \begin{bmatrix} V_c \cos\alpha + qy \\ V_c \sin\alpha - qx \end{bmatrix}, \tag{4.67}$$

As a consequence, to obtain a similar accuracy, for the case of simulation of generalized aerodynamically steady motions one may be required to have a finer grid than the grid one would normally use for uniform flows.

An alternative way to circumvent this problem is to try to get a more accurate evaluation of the exact residual $R^j(Q)$ at each control volume j. A more accurate evaluation of the residual would naturally lead to getting more accurate solutions and would have the additional advantage that accurate solutions could be obtained using grids normally used for classical uniform flows. By looking at the steady solution of the exact finite-volume equation (4.49)

$$R^j(Q) = \int_{\tau^j} W \, d\tau - \sum_{i=1}^{k^j} \int_{\sigma_i^j} \vec{F} \cdot \hat{n}_i^j \, d\sigma = 0 \tag{4.68}$$

one sees that an accurate evaluation of the residual at each control volume requires:

1. An accurate evaluation of $\int_{\sigma_i} \vec{F} \cdot \hat{n}_i \, d\sigma$ along each of the straight segments σ_i defining the boundary of the control volume, and
2. An accurate evaluation of the volume integral $\int_\tau W \, d\tau$.

Point 1 will be addressed in the next section. Point 2 will be addressed in Section 4.13.

4.12 Improving Accuracy in the Evaluation of Fluxes

4.12.1 Definitions and Properties of Segment Averages

Given a variable $A = A(\vec{x})$ and a straight segment of length σ_i^j, we define the *segment average* $\langle A \rangle_i^j$ of A as:

$$\langle A \rangle_i^j = \frac{1}{\sigma_i^j} \int_{\sigma_i^j} A(\vec{x}) \, d\sigma_i^j \tag{4.69}$$

From this definition it follows that the operation of computing segment averages is linear. In particular the following properties hold.

Property of Additivity. Given two arbitrary variables $A = A(\vec{x})$ and $B = B(\vec{x})$, their segments averages satisfy:

$$\langle A + B \rangle_i^j = \langle A \rangle_i^j + \langle B \rangle_i^j \tag{4.70}$$

Property of Average of a Constant. Given a physical variable λ which is constant along the segment, its segment average satisfies:

$$\langle \lambda \rangle_i^j = \lambda \tag{4.71}$$

Property of Multiplication by a Constant. Given an arbitrary variable $A = A(\vec{x})$ and a constant variable λ, the following property is valid:

$$\langle \lambda A \rangle_i^j = \lambda \, \langle A \rangle_i^j \tag{4.72}$$

4.12.2 Evaluation of Fluxes using Segment Averages

By definition of segment averages we have that:

$$\left\langle \vec{F}\cdot\hat{n}\right\rangle_i^j = \frac{1}{\sigma_i^j}\int_{\sigma_i^j}\vec{F}\cdot\hat{n}\;d\sigma_i^j \tag{4.73}$$

As a consequence. an accurate evaluation of the fluxes $\int_{\sigma_i^j}\vec{F}\cdot\hat{n}\;d\sigma_i^j$ along each straight segment σ_i^j of the control volume τ^j is equivalent to an accurate evaluation of the segment averaged fluxes $\left\langle \vec{F}\cdot\hat{n}\right\rangle_i^j$. Then, let's evaluate these segment averaged fluxes as accurately as possible. From now on we will drop the subscript i and the superscript j under the understanding that each segment average must be performed at each segment σ_i^j of the N control volumes.

Using equation (4.45) it follows that

$$\left\langle \vec{F}\cdot\hat{n}\right\rangle = \begin{bmatrix} \left\langle \rho\left[\vec{V}\cdot\hat{n}\right]\right\rangle \\ \left\langle \rho u\left[\vec{V}\cdot\hat{n}\right]+Pn_x\right\rangle \\ \left\langle \rho v\left[\vec{V}\cdot\hat{n}\right]+Pn_y\right\rangle \\ \left\langle (\rho E+P)\left[\vec{V}\cdot\hat{n}\right]\right\rangle \end{bmatrix} = \begin{bmatrix} \langle \rho\left[un_x+vn_y\right]\rangle \\ \langle \rho u\left[un_x+vn_y\right]+Pn_x\rangle \\ \langle \rho v\left[un_x+vn_y\right]+Pn_y\rangle \\ \left\langle \left(\rho\left[e+\frac{1}{2}\left(u^2+v^2\right)\right]+P\right)\left[un_x+vn_y\right]\right\rangle \end{bmatrix}$$

Expanding the terms in each of the rows of the RHS term we get

$$\left\langle \vec{F}\cdot\hat{n}\right\rangle = \begin{bmatrix} \langle \rho u n_x\rangle + \langle \rho v n_y\rangle \\ \langle \rho u u n_x\rangle + \langle \rho u v n_y\rangle + \langle P n_x\rangle \\ \langle \rho v u n_x\rangle + \langle \rho v v n_y\rangle + \langle P n_y\rangle \\ \langle \rho e u n_x\rangle + \langle \rho e v n_y\rangle + \frac{1}{2}\langle \rho u^2 u n_x\rangle + \frac{1}{2}\langle \rho u^2 v n_y\rangle + \frac{1}{2}\langle \rho v^2 u n_x\rangle + \\ +\frac{1}{2}\langle \rho v^2 v n_y\rangle + \langle P u n_x\rangle + \langle P v n_y\rangle \end{bmatrix} \tag{4.74}$$

From equations (4.73) and (4.74), it follows that to accurately determine the fluxes, we must accurately determine the segment averages of the quantities in the RHS of (4.74). To this end, we note that:

1. Since the segments σ_i^j are straight segments, the components of the normals are constant along each segment. So using property (4.72) we have that:

$$\langle n_x A\rangle = n_x\langle A\rangle; \qquad \langle n_y A\rangle = n_y\langle A\rangle \tag{4.75}$$

2. The scalar flow variables $\{\rho, P, e, T, a\}$ vary slowly and approach constant values as $\|x\| \longrightarrow \infty$. As a consequence, when evaluating these variables along a segment we can assume that they remain constant along each segment. The constant value will be

assumed to be the value of the variable at the mid-point of the segment. These values will be denoted with the subscript m. Under this assumption one has that:

$$\langle \rho A \rangle = \rho_m \langle A \rangle ; \qquad \langle PA \rangle = P_m \langle A \rangle ; \qquad \langle eA \rangle = e_m \langle A \rangle ; \qquad \langle aA \rangle = a_m \langle A \rangle \quad (4.76)$$

3. The same assumption is not valid for the velocity components u and v since they do not vary slowly and do not approach constant values as $\|x\| \longrightarrow \infty$.

4. Using average properties (4.70)-(4.72) and equations (4.75)-(4.76) in equation (4.74) we get that:

$$\left\langle \vec{F} \cdot \hat{n} \right\rangle =$$

$$\begin{bmatrix} \rho_m n_x \langle u \rangle + \rho_m n_y \langle v \rangle \\ \rho_m n_x \langle uu \rangle + \rho_m n_y \langle uv \rangle + P_m n_x \\ \rho_m n_x \langle vu \rangle + \rho_m n_y \langle vv \rangle + P_m n_y \\ \rho_m n_x e_m \langle u \rangle + \rho_m e_m n_y \langle v \rangle \quad + \frac{1}{2}\rho_m n_x \langle u^3 \rangle + \frac{1}{2}\rho_m n_y \langle u^2 v \rangle + \frac{1}{2}\rho_m n_x \langle v^2 u \rangle \\ + \frac{1}{2}\rho_m n_y \langle v^3 \rangle + P_m n_x \langle u \rangle + P_m n_y \langle v \rangle \end{bmatrix} \quad (4.77)$$

5. So to calculate the fluxes more accurately we must be able to calculate the following segment averages:

$$\langle u \rangle , \langle v \rangle , \left\langle u^2 \right\rangle , \langle uv \rangle , \left\langle v^2 \right\rangle , \left\langle u^3 \right\rangle , \left\langle v^3 \right\rangle , \left\langle vu^2 \right\rangle , \left\langle uv^2 \right\rangle \quad (4.78)$$

The calculation of these segment averages will be discussed in the following subsection.

4.12.3 Segment Averages of Velocity Components

To see how we can calculate the segment averages of equation (4.78), let's rewrite u and v in the following way:

$$u \doteq \overline{u} + qy \doteq \overline{u} + \widetilde{u} \quad (4.79)$$

$$v \doteq \overline{v} - qx \doteq \overline{v} + \widetilde{v} \quad (4.80)$$

By looking at the far-field conditions for u and v (equation (1)), it follows that the far-field conditions for $\overline{u}$ and $\overline{v}$ are:

$$\lim_{\|x\| \longrightarrow \infty} \begin{bmatrix} \overline{u}(x,y) \\ \overline{v}(x,y) \end{bmatrix} = \begin{bmatrix} V_c \cos\alpha \\ V_c \sin\alpha \end{bmatrix}.$$

As a consequence, $\overline{u}$ and $\overline{v}$ far from the perturbing effects of the airfoil vary slowly and approach constant values as $\|x\| \longrightarrow \infty$. Hence they can be assumed to be constant along any segment forming the boundary of any finite volume of reasonable size, i.e.

$$\langle \overline{u} \rangle = \overline{u}_m; \qquad \langle \overline{v} \rangle = \overline{v}_m \tag{4.81}$$

Using these results into equations (4.79)-(4.80) we deduce that:

$$\langle u \rangle = \overline{u}_m + \langle \widetilde{u} \rangle \tag{4.82}$$

$$\langle v \rangle = \overline{v}_m + \langle \widetilde{v} \rangle \tag{4.83}$$

We note that since $\widetilde{u} = qy$ and $\widetilde{v} = -qx$ we can not neglect the spatial variation of $\widetilde{u}$ and $\widetilde{v}$ and the segment averages must be calculated exactly.

Using equations (4.79)-(4.81) and the linearity of segment averages we can express the segment averages of powers of u and v in terms of the segment averages of powers of $\widetilde{u}$ and $\widetilde{v}$.

$$\left\langle u^2 \right\rangle = \left\langle (\overline{u} + \widetilde{u})^2 \right\rangle = \left\langle \overline{u}^2 + 2\overline{u}\widetilde{u} + \widetilde{u}^2 \right\rangle = \overline{u}_m^2 + 2\overline{u}_m \left\langle \widetilde{u} \right\rangle + \left\langle \widetilde{u}^2 \right\rangle$$

$$\left\langle v^2 \right\rangle = \overline{v}_m^2 + 2\overline{v}_m \left\langle \widetilde{v} \right\rangle + \left\langle \widetilde{v}^2 \right\rangle$$

$$\langle uv \rangle = \langle (\overline{u} + \widetilde{u})(\overline{v} + \widetilde{v}) \rangle = \langle \overline{u}\overline{v} + \overline{u}\widetilde{v} + \overline{v}\widetilde{u} + \widetilde{v}\widetilde{u} \rangle = \overline{u}_m \overline{v}_m + \overline{u}_m \langle \widetilde{v} \rangle + \overline{v}_m \langle \widetilde{u} \rangle + \langle \widetilde{u}\widetilde{v} \rangle$$

$$\left\langle u^2 v \right\rangle = \overline{u}_m^2 \overline{v}_m + 2\overline{u}_m \overline{v}_m \left\langle \widetilde{u} \right\rangle + \overline{v}_m \left\langle \widetilde{u}^2 \right\rangle + \overline{u}_m^2 \left\langle \widetilde{v} \right\rangle + 2\overline{u}_m \left\langle \widetilde{u}\widetilde{v} \right\rangle + \left\langle \widetilde{u}^2 \widetilde{v} \right\rangle$$

$$\left\langle v^2 u \right\rangle = \overline{v}_m^2 \overline{u}_m + 2\overline{v}_m \overline{u}_m \left\langle \widetilde{v} \right\rangle + \overline{u}_m \left\langle \widetilde{v}^2 \right\rangle + \overline{v}_m^2 \left\langle \widetilde{u} \right\rangle + 2\overline{v}_m \left\langle \widetilde{v}\widetilde{u} \right\rangle + \left\langle \widetilde{v}^2 \widetilde{u} \right\rangle$$

$$\left\langle v^3 \right\rangle = \overline{v}_m^3 + 3\overline{v}_m^2 \left\langle \widetilde{v} \right\rangle + 3\overline{v}_m \left\langle \widetilde{v}^2 \right\rangle + \left\langle \widetilde{v}^3 \right\rangle$$

$$\left\langle u^3 \right\rangle = \overline{u}_m^3 + 3\overline{u}_m^2 \left\langle \widetilde{u} \right\rangle + 3\overline{u}_m \left\langle \widetilde{u}^2 \right\rangle + \left\langle \widetilde{u}^3 \right\rangle$$

We will compute also the fourth order terms, since they will be required for the Van Leer scheme described in Subsection 4.12.5.

$$\left\langle v^3 u \right\rangle = \overline{u}_m \overline{v}_m^3 + 3\overline{u}_m \overline{v}_m^2 \left\langle \widetilde{v} \right\rangle + 3\overline{u}_m \overline{v}_m \left\langle \widetilde{v}^2 \right\rangle + \overline{u}_m \left\langle \widetilde{v}^3 \right\rangle +$$

$$+\overline{v}_m^3 \left\langle \widetilde{u} \right\rangle + 3\overline{v}_m^2 \left\langle \widetilde{u}\widetilde{v} \right\rangle + 3\overline{v}_m \left\langle \widetilde{u}\widetilde{v}^2 \right\rangle + \left\langle \widetilde{u}\widetilde{v}^3 \right\rangle$$

$$\left\langle u^3 v \right\rangle = \overline{v}_m \overline{u}_m^3 + 3\overline{v}_m \overline{u}_m^2 \left\langle \widetilde{u} \right\rangle + 3\overline{u}_m \overline{v}_m \left\langle \widetilde{u}^2 \right\rangle + \overline{v}_m \left\langle \widetilde{u}^3 \right\rangle$$

$$+\overline{u}_m^3 \left\langle \widetilde{v} \right\rangle + 3\overline{u}_m^2 \left\langle \widetilde{v}\widetilde{u} \right\rangle + 3\overline{u}_m \left\langle \widetilde{v}\widetilde{u}^2 \right\rangle + \left\langle \widetilde{v}\widetilde{u}^3 \right\rangle$$

$$\left\langle u^4 \right\rangle = \overline{u}_m^4 + 4\overline{u}_m^3 \left\langle \widetilde{u} \right\rangle + 6\overline{u}_m^2 \left\langle \widetilde{u}^2 \right\rangle + 4\overline{u}_m \left\langle \widetilde{u}^3 \right\rangle + \left\langle \widetilde{u}^4 \right\rangle$$

$$\left\langle v^4 \right\rangle = \overline{v}_m^4 + 4\overline{v}_m^3 \left\langle \widetilde{v} \right\rangle + 6\overline{v}_m^2 \left\langle \widetilde{v}^2 \right\rangle + 4\overline{v}_m \left\langle \widetilde{v}^3 \right\rangle + \left\langle \widetilde{v}^4 \right\rangle$$

As a consequence, to completely define the velocity averages:

$$\langle u \rangle, \langle v \rangle, \left\langle u^2 \right\rangle, \langle uv \rangle, \left\langle v^2 \right\rangle, \left\langle u^3 \right\rangle, \left\langle v^3 \right\rangle, \left\langle vu^2 \right\rangle, \left\langle uv^2 \right\rangle, \left\langle v^3 u \right\rangle, \left\langle u^3 v \right\rangle, \left\langle u^4 \right\rangle, \left\langle v^4 \right\rangle \tag{4.84}$$

and the flux average $\left\langle \vec{F} \cdot \hat{n} \right\rangle$ along a generic boundary segment we need to calculate:

$$\langle \widetilde{u} \rangle, \langle \widetilde{v} \rangle, \left\langle \widetilde{u}^2 \right\rangle, \langle \widetilde{u}\widetilde{v} \rangle, \left\langle \widetilde{v}^2 \right\rangle, \left\langle \widetilde{u}^3 \right\rangle, \left\langle \widetilde{v}^3 \right\rangle, \left\langle \widetilde{v}\widetilde{u}^2 \right\rangle, \left\langle \widetilde{u}\widetilde{v}^2 \right\rangle \left\langle \widetilde{v}^3\widetilde{u} \right\rangle, \left\langle \widetilde{u}^3\widetilde{v} \right\rangle, \left\langle \widetilde{u}^4 \right\rangle, \left\langle \widetilde{v}^4 \right\rangle \tag{4.85}$$

4.12.4 Segment Averages of $\widetilde{u}$ and $\widetilde{v}$

By definition, $\widetilde{u}$ and $\widetilde{v}$ are given by

$$\widetilde{u} = qy \tag{4.86}$$

$$\widetilde{v} = -qx \tag{4.87}$$

From the definition of segment averages it follows that to calculate $\langle \widetilde{u} \rangle$ and $\langle \widetilde{v} \rangle$ we must perfom the integrations $\frac{1}{\ell}\int_\ell \widetilde{u}\, d\ell$ and $\frac{1}{\ell}\int_\ell \widetilde{v}\, d\ell$, respectively, along all the straight segments $\ell = \sigma_i^j$.

To get a general expression, let's consider an generic straight segment of length ℓ with ends defined by the coordinates (x_0, y_0) and (x_1, y_1). So any point (x, y) on the line segment can be parameterized by

$$\begin{bmatrix} x \\ y \end{bmatrix} = \begin{bmatrix} x_0 \\ y_0 \end{bmatrix} (1-\lambda) + \begin{bmatrix} x_1 \\ y_1 \end{bmatrix} \lambda \tag{4.88}$$

with $\lambda \in [0, 1]$. Using the above parameterization the differential of length $d\ell$ is given by:

$$d\ell = \sqrt{dx^2 + dy^2} = \sqrt{(x_1 - x_0)^2 + (y_1 - y_0)^2} d\lambda = \ell\, d\lambda \tag{4.89}$$

As a consequence we have:

$$\langle A \rangle = \frac{1}{\ell}\int_\ell A(x, y)\, d\ell = \int_0^1 A(x(\lambda), y(\lambda))\, d\lambda \tag{4.90}$$

We can use equation (4.90) to calculate segment averages. Let's start by considering the calculation of $\langle\widetilde{u}\rangle$ and $\langle\widetilde{v}\rangle$

$$\langle\widetilde{u}\rangle = \int_0^1 \widetilde{u}\, d\lambda = \int_0^1 qy\, d\lambda = q\int_0^1 \left[y_0(1-\lambda) + y_1\lambda\right]\, d\lambda$$

$$\langle\widetilde{v}\rangle = \int_0^1 \widetilde{v}\, d\lambda = \int_0^1 -qx\, d\lambda = -q\int_0^1 \left[x_0(1-\lambda) + x_1\lambda\right]\, d\lambda$$

Performing the integrations we get that:

$$\langle\widetilde{u}\rangle = q\frac{(y_0+y_1)}{2} \quad \text{and} \quad \langle\widetilde{v}\rangle = -q\frac{(x_0+x_1)}{2}$$

Proceeding similarly it is possible to get all the segment averages associated with powers of $\widetilde{u}$ and $\widetilde{v}$. The resulting segment averages are:

$$\left\langle\widetilde{u}^2\right\rangle = q^2\frac{1}{3}\left(y_0^2 + y_1y_0 + y_1^2\right)$$

$$\left\langle\widetilde{v}^2\right\rangle = q^2\frac{1}{3}\left(x_1^2 + x_0x_1 + x_0^2\right)$$

$$\left\langle\widetilde{u}\widetilde{v}\right\rangle = -q^2\frac{1}{6}\left(2y_1x_1 + y_0x_1 + y_1x_0 + 2y_0x_0\right)$$

$$\left\langle\widetilde{u}\widetilde{v}^2\right\rangle = q^3\frac{1}{12}\left(3x_1^2y_1 + x_1^2y_0 + 2x_1y_1x_0 + 2x_1y_0x_0 + y_1x_0^2 + 3x_0^2y_0\right)$$

$$\left\langle\widetilde{u}^2\widetilde{v}\right\rangle = -q^3\frac{1}{12}\left(y_0^2x_1 + 3x_1y_1^2 + 2y_0x_1y_1 + y_1^2x_0 + 3x_0y_0^2 + 2y_1x_0y_0\right)$$

$$\left\langle\widetilde{v}^3\right\rangle = -q^3\frac{1}{4}\left(x_1 + x_0\right)\left(x_1^2 + x_0^2\right)$$

$$\left\langle\widetilde{u}^3\right\rangle = q^3\frac{1}{4}\left(y_1 + y_0\right)\left(y_1^2 + y_0^2\right)$$

$$\left\langle\widetilde{v}^3\widetilde{u}\right\rangle = -q^4\frac{1}{20}\left(x_0^3y_1 + 4x_0^3y_0 + 2x_0^2x_1y_1 + 3x_0^2y_0x_1 + 3x_0x_1^2y_1 + 2x_0y_0x_1^2 + 4x_1^3y_1 + y_0x_1^3\right)$$

$$\left\langle \widetilde{u}^3\widetilde{v}\right\rangle = -q^4\frac{1}{20}\left(3x_0y_1y_0^2 + 4x_0y_0^3 + x_0y_1^3 + 2x_0y_1^2y_0 + y_0^3x_1 + 3y_0x_1y_1^2 + 2y_0^2x_1y_1 + 4x_1y_1^3\right)$$

$$\begin{aligned}\left\langle \widetilde{u}^2\widetilde{v}^2\right\rangle &= q^4\frac{1}{30}\times\left(y_0^2x_1^2 + 6x_1^2y_1^2 + 3x_1^2y_1y_0 + 4x_0y_1y_0x_1 + \right.\\ &\qquad \left. + 3x_1x_0y_1^2 + 3x_0y_0^2x_1 + x_0^2y_1^2 + 3x_0^2y_1y_0 + 6x_0^2y_0^2\right)\end{aligned}$$

$$\left\langle \widetilde{v}^4\right\rangle = q^4\frac{1}{5}\left(x_0^4 + x_0^3x_1 + x_0^2x_1^2 + x_0x_1^3 + x_1^4\right)$$

$$\left\langle \widetilde{u}^4\right\rangle = q^4\frac{1}{5}\left(y_0^4 + y_0^3y_1 + y_0^2y_1^2 + y_0y_1^3 + y_1^4\right)$$

The above relationships define the required segment averages (4.85) associated with $\widetilde{u}$ and $\widetilde{v}$. These averages are given functions of the position coordinates (x_0, y_0) and (x_1, y_1) of the ends of the segment being considered. They also depend on the particular value of the pitch rate q. Once these segment averages are calculated, we can determine the velocity averages (4.84). Finally, after determining the velocity averages, the flux average $\left\langle \vec{F}\cdot\hat{n}\right\rangle$ (i.e the accurate fluxes along the boundary segments σ_i^j) can be determined from equation (4.77).

4.12.5 Segment Average of van Leer's Flux Splitting

Luckily, the same proceeding used to evaluate the segment averages of standard fluxes can be used to evaluate the segment average $\left\langle \vec{F}\cdot\hat{n}\right\rangle$ for van Leer's Flux Splitting scheme. The two-dimensional van Leer's Flux Splitting scheme is given by:

$$\vec{F}\cdot\hat{n} = \begin{bmatrix} f_1^+ \\ f_2^+ \\ f_3^+ \\ f_4^+ \end{bmatrix} + \begin{bmatrix} f_1^- \\ f_2^- \\ f_3^- \\ f_4^- \end{bmatrix}$$

where

$$f_1^+ = \frac{1}{4}\frac{\rho}{a}([un_x + vn_y] + a)^2 = \frac{1}{4}\frac{\rho}{a}([un_x + vn_y]^2 + 2a\left[un_x + vn_y\right] + a^2)$$

$$f_2^+ = \frac{1}{4}\frac{\rho}{a}([un_x + vn_y]^2 + 2a\left[un_x + vn_y\right] + a^2)\left(\frac{n_x}{\gamma}(2a - [un_x + vn_y]) + u\right)$$

$$f_3^+ = \frac{1}{4}\frac{\rho}{a}([un_x + vn_y]^2 + 2a\,[un_x + vn_y] + a^2)\left(\frac{n_y}{\gamma}(2a - [un_x + vn_y]) + v\right)$$

$$f_4^+ = \frac{1}{4}\frac{\rho}{a}([un_x + vn_y]^2 + 2a\,[un_x + vn_y] + a^2)\frac{1}{\gamma^2 - 1}\left(-(\gamma - 1)\,[un_x + vn_y]^2\right) +$$

$$+\frac{1}{4}\frac{\rho}{a}([un_x + vn_y]^2 + 2a\,[un_x + vn_y] + a^2)\frac{1}{\gamma^2 - 1}\left(2(\gamma - 1)\,a\,[un_x + vn_y]\right) +$$

$$+\frac{1}{4}\frac{\rho}{a}([un_x + vn_y]^2 + 2a\,[un_x + vn_y] + a^2)\frac{1}{\gamma^2 - 1}2a^2 +$$

$$+\frac{1}{4}\frac{\rho}{a}([un_x + vn_y]^2 + 2a\,[un_x + vn_y] + a^2)\frac{1}{2}\left(u^2 + v^2\right)$$

The expressions for f_1^-, f_2^-, f_3^-, and f_4^- are similar (except by the sign in some of the terms) to the expressions for f_1^+, f_2^+, f_3^+, and f_4^+, respectively.

To calculate

$$\left\langle \vec{F}\cdot\hat{n}\right\rangle = \begin{bmatrix} \left\langle f_1^+\right\rangle \\ \left\langle f_2^+\right\rangle \\ \left\langle f_3^+\right\rangle \\ \left\langle f_4^+\right\rangle \end{bmatrix} + \begin{bmatrix} \left\langle f_1^-\right\rangle \\ \left\langle f_2^-\right\rangle \\ \left\langle f_3^-\right\rangle \\ \left\langle f_4^-\right\rangle \end{bmatrix}$$

we need to determine the segment averages for

$$\left\langle f_1^+\right\rangle,\quad \left\langle f_2^+\right\rangle,\quad \left\langle f_3^+\right\rangle,\quad \left\langle f_4^+\right\rangle,\quad \left\langle f_1^-\right\rangle,\quad \left\langle f_2^-\right\rangle,\quad \left\langle f_3^-\right\rangle,\quad \left\langle f_4^-\right\rangle$$

From the definition of f_1^+, f_2^+, f_3^+, and f_4^+ then it follows that the above segment averages can be calculated if the following averages are determined:

$$\langle [un_x + vn_y]\rangle = [\langle u\rangle\, n_x + \langle v\rangle\, n_y]$$

$$\left\langle [un_x + vn_y]^2\right\rangle = \left\langle u^2n_x^2 + 2uvn_xn_y + v^2n_y^2\right\rangle = \left\langle u^2\right\rangle n_x^2 + 2\langle uv\rangle\, n_xn_y + \left\langle v^2\right\rangle n_y^2$$

$$\left\langle [un_x + vn_y]^3\right\rangle = \left\langle u^3n_x^3 + 3u^2vn_x^2n_y + 3uv^2n_xn_y^2 + v^3n_y^3\right\rangle$$

$$\left\langle [un_x + vn_y]^3\right\rangle = \left\langle u^3\right\rangle n_x^3 + 3\left\langle u^2v\right\rangle n_x^2n_y + 3\left\langle uv^2\right\rangle n_xn_y^2 + \left\langle v^3\right\rangle n_y^3$$

$$\left\langle [un_x + vn_y]^4\right\rangle = \left\langle u^4\right\rangle n_x^4 + 4\left\langle u^3v\right\rangle n_x^3n_y + 6\left\langle u^2v^2\right\rangle n_x^2n_y^2 + 4\left\langle uv^3\right\rangle n_y^3n_x + \left\langle v^4\right\rangle n_y^4$$

$$\left\langle [un_x + vn_y]\,u^2\right\rangle = \left[\left\langle u^3\right\rangle n_x + \left\langle vu^2\right\rangle n_y\right]$$

$$\left\langle [un_x + vn_y]\,v^2\right\rangle = \left[\left\langle uv^2\right\rangle n_x + \left\langle v^3\right\rangle n_y\right]$$

$$\left\langle [un_x + vn_y]^2\,u^2\right\rangle = \left\langle u^4\right\rangle n_x^2 + 2\left\langle u^3v\right\rangle n_xn_y + \left\langle u^2v^2\right\rangle n_y^2$$

$$\left\langle [un_x + vn_y]^2\,v^2\right\rangle = \left\langle u^2v^2\right\rangle n_x^2 + 2\left\langle uv^3\right\rangle n_xn_y + \left\langle v^4\right\rangle n_y^2$$

In turn these averages can be calculated once the velocity averages (4.84) are determined.

4.13 Evaluation of the Volume Integral

Now we address the problem of getting a more accurate evaluation of the volume integral associated to the source term W:

$$\int_{\tau^j} W \, d\tau \tag{4.91}$$

From equation (4.18) one knows that:

$$\begin{bmatrix} \Omega_x \\ \Omega_y \end{bmatrix} = \begin{bmatrix} q^2 x - qV_c \sin\alpha \\ q^2 y + qV_c \cos\alpha \end{bmatrix} \tag{4.92}$$

Using the definitions of u_c and v_c and the definitions of $\widetilde{u}$ and $\widetilde{v}$ (equations (4.86)-(4.87)) one can rewrite equation (4.92) as

$$\begin{bmatrix} \Omega_x \\ \Omega_y \end{bmatrix} = \begin{bmatrix} -q\widetilde{v} + qv_c \\ q\widetilde{u} - qu_c \end{bmatrix} \tag{4.93}$$

Inserting this expression into the definition of W (equation (4.17)), one gets

$$W(Q,\vec{x}) = \begin{bmatrix} 0 \\ \rho\left(-q\widetilde{v} + qv_c\right) + 2\rho qv \\ \rho\left(q\widetilde{u} - qu_c\right) - 2\rho qu \\ \rho\left(-q\widetilde{v} + qv_c\right)u + \rho\left(q\widetilde{u} - qu_c\right)v \end{bmatrix} = \begin{bmatrix} 0 \\ -\rho q\widetilde{v} + \rho qv_c + 2\rho qv \\ \rho q\widetilde{u} - \rho qu_c - 2\rho qu \\ -\rho q\widetilde{v}u + \rho qv_c u + \rho q\widetilde{u}v - \rho qu_c v \end{bmatrix} \tag{4.94}$$

As a consequence the volume integral of the source term W over any finite volume τ^j can be written as:

$$\int_{\tau^j} W(Q(\vec{x}),\vec{x}) \, d\tau = \begin{bmatrix} 0 \\ -\int_{\tau^j} \rho q\widetilde{v} \, d\tau + \int_{\tau^j} \rho qv_c \, d\tau + 2\int_{\tau^j} \rho qv \, d\tau \\ \int_{\tau^j} \rho q\widetilde{u} \, d\tau - \int_{\tau^j} \rho qu_c \, d\tau - 2\int_{\tau^j} \rho qu \, d\tau \\ -\int_{\tau^j} \rho q\widetilde{v}u \, d\tau + \int_{\tau^j} \rho qv_c u \, d\tau + \int_{\tau^j} \rho q\widetilde{u}v \, d\tau - \int_{\tau^j} \rho qu_c v \, d\tau \end{bmatrix} \tag{4.95}$$

Using the following observations:

1. q, u_c and v_c are constants
2. The density ρ can be assumed to remain constant over the control-volumes τ^j. Its constant value is assumed to be equal to the density at the inner node of the finite-volume: $\rho = \rho(\vec{x}^j) = \rho^j$

the volume integral (4.95)) can be simplified to

$$\int_{\tau^j} W(Q(\vec{x}),\vec{x})\ d\tau = \begin{bmatrix} 0 \\ -\rho^j q \int_{\tau^j} \widetilde{v}\ d\tau + \rho^j q v_c \tau^j + 2\rho^j q \int_{\tau^j} v\ d\tau \\ \rho^j q \int_{\tau^j} \widetilde{u}\ d\tau - \rho^j q u_c \tau^j - 2\rho^j q \int_{\tau^j} u\ d\tau \\ -\rho^j q \int_{\tau^j} \widetilde{v}u\ d\tau + \rho^j q v_c \int_{\tau^j} u\ d\tau + \rho^j q \int_{\tau^j} \widetilde{u}v\ d\tau - \rho^j q u_c \int_{\tau^j} v\ d\tau \end{bmatrix} \tag{4.96}$$

If we approximate the above integrals by:

$$\int_{\tau^j} \widetilde{v}\ d\tau \approx \widetilde{v}^j\tau^j; \qquad \int_{\tau^j} \widetilde{u}\ d\tau = \widetilde{u}^j\tau^j; \qquad \int_{\tau^j} v\ d\tau = v^j\tau^j; \qquad \int_{\tau^j} u\ d\tau = u^j\tau^j;$$

$$\int_{\tau^j} \widetilde{v}u\ d\tau = \widetilde{v}^j u^j \tau^j; \qquad \int_{\tau^j} \widetilde{u}v\ d\tau = \widetilde{u}^j v^j \tau^j$$

equation (4.96) reduces to the expresion:

$$\int_{\tau^j} W(Q(\vec{x}),\vec{x})\ d\tau = W(Q(\vec{x}^j),\vec{x}^j)\tau^j$$

which is exactly the first order approximation used to calculate the residual R^j in equation (4.56). If we want to calculate more accurately the volume integral of the source term W we must calculate the volume integrals

$$\int_{\tau^j} \widetilde{v}\ d\tau; \qquad \int_{\tau^j} \widetilde{u}\ d\tau; \qquad \int_{\tau^j} v\ d\tau; \qquad \int_{\tau^j} u\ d\tau; \qquad \int_{\tau^j} \widetilde{v}u\ d\tau; \qquad \int_{\tau^j} \widetilde{u}v\ d\tau \tag{4.97}$$

more accurately.

To this end, first, we use the definitions given in equations (4.79)-(4.80) to rewrite the integrals containing u and v terms as:

$$\int_{\tau^j} v\ d\tau = \int_{\tau^j} \overline{v}\ d\tau + \int_{\tau^j} \widetilde{v}\ d\tau; \qquad \int_{\tau^j} u\ d\tau = \int_{\tau^j} \overline{u}\ d\tau + \int_{\tau^j} \widetilde{u}\ d\tau \tag{4.98}$$

$$\int_{\tau^j} \widetilde{v}u\ d\tau = \int_{\tau^j} \widetilde{v}\overline{u}\ d\tau + \int_{\tau^j} \widetilde{v}\widetilde{u}\ d\tau; \qquad \int_{\tau^j} \widetilde{u}v\ d\tau = \int_{\tau^j} \widetilde{u}\overline{v}\ d\tau + \int_{\tau^j} \widetilde{u}\widetilde{v}\ d\tau \tag{4.99}$$

Since $\overline{u}$ and $\overline{v}$ remain approximately constant along the finite volume, the integrals (4.98)-(4.99) can be simplified to:

$$\int_{\tau^j} v\ d\tau = \overline{v}^j\tau^j + \int_{\tau^j} \widetilde{v}\ d\tau; \qquad \int_{\tau^j} u\ d\tau = \overline{u}^j\tau^j + \int_{\tau^j} \widetilde{u}\ d\tau \tag{4.100}$$

$$\int_{\tau^j} \widetilde{v}u \; d\tau = \overline{u}^j \int_{\tau^j} \widetilde{v} \; d\tau + \int_{\tau^j} \widetilde{v}\widetilde{u} \; d\tau; \qquad \int_{\tau^j} \widetilde{u}v \; d\tau = \overline{v}^j \int_{\tau^j} \widetilde{u} \; d\tau + \int_{\tau^j} \widetilde{u}\widetilde{v} \; d\tau \tag{4.101}$$

Replacing equations (4.100) and (4.101) into equation (4.98) we get:

$$\int_{\tau^j} W(Q(\vec{x}), \vec{x}) \; d\tau = \begin{bmatrix} 0 \\ -\rho^j q \int_{\tau^j} \widetilde{v} \; d\tau + \rho^j q v_c \tau^j \\ \rho^j q \int_{\tau^j} \widetilde{u} \; d\tau - \rho^j q u_c \tau^j \\ -\rho^j q \left(\overline{u}^j \int_{\tau^j} \widetilde{v} \; d\tau + \int_{\tau^j} \widetilde{v}\widetilde{u} \; d\tau \right) + \rho^j q v_c \left(\overline{u}^j \tau^j + \int_{\tau^j} \widetilde{u} \; d\tau \right) \end{bmatrix} +$$

$$+ \begin{bmatrix} 0 \\ +2\rho^j q \left(\overline{v}^j \tau^j + \int_{\tau^j} \widetilde{v} \; d\tau \right) \\ -2\rho^j q \left(\overline{u}^j \tau^j + \int_{\tau^j} \widetilde{u} \; d\tau \right) \\ +\rho^j q \left(\overline{v}^j \int_{\tau^j} \widetilde{u} \; d\tau + \int_{\tau^j} \widetilde{u}\widetilde{v} \; d\tau \right) - \rho^j q u_c \left(\overline{v}^j \tau^j + \int_{\tau^j} \widetilde{v} \; d\tau \right) \end{bmatrix} \tag{4.102}$$

As a consequence, to calculate $\int_{\tau^j} W \; d\tau$ with a higher accuracy we must calculate the following three volume integrals:

$$\int_{\tau^j} \widetilde{v} \; d\tau; \qquad \int_{\tau^j} \widetilde{u} \; d\tau; \qquad \int_{\tau^j} \widetilde{v}\widetilde{u} \; d\tau$$

These three integrals can be calculated using the definitions $\widetilde{u} = qy$ and $\widetilde{v} = -qx$ as follows:

$$\int_{\tau^j} \widetilde{v} \; d\tau = -q \int_{\tau^j} x \; d\tau = -q \int_{\tau^j} \frac{\partial}{\partial x} \left(\frac{1}{2} x^2 \right) \; d\tau = -q \int_{\tau^j} \nabla \cdot \left(\frac{1}{2} x^2 \hat{e}_x + 0 \hat{e}_y \right) \; d\tau$$

$$\int_{\tau^j} \widetilde{u} \; d\tau = q \int_{\tau^j} y \; d\tau = q \int_{\tau^j} \frac{\partial}{\partial y} \left(\frac{1}{2} y^2 \right) \; d\tau = q \int_{\tau^j} \nabla \cdot \left(0 \hat{e}_x + \frac{1}{2} y^2 \hat{e}_y \right) \; d\tau$$

$$\int_{\tau^j} \widetilde{v}\widetilde{u} \; d\tau = -q^2 \int_{\tau^j} yx \; d\tau = -q^2 \int_{\tau^j} \frac{\partial}{\partial y} \left(\frac{1}{2} x y^2 \right) \; d\tau = -q^2 \int_{\tau^j} \nabla \cdot \left(0 \hat{e}_x + \frac{1}{2} x y^2 \hat{e}_y \right) \; d\tau$$

Using the Divergence Theorem we get:

$$\int_{\tau^j} \widetilde{v} \; d\tau = -q \int_{\sigma^j} \left(\frac{1}{2} x^2 \hat{\imath} + 0 \hat{\jmath} \right) \cdot \hat{n} \; d\sigma^j = -q \int_{\sigma^j} \frac{1}{2} x^2 n_x \; d\sigma^j$$

$$\int_{\tau^j} \widetilde{u} \; d\tau = q \int_{\sigma^j} \left(0 \hat{e}_x + \frac{1}{2} y^2 \hat{e}_y \right) \cdot \hat{n} \; d\sigma^j = q \int_{\sigma^j} \frac{1}{2} y^2 n_y \; d\sigma^j$$

$$\int_{\tau^j} \widetilde{v}\widetilde{u}\ d\tau = -q^2 \int_{\sigma^j} \left(0\hat{e}_x + \frac{1}{2}xy^2\hat{e}_y\right) \cdot \hat{n}\ d\sigma^j = -q^2 \int_{\sigma^j} \frac{1}{2}xy^2 n_y\ d\sigma^j$$

where σ^j is the surface enclosing τ^j.

Since in our case σ^j is formed by union of k^j straight segments σ_i^j we can write the above equations as

$$\int_{\tau^j} \widetilde{v}\ d\tau = -q\frac{1}{2}n_x \sum_{i=1}^{k^j} \int_{\sigma_i^j} x^2\ d\sigma_i^j = -\frac{1}{2q}n_x \sum_{i=1}^{k^j} \left(\int_{\sigma_i^j} q^2x^2\ d\sigma_i^j\right)$$

$$\int_{\tau^j} \widetilde{u}\ d\tau = \frac{1}{2}n_y q \sum_{i=1}^{k^j} \int_{\sigma_i^j} y^2\ d\sigma_i^j = \frac{1}{2q}n_y \sum_{i=1}^{k^j} \left(\int_{\sigma_i^j} q^2y^2\ d\sigma_i^j\right)$$

$$\int_{\tau^j} \widetilde{v}\widetilde{u}\ d\tau = -\frac{1}{2}n_y q^2 \sum_{i=1}^{k^j} \int_{\sigma_i^j} xy^2\ d\sigma_i^j = -\frac{1}{2q}n_y \sum_{i=1}^{k^j} \left(\int_{\sigma_i^j} qxq^2y^2\ d\sigma_i^j\right)$$

Using the definitions of $\widetilde{u}$ and $\widetilde{v}$ we can write the three above integrals as:

$$\int_{\tau^j} \widetilde{v}\ d\tau = -\frac{1}{2q}n_x \sum_{i=1}^{k^j} \left(\int_{\sigma_i^j} \widetilde{v}^2\ d\sigma_i^j\right)$$

$$\int_{\tau^j} \widetilde{u}\ d\tau = \frac{1}{2q}n_y \sum_{i=1}^{k^j} \left(\int_{\sigma_i^j} \widetilde{u}^2\ d\sigma_i^j\right)$$

$$\int_{\tau^j} \widetilde{v}\widetilde{u}\ d\tau = \frac{1}{2q}n_y \sum_{i=1}^{k^j} \left(\int_{\sigma_i^j} \widetilde{v}\widetilde{u}^2\ d\sigma_i^j\right)$$

Finally from the definition of segment averages (equation (4.69)) we get that:

$$\int_{\tau^j} \widetilde{v}\ d\tau = -\frac{1}{2q}n_x \sum_{i=1}^{k^j} \sigma_i^j \left\langle \widetilde{v}^2 \right\rangle_i^j \tag{4.103}$$

$$\int_{\tau^j} \widetilde{u}\ d\tau = \frac{1}{2q}n_y \sum_{i=1}^{k^j} \sigma_i^j \left\langle \widetilde{u}^2 \right\rangle_i^j \tag{4.104}$$

$$\int_{\tau^j} \widetilde{v}\widetilde{u}\, d\tau = \frac{1}{2q} n_y \sum_{i=1}^{k^j} \sigma_i^j \left\langle \widetilde{v}\widetilde{u}^2 \right\rangle_i^j \tag{4.105}$$

From these three equations it follows that once the segment averages $\langle \widetilde{v}^2 \rangle, \langle \widetilde{v}^2 \rangle$ and $\langle \widetilde{v}\widetilde{u}^2 \rangle$ are calculated then equation (4.102) can be used to get a more accurate evaluation of the source terms.

Note. A similar method to the one presented in this section has been applied by Holmes and Tong [25] to turbomachinery flows for getting more accurate numerical simulations.

4.14 Numerical Results using Accurate Residuals

We have modified the `NISFLOW Code` in order to calculate the residuals $R^j(\hat{Q})$ using the more accurate expressions obtained in Sections 4.12 and 4.13. We will call this improved code `A-NISFLOW Code` (where the "`A`" stands for Accurate). The approximate Jacobian $\frac{\partial \hat{R}(\hat{Q})}{\partial \hat{Q}}$ employed to get `A-NISFLOW` solutions is the same approximate Jacobian used in the original `NISFLOW Code`.

In Figures (4.10) are shown the `A-NISFLOW` solutions corresponding to the cases shown in Figures (4.9) obtained using `NISFLOW`. Figures (4.10)(a)-(b) should be compared with Figures (4.9)(a)-(b) and Figures (4.10)(c)-(d) should be compared with Figures (4.9)(c)-(d). The close-view solutions seem very similar, and the same can be said for the streamlines shapes. However, when looking at the pressure coefficient contours it is clear that the solutions obtained using `A-NISFLOW` show the correct behavior, i.e. the pressure coefficient goes to zero as $\|\vec{x}\| \longrightarrow \infty$.

As the `NISFLOW Code` does, the `A-NISFLOW Code` allows us to simulate the flow corresponding to generalized aerodynamically steady motions. In particular, it is possible to construct functions of the form (4.64) using this accurate code. In Table (4.1) we show the values of the aerodynamic coefficients C_ℓ and C_m for the NACA 0012 airfoil obtained using `A-NISFLOW` for different Mach numbers and different pitch-rates $\hat{q}$ at $\alpha = 0.0^o$. Also, between parentheses the values obtained using `NISFLOW` are shown. The error of the `NISFLOW` solutions is less equal than 2% for the subsonic cases and less equal than 3% for the transonic case. These results show that the inaccuracies of `NISFLOW` in the evaluation of the residuals does not seem to have a large impact on the pressure distributions. This result can also be seeing in Figure (4.11) where the pressure coefficient distributions using the `A-NISFLOW Code` and the `NISFLOW` for the most sensitive case ($\hat{q} = 0.05$) are compared. For the case $M_c = 0.2$, $\alpha = 0.0^o$ shown in Figure (4.11a) the pressure distributions are nearly identical. For the case $M_c = 0.8$, $\alpha = 0.0^o$ shown in Figure (4.11b) there is also a good agreement, except near the shock (located on the lower surface) where `A-NISFLOW` seems to be better able to capture the shock (compare the peaks before the shock).

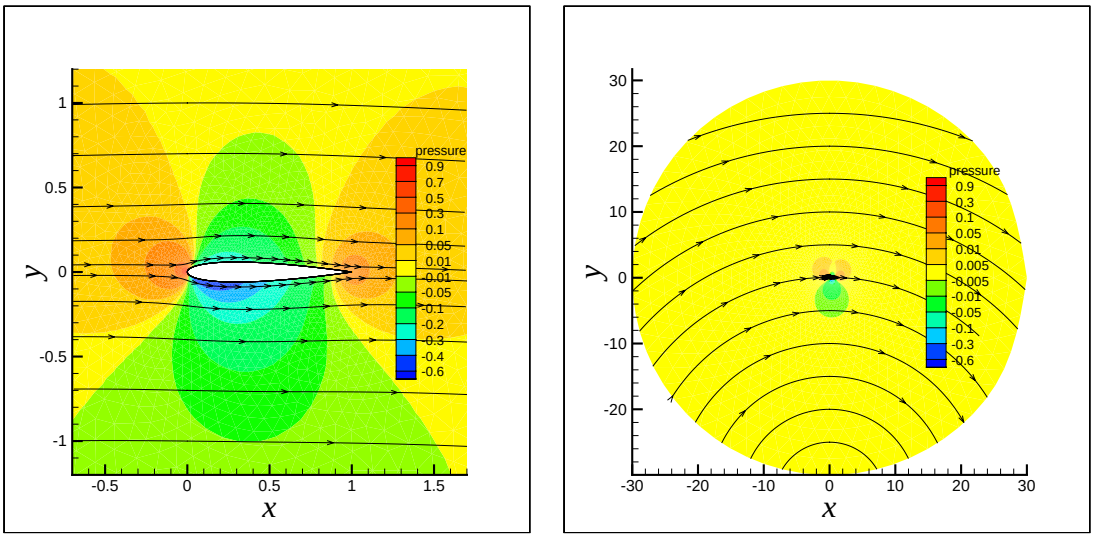

(a) Close-view, $M_c = 0.2$, $\hat{q} = 0.03$

(b) Wide-view, $M_c = 0.2$, $\hat{q} = 0.03$

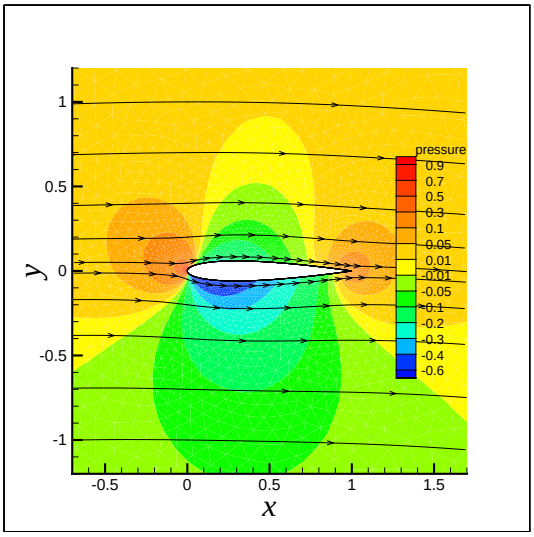

(c) Close-view, $M_c = 0.2$, $\hat{q} = 0.05$

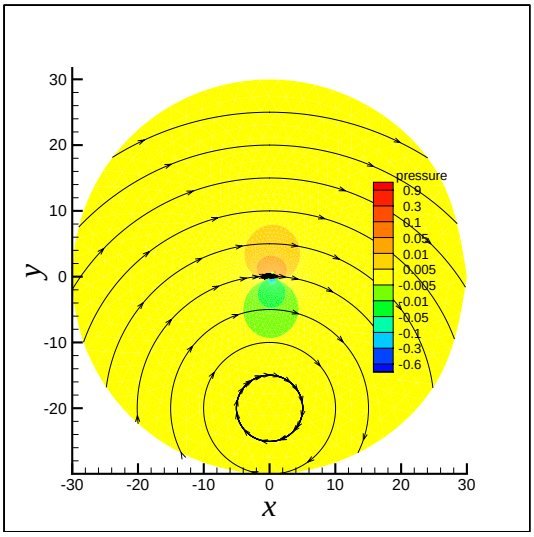

(d) Wide-view, $M_c = 0.2$, $\hat{q} = 0.05$

Figure 4.10: Pressure contours and velocity streamlines, obtained using the `A-NISFLOW Code`, for the air passing around a NACA 0012 airfoil moving in a steady circular trajectory at Mach $M_c = 0.2$, $\alpha = 0^o$ and with pitch rates $\hat{q} = 0.03$ and $\hat{q} = 0.05$.

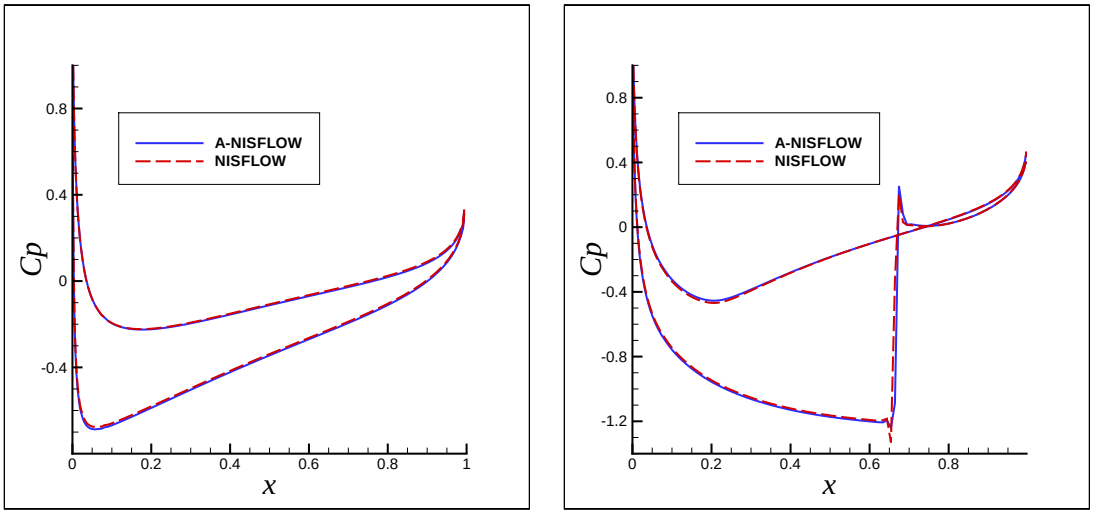

(a) $M_c = 0.2$, $\hat{q} = 0.05$ (b) $M_c = 0.8$, $\hat{q} = 0.05$

Figure 4.11: Pressure coefficient distributions along the surface of a NACA 0012 airfoil moving in steady circular motion. The airfoil is flying with $\alpha = 0^o$ and $\hat{q} = 0.05$.

The impact of grid discretization on the numerical solutions seems to follows the same patterns as classical (uniform flows) CFD solutions. The flow solutions improve with finer meshes at the expense of more computational time. For transonic flows, grids must be adjusted in order to get an accurate shock capture. In Table (4.2) we show the numerical values of lift, drag and pitching-moment coefficients of the NACA 0012 airfoil obtained for different grids for the most difficult case: $M_c = 0.8$, $\hat{q} = 0.05$ (strong shock at the lower surface and extremely high pitch rate). Grid 4 is the grid used in all other numerical calculations presented in this work. The `A-NISFLOW` solutions vary slightly for the four finest grids with a variation of less than 0.8% in the lift coefficient. The variation in the drag coefficient is of the same order (0.0004) as the variation in the drag coefficient at that Mach number for the standard classical case (uniform flow, $\hat{q} = 0.0$). The main contribution to these variations may be due to inaccuracies introduced by the strong shock located on the lower surface of the airfoil and to the fact that the grids had not been optimized to handle that shock. The `NISFLOW` solutions (shown between parentheses) show a much larger variation in the lift coefficient for the four finest grids (2.3%). Furthermore, a comparison of the values obtained with the coarsest grids (Grid 1 and Grid 2) seems to show that a major improvement is obtained in the lift and pitching-moment coefficients if the more accurate `A-NISFLOW Code` is used on such grids.

In Figures (4.12) we show a close view of the flow behavior around the NACA 0012 airfoil for the transonic case $M_c = 0.8$ and $\alpha = 0.0$ at different pitch-rates. It is particularly, interesting to note how the pressure coefficient changes as the pitch rate q increases (nose-

$M_c = 0.8,\ \hat{q} = 0.05$				
	N (gridpoints)	C_ℓ	C_d	C_m
Grid 1	1602	-0.4997 (-0.4662)	0.0205 (0.0191)	-0.2025 (-0.1885)
Grid 2	1739	-0.5005 (-0.4461)	0.0200 (0.0188)	-0.2015 (-0.1820)
Grid 3	6439	-0.4947 (-0.4871)	0.0176 (0.0173)	-0.1996 (-0.1965)
Grid 4	6691	-0.4980 (-0.4826)	0.0176 (0.0171)	-0.2005 (-0.1946)
Grid 5	10631	-0.4942 (-0.4789)	0.0172 (0.0166)	-0.1984 (-0.1926)
Grid 6	12300	-0.4967 (-0.4903)	0.0174 (0.0172)	-0.1999 (-0.1975)

Table 4.2: Variation of lift, drag and pitching-moment coefficients due to the use of different grids for the case of a NACA 0012 airfoil. The numbers between parentheses were obtained using the `NISFLOW Code`. The numbers without parentheses were obtained using the `A-NISFLOW Code`.

down). Observe that when $\hat{q} = 0$ there are two symmetric shocks, one on the upper surface and one on the lower surface. As $\hat{q}$ increases, the shock in the upper surface tends to decrease until disappearing. On the other hand the shock in the lower surface gets stronger as $\hat{q}$ increases. It is clear then that a more negative lift is produced as pitch-rate increases.

The results obtained using the aerodynamic model presented here were compared with the results obtained using *Etkin's Camber Theory* ([13] pp. 269-271). This theory is based on the approximation of thin airfoils and assumes linearity of the flow. It simulates the kinematics of the rotating flow due to the pitch-rate q by changing the camber of the airfoil according to the following law:

$$x' = x \quad y' = y + \frac{1}{2}\frac{q}{V_c}x^2 \tag{4.106}$$

As a consequence, if the effect of the pitch-rate q on an airfoil with coordinates (x, y) is desired, then the same effect can be reached if a transformed airfoil with coordinates x', y' is simulated in a rectilinear uniform flow ($q' = 0$).

The comparison of our results and the ones obtained using Etkin's Camber Theory are shown in Figures (4.13), and (4.14) for the cases $M_c = 0.2$, $M_c = 0.5$ and $M_c = 0.8$. The agreement at subsonic Mach numbers is really surprising. Particularly at low $\hat{q}$'s the coincidence is perfect. Observe that at the subsonic cases C_ℓ and C_m behave as linear functions of the pitch-rate. This result justifies why Bryan's linearized theory works so well, and remains the basis of many currently used aerodynamic models.

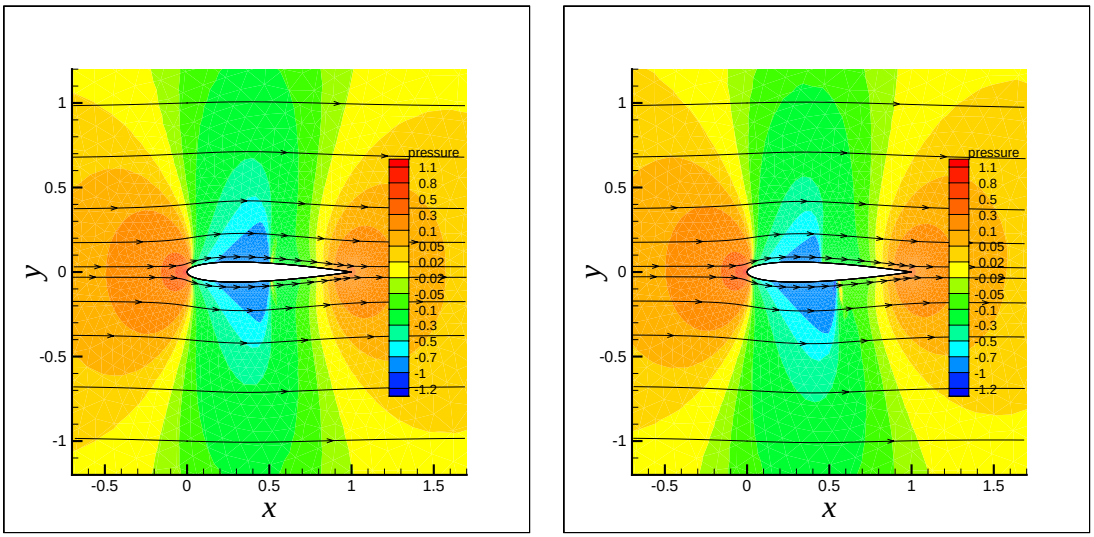

(a) Close-view, $M_c = 0.8$, $\hat{q} = 0.0$

(b) Close-view, $M_c = 0.8$, $\hat{q} = 0.01$

(c) Close-view, $M_c = 0.8$, $\hat{q} = 0.03$

(d) Close-view, $M_c = 0.8$, $\hat{q} = 0.05$

Figure 4.12: Pressure contours and velocity streamlines, obtained using the `A-NISFLOW Code`, around a NACA 0012 airfoil moving in steady circular motions at Mach $M_c = 0.8$ and $\alpha = 0^o$ but at different pitch rates.

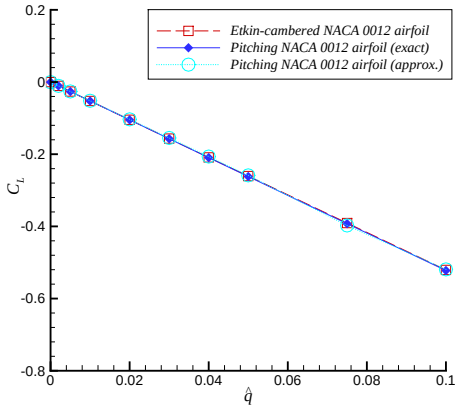

(a) Lift coefficient, $M_c = 0.2$

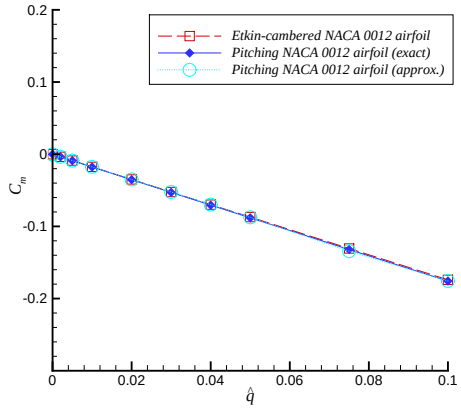

(b) Pitching-moment coef., $M_c = 0.2$

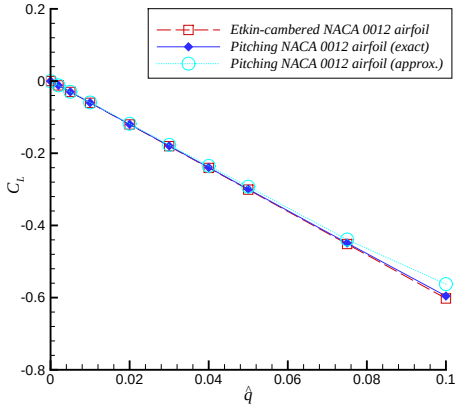

(c) Lift coefficient, $M_c = 0.5$

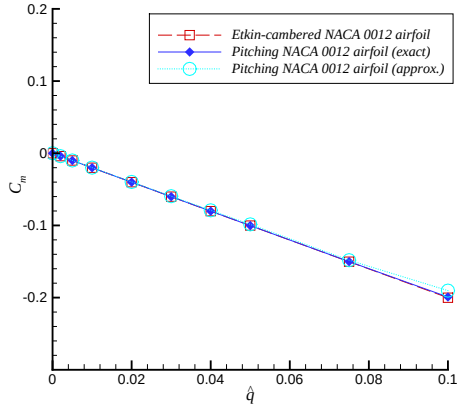

(d) Pitching-moment coef., $M_c = 0.5$

Figure 4.13: Variation of Lift coefficient and Pitching moment coefficient with respect to the pitch-rate for a NACA 0012 airfoil moving with $\alpha = 0^o$ at Mach numbers $M_c = 0.2$ and $M_c = 0.5$. The exact solution corresponds to solution using `A-NISFLOW`, and the approximate (approx.) solution corresponds to solution using `NISFLOW`

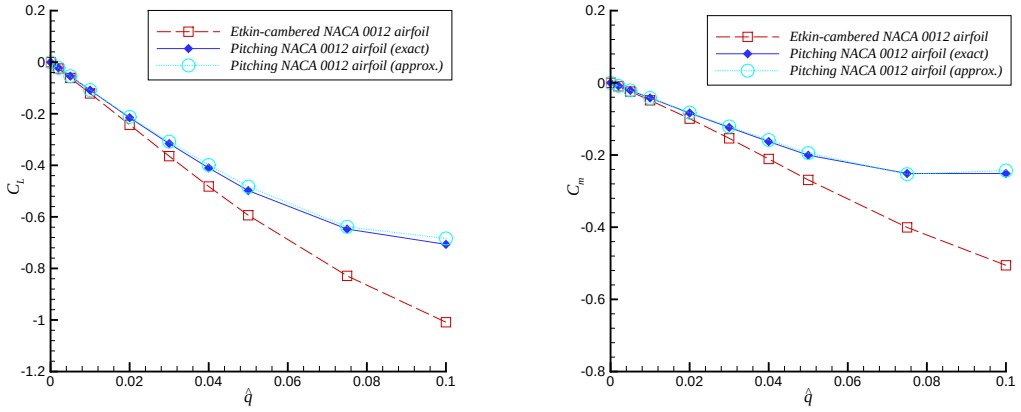

(a) Lift Coefficient

(b) Pitching-moment Coefficient

Figure 4.14: Variation of Lift coefficient and Pitching moment coefficient with respect to the pitch-rate for a NACA 0012 airfoil at Mach $M_c = 0.8$ and $\alpha = 0^o$. The "exact" solution corresponds to solution using `A-NISFLOW Code`, and the approximate ("approx.") solution corresponds to solution using `NISFLOW`

Chapter 5

The Sensitivity Equation Method and its Application in the Determination of Stability Derivatives

5.1 Stability Derivatives

The idea of stability derivatives appears as a consequence of the standard stability analysis of the aircraft. This stability analysis consist basically in the linearization of the non-linear equations of motion around an equilibrium flight condition (see for example reference [46]). The linearization is performed by considering small perturbations of the state variables

$$X = \{V_c, \alpha, \beta, \phi, \theta, \psi, p, q, r\}$$

and their time-rates of change $\{\dot{V}_c, \dot{\alpha}, \dot{\beta}, \dot{\phi}, \dot{\theta}, \dot{\psi}, \dot{p}, \dot{q}, \dot{r}\}$. This procedure naturally leads to the requirement of getting a linearized expansion of the aerodynamic forces in terms of the eighteen variables defined above.

Since by the kinematics equations $\dot{\phi}, \dot{\theta}, \dot{\psi}$ are explicit functions of p, q, r and ϕ, θ, ψ, it follows that the linearized expansion of the aerodynamic forces can be expressed completely in terms of the following state variables:

$$\{V_c, \alpha, \beta, \phi, \theta, \psi, p, q, r, \dot{V}_c, \dot{\alpha}, \dot{\beta}, \dot{p}, \dot{q}, \dot{r}\}$$

Under the assumption of a homogeneous, isentropic air, the aerodynamic forces do not depend on the particular attitude (ϕ, θ, ψ) of the aircraft. So the set of variables reduce further to:

$$\{V_c, \alpha, \beta, p, q, r, \dot{V}_c, \dot{\alpha}, \dot{\beta}, \dot{p}, \dot{q}, \dot{r}\}$$

Usually the dependence of the rates $\dot{p}, \dot{q}, \dot{r}$ is neglected so the linearized expansion of any component $\mathcal{F}$ of the aerodynamic forces or moments has the form:

$$\mathcal{F} = c_0 + c_V V_c + c_\alpha \alpha + c_\beta \beta + c_p p + c_q q + c_r r + c_{\dot{V}} \dot{V}_c + c_{\dot{\alpha}} \dot{\alpha} + c_{\dot{\beta}} \dot{\beta} \tag{5.1}$$

This linearization may also be applied for any non-dimensional force or moment coefficient. For example, for the pitching-moment coefficient one can write:

$$C_m = C_{m_0} + C_{m_V} V_c + C_{m_\alpha} \alpha + C_{m_\beta} \beta + C_{m_p} p + C_{m_q} q + C_{m_r} r + C_{m_{\dot{V}}} \dot{V}_c + C_{m_{\dot{\alpha}}} \dot{\alpha} + C_{m_{\dot{\beta}}} \dot{\beta} \tag{5.2}$$

The aerodynamic coefficients c_V, c_α,..., C_{m_V}, C_{m_α},..., etc. of the linear expressions (5.1) and (5.2) are usually called *stability derivatives*.

The substitution of the linear terms of the aerodynamic forces into the linearized equations of motions, leads to a linear system of state equations of the form:

$$E\dot{X} = AX + Bu$$

where E, A and B are constant matrices. This linearization forms the basis for the application of linear control theory and the design of systems of control. The word "stability" to name the coefficients of equations (5.1) and (5.2) comes from the fact that these coefficients determine the stability of the aircraft [1]. The word "derivatives" in the name of the stability derivatives comes from the fact that these coefficients can be interpreted as partial derivatives of the aerodynamic forces. For example, one can loosely write equations (5.1) and (5.2) as:

$$\mathcal{F} = \mathcal{F}_0 + \frac{\partial \mathcal{F}}{\partial V_c} V_c + \frac{\partial \mathcal{F}}{\partial \alpha} \alpha + \frac{\partial \mathcal{F}}{\partial \beta} \beta + \frac{\partial \mathcal{F}}{\partial p} p + \frac{\partial \mathcal{F}}{\partial q} q + \frac{\partial \mathcal{F}}{\partial r} r + \frac{\partial \mathcal{F}}{\partial \dot{V}_c} \dot{V}_c + \frac{\partial \mathcal{F}}{\partial \dot{\alpha}} \dot{\alpha} + \frac{\partial \mathcal{F}}{\partial \dot{\beta}} \dot{\beta}$$

$$C_m = C_{m_0} +$$

$$\frac{\partial C_m}{\partial V_c} V_c + \frac{\partial C_m}{\partial \alpha} \alpha + \frac{\partial C_m}{\partial \beta} \beta + \frac{\partial C_m}{\partial p} p + \frac{\partial C_m}{\partial q} q + \frac{\partial C_m}{\partial r} r + \frac{\partial C_m}{\partial \dot{V}_c} \dot{V}_c + \frac{\partial C_m}{\partial \dot{\alpha}} \dot{\alpha} + \frac{\partial C_m}{\partial \dot{\beta}} \dot{\beta}$$

However, this interpretation may be misleading since for example α and $\dot{\alpha}$ are obviously not independent variables.

Stability derivatives (also called stability parameters) can be obtained from flight-test measurements but the results of these tests can only be used in the very late steps of the design of a new aircraft. As a consequence, they are usually determined experimentally

[1] These coefficients determine the stability of the aircraft because the matrix elements of E and A contain these coefficients and the particular values of these matrix elements define the stability properties of the aircraft.

using wind-tunnel testing. The experimental techniques to obtain these parameters basically remain the same as in the past. The only change being an increase in the number of required experiments to simulate a greater number of parameters and a wider set of conditions. A review of the mathematical theory behind the main methods used to obtain stability derivatives is presented in reference [42]. Reference [40] presents a review of the methods employed up to the end of 1981. Reference [12] describes the static and oscillatory tests conducted to determine the stability derivatives of a model transport aircraft. Reference [20] provides a discussion of the direct forced oscillation technique. In reference [31] Lutze et al. discussed the determination of rotary stability derivatives using the curved wind tunnel at the Virginia Polytechnic Institute and State University. This data set of stability derivatives together with other data set obtained from NASA were used in [30] to perform the analysis of the poststall gyrations of a high-performance aircraft. More recent experimental techniques for the calculation of stability derivatives can be found in [26], [43] and [17]. Brinker [8] has studied the robustness of dynamic inversion based control laws based on uncertain stability derivatives.

Some authors have used semi-analytical techniques to calculate stability derivatives. Hemdan [21] have obtained closed-form formulas for C_{m_α} and $C_{m_{\dot{\alpha}}}$ for the case of airfoils at small angles of attack and hypersonic Mach numbers. Bryson [10], developed a technique to determine static and dynamic stability derivatives on slender bodies based on a transformation of three-dimensional flow problems into two-dimensional, incompressible flow problems in the cross-section perpendicular to the long axis of the body and using the concept of apparent-mass coefficients. More recently Suzuki and Fukuda [47] have slightly generalized Bryson's idea by using the boundary element method [7] to calculate the apparent-mass coefficients.

Other researchers have implemented numerical techniques to simulate oscillating, spinning or coning motions to get stability derivatives. Guruswami and Tu [19] performed time-accurate numerical solutions to simulate forced-oscillations in a rigid/flexible wing-body configuration. Through these numerical solutions they were able to get longitudinal dynamic stability derivatives. Weinacht [59] has simulated numerically the flow around projectiles which are moving in a specific combination of coning and spinning motions. In these particular motions the flow is steady and Weinacht used a time-marching Navier-Stokes scheme to compute the steady-state aerodynamic forces and moments. Using these flow solutions the pitch-damping force and moment coefficients can be determined using analytical expressions derived in [58].

5.2 Determination of Stability Derivatives using Aerodynamically Steady Motions

The mathematical model introduced in Chapter 2 has the advantage that it allows us to determine the complete set of static and dynamic stability derivatives [2]. Furthermore, the mathematical model allows us to recover the traditional way of interpreting the stability derivatives as partial derivatives of aerodynamic functions.

Let's consider again the steady aerodynamic function (2.18):

$$\mathcal{F} = \overline{F}\left(V_c, \alpha, \beta, p, q, r\right) \tag{5.3}$$

representing each of the components of the aerodynamic forces and moments acting on an arbitrary aircraft. This expression is valid also for the non-dimensional coefficients of the aerodynamic forces. For example for the pitching moment coefficent we have:

$$C_m = \overline{C}_m\left(V_c, \alpha, \beta, p, q, r\right) \tag{5.4}$$

The steady aerodynamic functions (5.3)-(5.4) can be constructed by performing experimental measurements or numerical simulations along aerodynamically steady motions. In Chapter 3, it was discussed how CFD tecniques can be used to determine these forces, and in Chapter 4, we have shown actual results of the determination of these functions for the two-dimensional case.

Under this steady-state approach, the function (5.3) uniquely defines the dependence of the aerodynamic forces with respect to the motion variables. As a consequence, a (first order) expansion in Taylor series of equations (5.3)-(5.4) naturally leads to:

$$\mathcal{F} = \overline{F}_0 + \frac{\partial \overline{F}}{\partial V_c}V_c + \frac{\partial \overline{F}}{\partial \alpha}\alpha + \frac{\partial \overline{F}}{\partial \beta}\beta + \frac{\partial \overline{F}}{\partial p}p + \frac{\partial \overline{F}}{\partial q}q + \frac{\partial \overline{F}}{\partial r}r + ... + \tag{5.5}$$

$$C_m = \overline{C}_{m_0} + \frac{\partial \overline{C}_m}{\partial V_c}V_c + \frac{\partial \overline{C}_m}{\partial \alpha}\alpha + \frac{\partial \overline{C}_m}{\partial \beta}\beta + \frac{\partial \overline{C}_m}{\partial p}p + \frac{\partial \overline{C}_m}{\partial q}q + \frac{\partial \overline{C}_m}{\partial r}r + ... + \tag{5.6}$$

After comparing the above equations with the linear expansions (5.1) and (5.2), it follows that the stability derivatives can be determined by calculating the appropiate partial derivatives of the steady aerodynamic functions (5.3). For example, the damping-in-pitch stability derivative C_{m_q} can be calculated from:

$$C_{m_q} = \frac{\partial \overline{C}_m\left(V_c, \alpha, \beta, p, q, r\right)}{\partial q} \tag{5.7}$$

[2] Excluding the time-rate stability derivatives associated with $\dot{V}_c, \dot{\alpha}, \dot{\beta}$

Observe that these stability derivatives can be calculated using finite differences. For example:

$$C_{m_q} \approx \frac{\overline{C}_m\left(V_c, \alpha, \beta, p, q + \triangle q, r\right) - \overline{C}_m\left(V_c, \alpha, \beta, p, q, r\right)}{\triangle q}. \tag{5.8}$$

From this expression it follows that for getting each stability derivative we need two non-linear flow simulations. This method can be very time consuming. Also, the use of finite differences may introduce problems due to round-off errors.

An alternative and promisingly better approach to calculate the whole set of stability derivatives with respect to the motion variables $\{V_c, \alpha, \beta, p, q, r\}$ is to use the Sensitivity Equation Method. This method can be employed here because of the identification of the stability derivatives as partial derivatives of the steady aerodynamic functions.

Consider, for example, the pitching moment coefficient $\hat{M}$. Under the assumption of inviscid flow, this pitching moment can be calculated from the aerodynamically steady flow solutions by an appropiate integration of the static pressure:

$$\hat{M} = \int_\sigma \left[\vec{x} \times -P\hat{n}\right]_y \, d\sigma$$

along the aircraft surface σ. The non-dimensional pitching moment coefficient can be determined from:

$$\overline{C}_m = \frac{2}{\rho_\infty V_c^2 Sc} \int_\sigma \left[\vec{x} \times -P\hat{n}\right]_y \, d\sigma$$

where S is the area of the aircraft's wing and where c is the mean aerodynamic chord of the wing. Differentiating the above expresion with respect to the angular rate q one gets:

$$\frac{\partial \overline{C}_m}{\partial q} = \frac{2}{\rho_\infty V_c^2 Sc} \frac{\partial}{\partial q} \int_\sigma \left[\vec{x} \times -P\hat{n}\right]_y \, d\sigma = \frac{2}{\rho_\infty V_c^2 Sc} \int_\sigma \left[\vec{x} \times -\frac{\partial P}{\partial q}\hat{n}\right]_y \, d\sigma \tag{5.9}$$

So it follows that an alternative way to calculate the damping-in-pitch stability derivative is to calculate the sensitivity $\frac{\partial P}{\partial q}$ of the pressure with respect to the pitch rate q. Similarly, if we want to calculate the stability derivative of the pitching moment with respect to any other motion variables we have that:

$$\frac{\partial \overline{C}_m}{\partial \eta} = \frac{2}{\rho_\infty V_c^2 Sc} \int_\sigma \left[\vec{x} \times -\frac{\partial P}{\partial \eta}\hat{n}\right]_y \, d\sigma \quad \text{where} \quad \eta = \{V_c, \alpha, \beta, p, q, r\} \tag{5.10}$$

A similar procedure can be done for calculating the stability derivatives of the other aerodynamic forces and moments. Then, it follows that, an alternative way to calculate the stability-derivatives is to determine the pressure sensitivities:

$$\frac{\partial P}{\partial \eta}(\vec{x}, t; \eta) \quad \text{with} \quad \eta = \{V_c, \alpha, \beta, p, q, r\}.$$

In the next section, we introduce the Sensitivity Equation Method which will allow us to calculate these sensitivities.

5.3 The Sensitivity Equation Method

Consider any system defined in a certain fixed region Γ of our physical space. Assume that the points of the space are described in an arbitrary reference frame through the position vector $\vec{x}$ and that the system can evolve with time t. Let us suppose that a certain property A of the system is described in an Eulerian (local) way: $A = A(\vec{x}, t)$. For example, the system could be the flow passing around an aircraft that is flying in a particular motion. In this case Γ would be all the flow region surrounding the aircraft surface and the property A could be the pressure of the fluid particles.

Now, assume that a certain parameter η induces a continuous modification of the system and that accordingly the property A is modified so that:

$$A = A(\vec{x}, t; \eta) \tag{5.11}$$

For the example given above, the parameter η could be the angle of incidence α at which the aircraft is flying or the velocity of rotation ω at which the aircraft is performing a steady maneuver. It is clear in both cases that the flow field and in particular the pressure field on the aircraft's surface changes as the parameter varies.

Even more, the parameter also could modify the geometry of the region Γ (for example a change in the aircraft shape) producing a change in the system and therefore in the property A. So in general one can have that

$$A = A(\vec{x}(\eta), t; \eta) \tag{5.12}$$

Although, the study of the general dependence (5.12) is important, particularly because of its application in the problems of design of optimal shapes, in the present work it will be assumed that the parameter η does not modify the geometry of our physical domain Γ.

As a consequence, starting from (5.11), the sensitivity $S_{A/\eta}$ of A with respect to η is defined to be

$$S_{A/\eta}(\vec{x}, t; \eta) = \frac{\partial A(\vec{x}, t; \eta)}{\partial \eta} \tag{5.13}$$

Then, by definition, the sensitivity $S_{A/\eta}$ measures the degree of change of A as the parameter η changes, keeping fixed the position and time of observation.

Assume that the system's behavior can be described mathematically in terms of a boundary value problem (BVP), i.e. a set of partial differential equations (PDE) plus a set of boundary conditions (BC). For each given value of $\eta = \eta_0$, the property $A(\vec{x}, t; \eta_0)$ can be (directly or indirectly) determined by solving the PDE plus its respective BC:

$$[A(\vec{x}, t; \eta)] \quad \Longleftarrow \text{solving} \quad \begin{bmatrix} \text{PDE} \\ + \\ \text{BC} \end{bmatrix} \tag{5.14}$$

The sensitivity $S_{A/\eta}$ at any η_0 could be determined numerically by using two close solutions of the BVP:

$$S_{A/\eta} = \frac{\partial A(\vec{x}, t; \eta_0)}{\partial \eta} \approx \frac{A(\vec{x}, t; \eta_0 + \triangle\eta) - A(\vec{x}, t; \eta_0)}{\triangle\eta} \tag{5.15}$$

However, a calculation such as the one described in equation (5.15) has two major drawbacks:

1. Determining the sensitivities using finite-differences would require at least two non-linear solutions. If the BVP is a complex non-linear problem then getting an additional solution may take a lot of time.

2. Finite-precision arithmethic can be a very important source of errors.

A promising alternative procedure to the evaluation of sensitivities consists in employing the Sensitivity Equation Method. In this method the sensitivities $S_{A/\eta}$ can be obtained by solving a Sensitivity BVP. The Sensitivity PDE is obtained by differentiating the original PDE with respect to η and the Sensitivity BC is obtained by differentiating the original BC with respect to η:

$$\left[S_{A/\eta}(\vec{x}, t; \eta)\right] \quad \Longleftarrow \text{solving} \quad \begin{bmatrix} \text{Sensitivity PDE} \\ + \\ \text{Sensitivity BC} \end{bmatrix} = \begin{bmatrix} \frac{d}{d\eta}[\text{original PDE}] \\ + \\ \frac{d}{d\eta}[\text{original BC}] \end{bmatrix} \tag{5.16}$$

Some of the advantages of this approach are the following:

1. Even if the original problem is a non-linear problem, the Sensitivity BVP is a linear BVP.

2. Only one non-linear solution of the original BVP is required.

3. Evaluation of the Sensitivities using Sensitivity Equations are potentially faster than using finite-differences.

4. No subtraction errors

In the next section we will apply the Sensitivity Equation Method to the BVP of aerodynamically steady flows. Other applications of the Sensitivity Equation Method can be found in [15] and [6].

5.4 Flow Sensitivity Equations

In this section we develop the equations that will allow us to determine the flow sensitivities (including pressure sensitivities) with respect to an arbitrary parameter η. The parameter

could be a parameter that modifies the far-field conditions or even the flow equations. The only restriction will be that η doesn't modify the space geometry or the boundary geometries. We will assume also that η is independent of the time t. For the applications in which we are interested, the parameter η could be the angle of attack α, the Mach number M_c or the pitch rate q of the aircraft.

The state of the flow is completely defined in terms of the five conserved quantities defined in equation (3.55), then, the sensitivities S_η of the conserved quantities Q with respect to the parameter η will be a vector array with five components:

$$\begin{bmatrix} S_{\eta 1} \\ S_{\eta 2} \\ S_{\eta 3} \\ S_{\eta 4} \\ S_{\eta 5} \end{bmatrix} = S_\eta = \frac{\partial}{\partial \eta} Q(\vec{x},t;\eta) = \begin{bmatrix} \frac{\partial Q_1(\vec{x},t;\eta)}{\partial \eta} \\ \frac{\partial Q_2(\vec{x},t;\eta)}{\partial \eta} \\ \frac{\partial Q_3(\vec{x},t;\eta)}{\partial \eta} \\ \frac{\partial Q_3(\vec{x},t;\eta)}{\partial \eta} \\ \frac{\partial Q_5(\vec{x},t;\eta)}{\partial \eta} \end{bmatrix} = \begin{bmatrix} \frac{\partial \rho(\vec{x},t;\eta)}{\partial \eta} \\ \frac{\partial \rho u(\vec{x},t;\eta)}{\partial \eta} \\ \frac{\partial \rho v(\vec{x},t;\eta)}{\partial \eta} \\ \frac{\partial \rho w(\vec{x},t;\eta)}{\partial \eta} \\ \frac{\partial \rho E(\vec{x},t;\eta)}{\partial \eta} \end{bmatrix} \tag{5.17}$$

If we determine the sensitivities of the conserved variables we can determine the sensitivitites of any flow variable by using the definition (5.17) and equations (3.21)-(3.29). For example, the sensitivity $S_{u/\eta}$ of the x-component of the flow velocity vector can be determined from

$$S_{u/\eta} = \frac{\partial u}{\partial \eta} = \frac{\partial Q_2/Q_1}{\partial \eta} = -\frac{Q_2}{Q_1^2}\frac{\partial Q_1}{\partial \eta} + \frac{1}{Q_1}\frac{\partial Q_2}{\partial \eta} = -\frac{Q_2}{Q_1^2} S_{\eta 1} + \frac{1}{Q_1} S_{\eta 2}$$

From the flow equations it is possible to determine the PDE satisfied by the sensitivity vector S_η. For simplicity we will assume our fluid is inviscid and non-heat conducting. We are interested in calculating sensitivities along aerodynamically steady motions so we will consider the aerodynamically steady Euler equation (3.54):

$$\frac{\partial Q}{\partial t} + \frac{\partial F}{\partial x} + \frac{\partial G}{\partial y} + \frac{\partial H}{\partial z} = W \tag{5.18}$$

Taking the derivative $\frac{d}{d\eta}$ of the flow equation (5.18) with respect to the parameter η we get:

$$\frac{\partial}{\partial \eta}\frac{\partial}{\partial t} Q(\vec{x},t;\eta) + \frac{\partial}{\partial \eta}\frac{\partial}{\partial x} F(\vec{x},t;\eta) + \frac{\partial}{\partial \eta}\frac{\partial}{\partial y} G(\vec{x},t;\eta) + \frac{\partial}{\partial \eta}\frac{\partial}{\partial z} H(\vec{x},t;\eta) = \frac{\partial}{\partial \eta} W(\vec{x},t;\eta)$$

Since the coordinates $\vec{x}$ and the time t are independent of η, we can interchange partial derivatives (assuming certain smoothness) in the above equation to get:

$$\frac{\partial}{\partial t}\frac{\partial}{\partial \eta} Q(\vec{x},t;\eta) + \frac{\partial}{\partial x}\frac{\partial}{\partial \eta} F(\vec{x},t;\eta) + \frac{\partial}{\partial y}\frac{\partial}{\partial \eta} G(\vec{x},t;\eta) + \frac{\partial}{\partial z}\frac{\partial}{\partial \eta} H(\vec{x},t;\eta) = \frac{\partial}{\partial \eta} W(\vec{x},t;\eta). \tag{5.19}$$

By differentiating equation (3.30) with respect to η we can deduce that

$$\frac{\partial}{\partial\eta}F(\vec{x},t;\eta)=\frac{\partial F}{\partial Q}\cdot\frac{\partial Q}{\partial\eta}(\vec{x},t;\eta)=\nabla_Q F\cdot\frac{\partial Q}{\partial\eta}(\vec{x},t;\eta) \tag{5.20}$$

where $\nabla_Q F$ is the Jacobian of F with respect to the conserved quantities Q:

$$\nabla_Q F=$$

$$\begin{bmatrix} 0 & 1 & 0 & 0 & 0 \\ -\frac{Q_2^2}{Q_1^2}+\frac{(\gamma-1)V^2}{2} & \frac{(3-\gamma)Q_2}{Q_1} & \frac{(1-\gamma)Q_3}{Q_1} & \frac{(1-\gamma)Q_4}{Q_1} & (\gamma-1) \\ -\frac{Q_2Q_3}{Q_1^2} & \frac{Q_3}{Q_1} & \frac{Q_2}{Q_1} & 0 & 0 \\ -\frac{Q_2Q_4}{Q_1^2} & \frac{Q_4}{Q_1} & 0 & \frac{Q_2}{Q_1} & 0 \\ -\frac{\gamma Q_5Q_2}{Q_1^2}+\frac{Q_2(\gamma-1)V^2}{Q_1} & \frac{\gamma Q_5}{Q_1}-\frac{(\gamma-1)V^2}{2}-\frac{(\gamma-1)Q_2^2}{Q_1^2} & -\frac{(\gamma-1)Q_3Q_2}{Q_1^2} & -\frac{(\gamma-1)Q_4Q_2}{Q_1^2} & \gamma\frac{Q_2}{Q_1} \end{bmatrix}$$

where

$$V=\sqrt{u^2+v^2+w^2}=\frac{\sqrt{Q_2^2+Q_3^2+Q_4^2}}{Q_1}$$

A similar equation to equation (5.20) holds for the conservative fluxes G and H, and as a consequence, equation (5.19) can be written as:

$$\frac{\partial}{\partial t}\frac{\partial}{\partial\eta}Q(\vec{x},t;\eta)+\frac{\partial}{\partial x}\left[\nabla_Q F\cdot\frac{\partial}{\partial\eta}Q(\vec{x},t;\eta)\right]+$$

$$\frac{\partial}{\partial y}\left[\nabla_Q G\cdot\frac{\partial}{\partial\eta}Q(\vec{x},t;\eta)\right]+\frac{\partial}{\partial z}\left[\nabla_Q H\cdot\frac{\partial}{\partial\eta}Q(\vec{x},t;\eta)\right]=\frac{\partial}{\partial\eta}W(\vec{x},t;\eta).$$

Using the definition (5.17) the above equation can be rewritten as

$$\frac{\partial S_\eta}{\partial t}+\frac{\partial}{\partial x}\left[\nabla_Q F(\vec{x},t;\eta)\cdot S_\eta\right]+$$

$$\frac{\partial}{\partial y}\left[\nabla_Q G(\vec{x},t;\eta)\cdot S_\eta\right]+\frac{\partial}{\partial z}\left[\nabla_Q H(\vec{x},t;\eta)\cdot S_\eta\right]=\frac{\partial}{\partial\eta}W(\vec{x},t;\eta) \tag{5.21}$$

Now, let us calculate the RHS term of equation (5.21) using equation (3.59)

$$\frac{\partial}{\partial\eta}W(\vec{x},t;\eta)=\begin{bmatrix} 0 \\ \frac{\partial Q_1}{\partial\eta}\left[f_x+\Omega_x\right]-2(q\frac{\partial Q_4}{\partial\eta}-r\frac{\partial Q_3}{\partial\eta}) \\ \frac{\partial Q_1}{\partial\eta}\left[f_y+\Omega_y\right]-2(r\frac{\partial Q_2}{\partial\eta}-p\frac{\partial Q_4}{\partial\eta}) \\ \frac{\partial Q_1}{\partial\eta}\left[f_z+\Omega_z\right]-2(p\frac{\partial Q_3}{\partial\eta}-q\frac{\partial Q_2}{\partial\eta}) \\ \left[f_x+\Omega_x\right]\frac{\partial Q_2}{\partial\eta}+\left[f_y+\Omega_y\right]\frac{\partial Q_3}{\partial\eta}+\left[f_z+\Omega_z\right]\frac{\partial Q_4}{\partial\eta} \end{bmatrix}+$$

$$\begin{bmatrix} 0 \\ Q_1\frac{\partial[f_x+\Omega_x]}{\partial\eta} - 2(\frac{\partial q}{\partial\eta}Q_4 - \frac{\partial r}{\partial\eta}Q_3) \\ Q_1\frac{\partial[f_y+\Omega_y]}{\partial\eta} - 2(\frac{\partial r}{\partial\eta}Q_2 - \frac{\partial p}{\partial\eta}Q_4) \\ Q_1\frac{\partial[f_z+\Omega_z]}{\partial\eta} - 2(\frac{\partial p}{\partial\eta}Q_3 - \frac{\partial q}{\partial\eta}Q_2) \\ \frac{\partial[f_x+\Omega_x]}{\partial\eta}Q_2 + \frac{\partial[f_y+\Omega_y]}{\partial\eta}Q_3 + \frac{\partial[f_z+\Omega_z]}{\partial\eta}Q_4 \end{bmatrix}$$

As a consequence, we can write

$$\frac{\partial}{\partial\eta}W(\vec{x},t;\eta) = W_A(\vec{x},t;\eta)\cdot\begin{bmatrix} \frac{\partial Q_1}{\partial\eta} \\ \frac{\partial Q_2}{\partial\eta} \\ \frac{\partial Q_3}{\partial\eta} \\ \frac{\partial Q_3}{\partial\eta} \\ \frac{\partial Q_5}{\partial\eta} \end{bmatrix} + W_B(\vec{x},t;\eta) = W_A(\vec{x},t;\eta)\cdot S_\eta + W_B(\vec{x},t;\eta) \quad (5.22)$$

where

$$W_A(\vec{x},t;\eta) = \begin{bmatrix} 0 & 0 & 0 & 0 & 0 \\ f_x+\Omega_x & 0 & 2r & -2q & 0 \\ f_y+\Omega_y & -2r & 0 & 2p & 0 \\ f_z+\Omega_z & 2q & -2p & 0 & 0 \\ 0 & f_x+\Omega_x & f_y+\Omega_y & f_z+\Omega_z & 0 \end{bmatrix} \quad (5.23)$$

$$W_B(\vec{x},t;\eta) = \begin{bmatrix} 0 \\ Q_1\frac{\partial[f_x+\Omega_x]}{\partial\eta} - 2(\frac{\partial q}{\partial\eta}Q_4 - \frac{\partial r}{\partial\eta}Q_3) \\ Q_1\frac{\partial[f_y+\Omega_y]}{\partial\eta} - 2(\frac{\partial r}{\partial\eta}Q_2 - \frac{\partial p}{\partial\eta}Q_4) \\ Q_1\frac{\partial[f_z+\Omega_z]}{\partial\eta} - 2(\frac{\partial p}{\partial\eta}Q_3 - \frac{\partial q}{\partial\eta}Q_2) \\ \frac{\partial[f_x+\Omega_x]}{\partial\eta}Q_2 + \frac{\partial[f_y+\Omega_y]}{\partial\eta}Q_3 + \frac{\partial[f_z+\Omega_z]}{\partial\eta}Q_4 \end{bmatrix} \quad (5.24)$$

Replacing equation (5.22) into (5.21) we finally get that the sensitivities S_η satisfy

$$\frac{\partial S_\eta}{\partial t} + \frac{\partial}{\partial x}\left[\nabla_Q F\cdot S_\eta\right] + \frac{\partial}{\partial y}\left[\nabla_Q G\cdot S_\eta\right] + \frac{\partial}{\partial z}\left[\nabla_Q H\cdot S_\eta\right] = W_A\cdot S_\eta + W_B \quad (5.25)$$

If the PDE defined by equation (5.25) is solved with the appropiate boundary conditions the flow sensitivities can be determined. Equation (5.25) may seem very complicated but it is not so. Observe that the Jacobians $\nabla_Q F$, $\nabla_Q G$, $\nabla_Q H$ are known functions of the flow solution and they are independent of the sensitivities. Also since the pseudo force vector $\vec{\Omega}$ and the external forces components f_x, f_y and f_z are independent of the state variables the matrices W_A and W_B do not depend on S_η. From these properties, it follows that the flow sensitivity equation (5.25) is a linear equation. Furthermore, the same numerical techniques applied to the flow solutions can be used to solve this linear equation.

Observe also that in the case there are no external forces the expressions for W_A and W_B simplify to:

$$W_A(\vec{x},t;\eta) = \begin{bmatrix} 0 & 0 & 0 & 0 & 0 \\ \Omega_x & 0 & 2r & -2q & 0 \\ \Omega_y & -2r & 0 & 2p & 0 \\ \Omega_z & 2q & -2p & 0 & 0 \\ 0 & \Omega_x & \Omega_y & \Omega_z & 0 \end{bmatrix} \tag{5.26}$$

$$W_B(\vec{x},t;\eta) = \begin{bmatrix} 0 \\ Q_1\frac{\partial\Omega_x}{\partial\eta} - 2(\frac{\partial q}{\partial\eta}Q_4 - \frac{\partial r}{\partial\eta}Q_3) \\ Q_1\frac{\partial\Omega_y}{\partial\eta} - 2(\frac{\partial r}{\partial\eta}Q_2 - \frac{\partial p}{\partial\eta}Q_4) \\ Q_1\frac{\partial\Omega_z}{\partial\eta} - 2(\frac{\partial p}{\partial\eta}Q_3 - \frac{\partial q}{\partial\eta}Q_2) \\ \frac{\partial\Omega_x}{\partial\eta}Q_2 + \frac{\partial\Omega_y}{\partial\eta}Q_3 + \frac{\partial\Omega_z}{\partial\eta}Q_4 \end{bmatrix} \tag{5.27}$$

5.5 Rotary Stability Derivatives

We complete our mathematical work by determining the flow sensitivity equations with respect to the angular rates. These sensitivity equations can be determined by choosing the parameter η to be the roll rate p, the pitch rate q or the yaw rate r. We are interested in getting these sensitivity equations because from their solutions we will be able to determine the pressure sensitivities $\frac{\partial P}{\partial p}$, $\frac{\partial P}{\partial q}$ and $\frac{\partial P}{\partial r}$. Then with these pressure sensitivities one can use relationships of the type of equation (5.9) to easily calculate the complete set of rotary stability derivatives.

Observe also that choosing η to be the speed of the aircraft V_c, the angle of attack α or the angle of sideslip β will also allow us to determine the complete set of static stability derivatives. This approach was used by Godfrey and Cliff [14] to calculate the set of static stability derivatives. However, their approach was unable to get rotary stability derivatives since it was only valid for the case of rectilinear steady flights. The approach presented is more general and allows the calculation of stability derivatives even when the aircraft has arbitrary (non-zero) angular rates.

By replacing η by the roll-rate p in equation (5.25) we can get the sensitivity equation with respect to the roll-rate:

$$\frac{\partial S_p}{\partial t} + \frac{\partial}{\partial x}\left[\nabla_Q F \cdot S_p\right] + \frac{\partial}{\partial y}\left[\nabla_Q G \cdot S_p\right] + \frac{\partial}{\partial z}\left[\nabla_Q H \cdot S_p\right] = W_A \cdot S_p + W_B. \tag{5.28}$$

In the above equation W_A is given by (5.23) with p instead of η while $W_B(\vec{x},t;p)$ (*cf.* equation

(5.25)) is given by:

$$W_B(\vec{x},t;p)=\begin{bmatrix} 0 \\ Q_1\frac{\partial[f_x+\Omega_x]}{\partial p}-2(\frac{\partial q}{\partial p}Q_4-\frac{\partial r}{\partial p}Q_3) \\ Q_1\frac{\partial[f_y+\Omega_y]}{\partial p}-2(\frac{\partial r}{\partial p}Q_2-\frac{\partial p}{\partial p}Q_4) \\ Q_1\frac{\partial[f_z+\Omega_z]}{\partial p}-2(\frac{\partial p}{\partial p}Q_3-\frac{\partial q}{\partial p}Q_2) \\ \frac{\partial[f_x+\Omega_x]}{\partial p}Q_2+\frac{\partial[f_y+\Omega_y]}{\partial p}Q_3+\frac{\partial[f_z+\Omega_z]}{\partial p}Q_4 \end{bmatrix}$$

Assuming that any external forces are independent of the roll-rate of the aircraft and simplifying some of the partial derivatives, $W_B(\vec{x},t;p)$ reduces to:

$$W_B(\vec{x},t;p)=\begin{bmatrix} 0 \\ Q_1\frac{\partial\Omega_x}{\partial p} \\ Q_1\frac{\partial\Omega_y}{\partial p}+2Q_4 \\ Q_1\frac{\partial\Omega_z}{\partial p}-2Q_3 \\ \frac{\partial\Omega_x}{\partial p}Q_2+\frac{\partial\Omega_y}{\partial p}Q_3+\frac{\partial\Omega_z}{\partial p}Q_4 \end{bmatrix} \tag{5.29}$$

Now, we need to determine the partial derivatives with respect to p of the components of the 'pseudo force vector' $\vec{\Omega}$. Here we should be very careful in calculating the derivatives. From the original definition of $\vec{\Omega}$:

$$\vec{\Omega}=-\vec{\omega}\times(\vec{\omega}\times\vec{x})-\frac{d\vec{\omega}}{dt}\times\vec{x}-\vec{a}_{\mathcal{R}/\mathcal{S}},$$

one may think that the only contribution to the partial derivatives $\frac{\partial\Omega_x}{\partial p}$, $\frac{\partial\Omega_y}{\partial p}$, $\frac{\partial\Omega_z}{\partial p}$ comes from the term $-\vec{\omega}\times(\vec{\omega}\times\vec{x})$. This is not correct. We must perturb the state of the motion $X=\{V_c,\alpha,\beta,p,q,r\}$ in such a way that in the new perturbed state only one state variable has changed (in this case p) while the others remain constant.

In our discussion of aerodynamically steady motions the dependence of $\vec{\Omega}$ on the state variables was given by equation (3.60) or equation (3.61). By differentiating each of the rows of these equations we get:

$$\begin{bmatrix} \frac{\partial\Omega_x}{\partial p} \\ \frac{\partial\Omega_y}{\partial p} \\ \frac{\partial\Omega_z}{\partial p} \end{bmatrix}=\begin{bmatrix} -(qy+rz) \\ -qx+2yp+w_c \\ -rx+2zp-v_c \end{bmatrix} \tag{5.30}$$

So replacing (5.30) into (5.29) we get:

$$W_B(\vec{x},t;p)=\begin{bmatrix} 0 \\ -Q_1(qy+rz) \\ Q_1(-qx+2yp+w_c)+2Q_4 \\ Q_1(-rx+2zp-v_c)-2Q_3 \\ -(qy+rz)Q_2+(-qx+2yp+w_c)Q_3+(-rx+2zp-v_c)Q_4 \end{bmatrix} \tag{5.31}$$

We can proceed similarly with the other angular rates components.

For the pitch-rate sensitivities we have:

$$\frac{\partial S_q}{\partial t} + \frac{\partial}{\partial x}\left[\nabla_Q F \cdot S_q\right] + \frac{\partial}{\partial y}\left[\nabla_Q G \cdot S_q\right] + \frac{\partial}{\partial z}\left[\nabla_Q H \cdot S_q\right] = W_A \cdot S_q + W_B. \tag{5.32}$$

where W_A is given by (5.23) and where $W_B(\vec{x}, t; q)$ is given by:

$$W_B(\vec{x}, t; q) = \begin{bmatrix} 0 \\ Q_1\left(-py + 2xq - w_c\right) - 2Q_4 \\ -Q_1\left(px + rz\right) \\ Q_1\left(-ry + 2zq + u_c\right) + 2Q_2 \\ \left(-py + 2xq - w_c\right)Q_2 - \left(px + rz\right)Q_3 + \left(-ry + 2zq + u_c\right)Q_4 \end{bmatrix}$$

For the yaw-rate sensitivities we have:

$$\frac{\partial S_r}{\partial t} + \frac{\partial}{\partial x}\left[\nabla_Q F \cdot S_r\right] + \frac{\partial}{\partial y}\left[\nabla_Q G \cdot S_r\right] + \frac{\partial}{\partial z}\left[\nabla_Q H \cdot S_r\right] = W_A \cdot S_r + W_B. \tag{5.33}$$

where W_A is given by (5.23) and where $W_B(\vec{x}, t; r)$ is given by:

$$W_B(\vec{x}, t; r) = \begin{bmatrix} 0 \\ Q_1\left(-pz + 2xr + v_c\right) + 2Q_3 \\ Q_1\left(-qz + 2yr - u_c\right) - 2Q_2 \\ -Q_1\left(px + qy\right) \\ \left(-pz + 2xr + v_c\right)Q_2 + \left(-qz + 2yr - u_c\right)Q_3 - \left(px + qy\right)Q_4 \end{bmatrix}$$

Note that if we are calculating the stability derivatives respect to the angular rates for the case of steady rectlinear motion ($p = q = r = 0$), the term W_A vanishes in all cases (if we assume there are no external forces applied on the fluid) and W_B reduces to:

$$W_B(\vec{x}, t; p) = \begin{bmatrix} 0 \\ 0 \\ Q_1 w_c + 2Q_4 \\ -Q_1 v_c - 2Q_3 \\ w_c Q_3 - v_c Q_4 \end{bmatrix}$$

$$W_B(\vec{x}, t; q) = \begin{bmatrix} 0 \\ -Q_1 w_c - 2Q_4 \\ 0 \\ Q_1 u_c + 2Q_2 \\ -w_c Q_2 + u_c Q_4 \end{bmatrix}$$

$$W_B(\vec{x},t;r) = \begin{bmatrix} 0 \\ Q_1 v_c + 2Q_3 \\ -Q_1 u_c - 2Q_2 \\ 0 \\ v_c Q_2 - u_c Q_3 \end{bmatrix},$$

respectively.

5.6 Boundary Conditions for Flow Sensitivities

The boundary conditions for the sensitivities of the conserved variables Q can be obtained using the same procedure by which we derived the sensitivity equations. That is, by differentiating the boundary conditions of the flow equations with respect to the sensitivity parameter η. Here we will only derive the boundary conditions for the case the parameter η is the roll-rate p. As a consequence we will obtain the boundary-conditions corresponding to the roll-rate sensitivities S_p. The procedures for any other sensitivity parameter are similar.

5.6.1 Far-Field Boundary Condititions

The far-field boundary conditions for the velocity sensitivities $S_{u/p}$, $S_{v/p}$ and $S_{w/p}$ can be obtained by direct differentiation of the velocity far-field boundary conditions defined in equation (3.63):

$$\lim_{\|\vec{x}\|\to\infty} \begin{bmatrix} S_{u/p} \\ S_{v/p} \\ S_{w/p} \end{bmatrix} = \lim_{\|\vec{x}\|\to\infty} \begin{bmatrix} \frac{\partial u}{\partial p} \\ \frac{\partial v}{\partial p} \\ \frac{\partial w}{\partial p} \end{bmatrix} = \lim_{\|\vec{x}\|\to\infty} \frac{d}{dp} \begin{bmatrix} u \\ v \\ w \end{bmatrix} = \lim_{\|\vec{x}\|\to\infty} \frac{d}{dp} \begin{bmatrix} -u_c - (qz - ry) \\ -v_c - (rx - pz) \\ -w_c - (py - qx) \end{bmatrix}.$$

$$\lim_{\|\vec{x}\|\to\infty} \begin{bmatrix} S_{u/p} \\ S_{v/p} \\ S_{w/p} \end{bmatrix} = \lim_{\|\vec{x}\|\to\infty} \begin{bmatrix} \frac{\partial}{\partial p}\left[-u_c - (qz - ry)\right] \\ \frac{\partial}{\partial p}\left[-v_c - (rx - pz)\right] \\ \frac{\partial}{\partial p}\left[-w_c - (py - qx)\right] \end{bmatrix} = \lim_{\|\vec{x}\|\to\infty} \begin{bmatrix} 0 \\ z \\ -y \end{bmatrix} \tag{5.34}$$

Differentiating the boundary conditions (3.62) with respect to the roll-rate p we get that the far-field boundary conditions for the sensitivities of scalar quantities such as $f = \{\rho, P, T, e, a\}$ can be written as:

$$\lim_{\|\vec{x}\|\to\infty} S_{f/p}(\vec{x}) = \lim_{\|\vec{x}\|\to\infty} \frac{\partial f}{\partial p}(\vec{x}) = \frac{\partial f_\infty}{\partial p} = 0 \tag{5.35}$$

For example for the density sensitivity we have:

$$\lim_{\|\vec{x}\|\to\infty} S_{\rho/p}(\vec{x}) = 0 \tag{5.36}$$

5.6.2 Solid Walls Boundary Conditions

The boundary conditions for the sensitivities at solid walls can be determined by direct differentiation of the flow boundary conditions (3.64) with respect to the roll-rate p. We get:

$$\frac{\partial u}{\partial p}n_x + \frac{\partial v}{\partial p}n_y + \frac{\partial w}{\partial p}n_z = \frac{d}{dp}\left[un_x + vn_y + wn_z\right] = \frac{d}{dp}\left[0\right] = 0$$

So we have that:

$$S_{u/p}n_x + S_{v/p}n_y + S_{w/p}n_z = 0. \tag{5.37}$$

Chapter 6

Numerical Determination of Longitudinal Stability Derivatives

In this chapter we implement numerically the sensitivity equation method for the determination of stability derivatives for the two-dimensional case.

6.1 Preliminary Remarks

In the two-dimensional application the aerodynamically-steady motions correspond to planar motions consisting of circular trajectories as shown in Figure (4.4). In Chapter 4 we introduced a flow solver called `A-NISFLOW` which can be used to obtain numerical solutions for the flows around airfoils moving along these planar aerodynamically steady motions. From the numerical solutions it was possible to obtain by integration the lift, drag and pitching moment for different values of Mach numbers M_c, angles of attack α and pitch rates q. With these simulations it is possible to construct functions of the form:

$$\left[\begin{array}{rcl} C_\ell & = & \overline{C}_\ell(M_c,\alpha,q) \\ C_d & = & \overline{C}_d(M_c,\alpha,q) \\ C_m & = & \overline{C}_m(M_c,\alpha,q) \end{array}\right] \tag{6.1}$$

for the evaluation of the non-dimensional lift, drag and pitching moment coefficients. With the functions defined in equation (6.1) one can determine the following nine longitudinal stability derivatives:

$$\left[\begin{array}{rcl} C_{\ell_\kappa} & = & \frac{\partial \overline{C}_\ell}{\partial \kappa}(M_c,\alpha,q) \\ C_{d_\kappa} & = & \frac{\partial \overline{C}_d}{\partial \kappa}(M_c,\alpha,q) \\ C_{m_\kappa} & = & \frac{\partial \overline{C}_m}{\partial \kappa}(M_c,\alpha,q) \end{array}\right] \quad \text{with} \quad \kappa = \{M_c,\alpha,q\} \tag{6.2}$$

This stability derivatives can be calculated using finite-differences by using the numerical solutions obtained by `A-NISFLOW`. For example, the damping-in-pitch C_{m_q} can be calculated as:

$$C_{m_q} = \frac{\overline{C}_m(M_c, \alpha, q + \triangle q) - \overline{C}_m(M_c, \alpha, q)}{\triangle q}. \tag{6.3}$$

Equation (6.3) is a particular case of the general equation (5.8).

Here we are interested in using the sensitivity equation method as an alternative method for the calculation of the stability derivatives defined in equation (6.2).

6.2 Two-Dimensional Flow Sensitivity Equations

In this section the equations for the two-dimensional flow sensitivities with respect to a general parameter η are described. Attention is restricted to the flows associated with planar aerodynamically steady motions. We will assume there are no external forces (i.e. $f_x = f_y = f_z = 0$) . The coordinate system is chosen to be the same as the one used in Chapter 4 for the Euler flows associated to planar aerodynamically steady motions. The x, y axes are in the plane of the motion while the z-axis is perpendicular to it. As a consequence, the airfoil pitches around the z-axis (positive pitch $\rightarrow$ nose-down).

The two-dimensional sensitivity equations can be obtained from the three-dimensional sensitivity equations of Section 5.4 by setting $w = 0$, $H = 0$, $\nabla_Q H = 0$, $p = 0$, $q = 0$ and replacing r by q. Doing this setting we get the following results:

1. The sensitivities S_η of the conserved quantities with respect to the parameter η form a vector array with four components:

$$\begin{bmatrix} S_{\eta 1} \\ S_{\eta 2} \\ S_{\eta 3} \\ S_{\eta 4} \end{bmatrix} = S_\eta = \frac{\partial Q}{\partial \eta} = \begin{bmatrix} \frac{\partial Q_1}{\partial \eta} \\ \frac{\partial Q_2}{\partial \eta} \\ \frac{\partial Q_3}{\partial \eta} \\ \frac{\partial Q_4}{\partial \eta} \end{bmatrix} = \begin{bmatrix} \frac{\partial \rho}{\partial \eta} \\ \frac{\partial \rho u}{\partial \eta} \\ \frac{\partial \rho v}{\partial \eta} \\ \frac{\partial \rho E}{\partial \eta} \end{bmatrix}. \tag{6.4}$$

2. These sensitivities satisfy the following linear PDE:

$$\frac{\partial S_\eta}{\partial t} + \frac{\partial}{\partial x}\left[\nabla_Q F \cdot S_\eta\right] + \frac{\partial}{\partial y}\left[\nabla_Q G \cdot S_\eta\right] = W_A \cdot S_\eta + W_B. \tag{6.5}$$

   where $\nabla_Q F$ and $\nabla_Q G$ are the Jacobians with respect to the conserved quantities Q of F and of G, respectively.

3. W_A and W_B are given by

$$W_A(Q;\eta) = \begin{bmatrix} 0 & 0 & 0 & 0 \\ \Omega_x & 0 & 2q & 0 \\ \Omega_y & -2q & 0 & 0 \\ 0 & \Omega_x & \Omega_y & 0 \end{bmatrix} \tag{6.6}$$

and

$$W_B(Q;\eta) = \begin{bmatrix} 0 \\ Q_1 \frac{\partial \Omega_x}{\partial \eta} + 2\frac{\partial q}{\partial \eta} Q_3 \\ Q_1 \frac{\partial \Omega_y}{\partial \eta} - 2\frac{\partial q}{\partial \eta} Q_2 \\ \frac{\partial \Omega_x}{\partial \eta} Q_2 + \frac{\partial \Omega_y}{\partial \eta} Q_3 \end{bmatrix}. \tag{6.7}$$

Observe that the Jacobians $\nabla_Q F,\ \nabla_Q G$ are known functions of the flow solution and independent of the sensitivities, as are the matrices W_A and W_B.

4. $\vec{\Omega}$ reduces to:

$$\begin{bmatrix} \Omega_x \\ \Omega_z \end{bmatrix} = \begin{bmatrix} q^2 x + q v_c \\ q^2 y - q u_c \end{bmatrix}. \tag{6.8}$$

6.3 Rotary Stability Derivatives

As an example of the use of the sensitivity equation method in flight mechanics the flow sensitivity with respect to the pitch rate q is determined. From equation (6.5) the sensitivity vector for the pitch rate q satisfies the linear PDE

$$\frac{\partial S_q}{\partial t} + \frac{\partial}{\partial x}\left[\nabla_Q F \cdot S_q\right] + \frac{\partial}{\partial y}\left[\nabla_Q G \cdot S_q\right] = W_A \cdot S_q + W_B, \tag{6.9}$$

where W_A is given by equation (6.6), and $W_B(Q;q)$, from (6.7) and (6.8), is given by

$$W_B(Q;q) = \begin{bmatrix} 0 \\ Q_1 \frac{\partial \Omega_x}{\partial q} + 2Q_3 \\ Q_1 \frac{\partial \Omega_y}{\partial q} - 2Q_2 \\ \frac{\partial \Omega_x}{\partial q} Q_2 + \frac{\partial \Omega_y}{\partial q} Q_3 \end{bmatrix} = \begin{bmatrix} 0 \\ Q_1 \left(2qx + v_c\right) + 2Q_3 \\ Q_1 \left(2qy - u_c\right) - 2Q_2 \\ \left(2qx + v_c\right) Q_2 + \left(2qy - u_c\right) Q_3 \end{bmatrix}. \tag{6.10}$$

Once equation (6.9) is solved, the pressure sensitivity $\frac{\partial P}{\partial q}$ is available at any point in the flow field. In the case of inviscid flows, $\frac{\partial P}{\partial q}$ and relationships of the type given in equations (5.9) or (5.10) are sufficient to calculate the stability derivatives of each of the aerodynamic forces and moments with respect to the pitch rate. Observe that all the procedures used to compute the aerodynamic forces can be used to compute their sensitivities by simply replacing the pressure by the pressure sensitivity.

6.4 Numerical Results: Pitch Rate Sensitivity

A solution procedure for the two dimensional sensitivity equation (6.9) was implemented using a finite-volume formulation. The sensitivity solver is called `S-NISFLOW` and it is based in the same implicit time-marching iterative technique employed in the flow solvers `NISFLOW` and `A-NISFLOW`. The `S-NISFLOW Code` can be used to calculate sensitivities with respect to the angle of attack α, the flight Mach number M_c and the pitch rate q.

The same unstructured grid that was used for the flow solution was used to compute the flow sensitivities. Note that while it may be convenient to solve the sensitivity equation using the same scheme and discretization as for the nonlinear flow it is not necessary to do so. Indeed when using adaptive grid technology one should be aware that an acceptable refinement for the flow problem may not be acceptable for the sensitivity problem [6].

Figures (6.1)-(6.3) display some of the pitch-rate flow-sensitivities results for the case of a NACA 0012 airfoil at different Mach Numbers and at $\alpha = 0.0^o$ and $q = 0$. The origin of coordinates of the body-fixed reference frame was chosen to be at the leading edge. The fact that $q = 0$ implies that the flow solutions required to calculate the source term W_B, and the Jacobians $\nabla_Q F$ and $\nabla_Q G$, can be simply extracted from the `Class Code`. That is to say when $q = 0$ the flow solutions can be obtained from a standard (inertial) CFD code for uniform flows. However, this approach is not valid in cases where q is non-zero. In such cases, the flow solutions must be obtained using the `A-NISFLOW Code`.

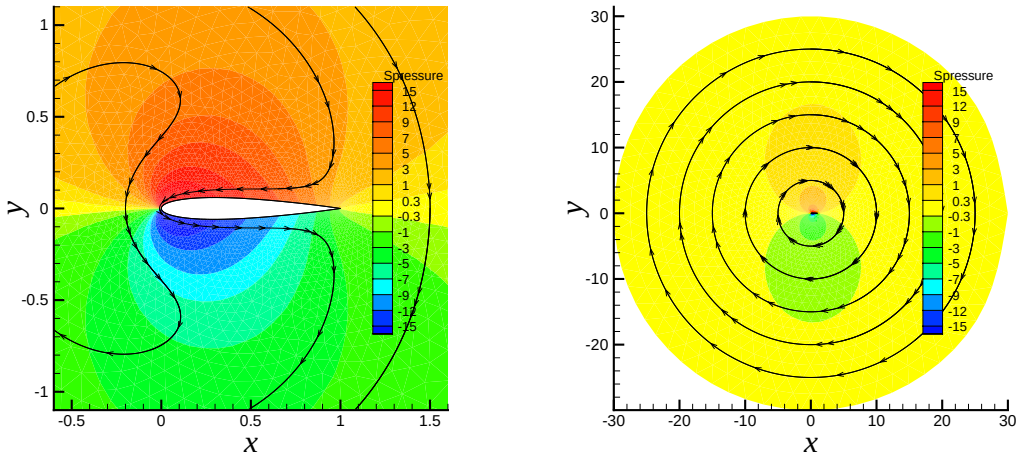

(a) Close-view, $M_c = 0.2$

(b) Wide-view, $M_c = 0.2$

Figure 6.1: Pitch-rate pressure sensitivity contours and velocity sensitivity streamlines for a NACA 0012 airfoil moving in rectilinear steady motion ($\hat{q} = 0$) at $M_c = 0.2$ and $\alpha = 0.0^o$

In Figure (6.1)-(a) the pitch-rate pressure sensitivity contours and the velocity sensitivity streamlines are shown for a NACA 0012 airfoil at $M_c = 0.2$; these flow sensitivities were computed using the flow solution shown in Figures (4.8)(a)-(b). The pressure sensitivities measure how the pressure is going to vary if the airfoil tends to rotate nose-down (positive q). Similarly, the velocity sensitivity streamlines indicate how the velocities are going to change if the airfoil tends to move nose-down. Observe that for a positive q (nose-down) the pressure tends to increase on the airfoil's upper surface while it tends to decrease on the lower surface. From this behavior we expect a negative (downward) C_{ℓ_q}. From the velocity sensitivity streamlines one sees that near the upper surface the flow tends to decelerate while on the lower surface it tends to accelerate. Also, the stagnation point tends to move to the upper surface.

In Figure (6.1)-(b), a zoom-out of the sensitivity field is shown to display the pressure sensitivity and velocity sensitivity streamlines in the far-field. Observe that the pressure sensitivity goes to zero at the far-field. This behavior is expected since airfoil pitch motions should not change the air pressure in the far-field. Also observe that the sensitivity streamlines tend to be concentric circles with center at the origin of coordinates (i.e. at the airfoil's leading edge). This phenomenon is also expected and can be proved mathematically by differentiating the velocity far-field boundary condition with respect to the pitch-rate. Observe that for a positive pitch q (i.e. a pitch in the counterclockwise sense) the far-field streamlines run clockwise.

Note that the finite-volume sensitivity formulation allows one to treat the range of subsonic, supersonic and transonic speeds. In Figures (6.2) and (6.3) the pitch-rate pressure sensitivity and the pitch-rate velocity sensitivity streamlines of the same airfoil are shown but at the higher Mach numbers $M_c = 0.5$ and $M_c = 0.8$, respectively. The main features of the resulting pressure sensitivity and velocity sensitivity streamlines for the case $M_c = 0.5$ are similar to the low subsonic case.

The case $M_c = 0.8$ corresponds to the transonic flow shown in Figure (4.3). In particular, as shown in Figure (4.3)-(a), at $\alpha = 0.0^o$ a shock exists on both the upper and lower surfaces of the airfoil and by symmetry the shocks are located at the same location along the chord. From the corresponding pressure sensitivity shown in Figure (6.3)-(a), it can be seen that on the upper surface, between the leading edge and some distance before the shock location, the expected change in pressure is a more or less uniform pressure increase. On the lower surface the expected change is a more or less uniform pressure drop. On the other hand on the upper surface, near the shock location the expected change is a large pressure increase. This pressure increase is an indication that if the airfoil tends to pitch nose-down, the shock on the upper surface would tend to move towards the leading edge. The opposite phenomenon occurs on the lower surface where the pressure sensitivity is large but negative. This result indicates that if the airfoil tends to pitch nose-down, the lower-surface shock would tend to move towards the trailing edge. These expected motions of the shocks are in complete agreement with the shock motion phenomena observed in the flow solutions shown in Figures (4.12).

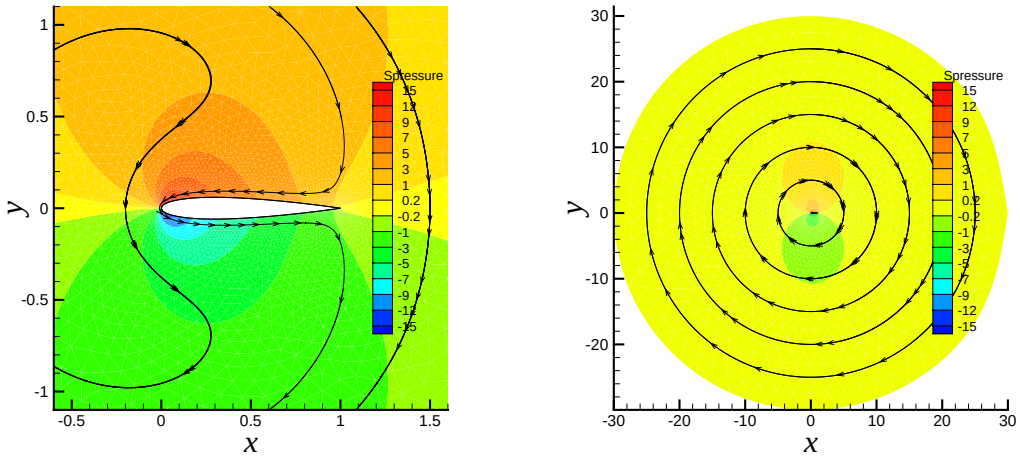

(a) Close-view, $M_c = 0.5$

(b) Wide-view, $M_c = 0.5$

Figure 6.2: Pitch-rate pressure sensitivity contours and velocity sensitivity streamlines for a NACA 0012 airfoil moving in rectilinear steady motion ($\hat{q} = 0$) at $M_c = 0.5$ and $\alpha = 0.0^o$

It must be noted that the anti-symmetry observed in the pressure-sensitivity contours with respect to the x-axis is a special phenomenon that only occurs at $\alpha = 0.0^o$ due to the symmetry of the airfoil and the symmetry of the flow solution at that angle of attack.

Table 6.1, shows a comparison of the non-dimensional pitch-rate derivatives $C_{\ell_{\hat{q}}} = \frac{\partial \overline{C}_\ell}{\partial \hat{q}}$ and $C_{m_{\hat{q}}} = \frac{\partial \overline{C}_m}{\partial \hat{q}}$ obtained for four different Mach numbers $M_c = 0.1$, $M_c = 0.2$, $M_c = 0.5$ and $M_c = 0.8$ at $\alpha = 0.0^o$. As mentioned before, the non-dimensional pitch rate $\hat{q}$ is defined to be $\hat{q} = \frac{qc}{V_c}$. The damping-in-pitch $C_{m_{\hat{q}}}$ is computed using

$$\frac{\partial \overline{C}_m}{\partial \hat{q}} = \frac{2}{\rho_\infty V_c^2 c^2} \int_\sigma \left[\vec{x} \times -\frac{\partial P}{\partial \hat{q}} \hat{n} \right]_z d\sigma$$

To validate the results Table 6.1 also shows the same aerodynamic derivatives calculated using `QUADPAN` [61], [62] and `VORLAX` [36] which are two panel methods developed at Lockheed. Both methods use potential flow formulations to estimate the local velocity and they recover the pressure from approximations to the isentropic, compressible Bernoulli equation. The results show good agreement between `QUADPAN` and `S-NISFLOW` at $M_c = 0.1$ and $M_c = 0.5$. The difference in $C_{\ell_{\hat{q}}}$ is around 2%-3% at $M_c = 0.1$ and increases to 4%-5% at $M_c = 0.5$. For $C_{m_{\hat{q}}}$ the difference is less than 2% at $M_c = 0.1$ and increases slightly to less than 4% at $M_c = 0.5$. This small difference may be due to inaccuracies of the discretization and/or to the different approaches used in simulating the pitching motion effect. The estimates at $M_c = 0.8$ are quite different. One explanation is that `VORLAX` and `QUADPAN` can not model

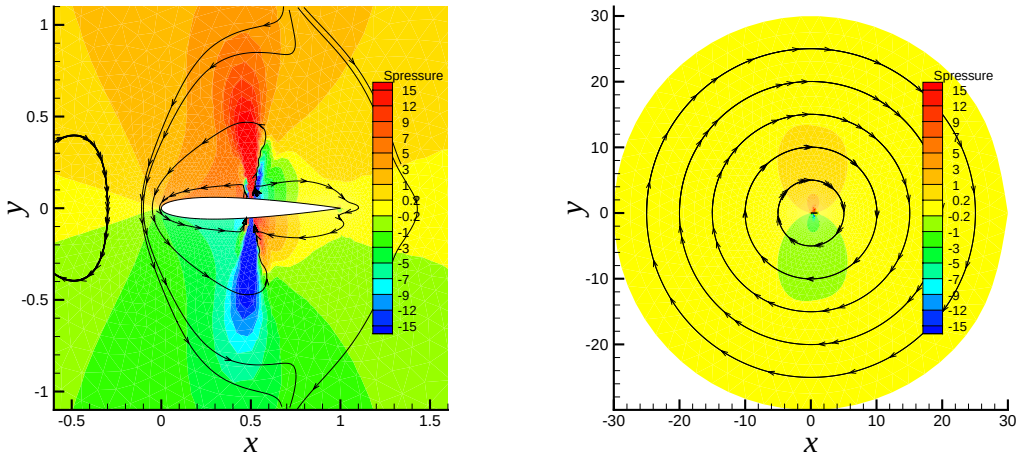

(a) Close-view, $M_c = 0.8$

(b) Wide-view, $M_c = 0.8$

Figure 6.3: Pitch-rate pressure sensitivity contours and velocity sensitivity streamlines for a NACA 0012 airfoil moving in rectilinear steady motion ($\hat{q} = 0$) at $M_c = 0.8$ and $\alpha = 0.0^o$

embedded shocks, whereas it is clear from the flow solution (see Figure (4.3)-(a)) that at $M_c = 0.8$ there is an embedded shock.

The comparisons with `VORLAX`, also shown in Table 6.1, are somewhat worse. At the lower Mach numbers, the `VORLAX` values are around 6%/9% smaller in magnitude than those obtained using `QUADPAN/S-NISFLOW`. Actually, we expect that the values generated by `VORLAX` to be less accurate because `VORLAX` implements a lifting surface panel method, *i.e.* it is based on the approximation that the airfoil has zero-thickness. The values produced by `VORLAX` at low Mach numbers are close to the incompressible predictions: $C_{\ell_{\hat{q}}} = -\frac{3\pi}{2}$ and $C_{m_{\hat{q}}} = -\frac{\pi}{2}$, obtained from thin airfoil theory using the fictitious Etkin's camber defined by equation (4.106).

In addition, the `S-NISFLOW` results have been validated by comparisons to finite-difference estimates based on nonlinear flow solutions obtained using `A-NISFLOW`. These finite-difference estimates correspond to column FD `A-NISFLOW` of Table 6.1. In subsonic cases, these finite-difference estimates are within 0.3% of the `S-NISFLOW` values. For the case $M_c = 0.8$ the comparison degrades to about 3% but some of this degrading may be explained by insufficient grid-refinement in solving the linear sensitivity equation and/or the nonlinear flow equation. Observe that the negative values of $C_{m_{\hat{q}}}$ indicates that the moment produced is always in the opposite direction of the pitch rotation (i.e. damping-in-pitch). It also follows from the results that both $C_{\ell_{\hat{q}}}$ and $C_{m_{\hat{q}}}$ tend to increase in magnitude when the Mach number increases.

$M_c = 0.1$	QUADPAN	S-NISFLOW	FD A-NISFLOW	VORLAX
$C_{\ell_{\hat{q}}}$	-5.049	-5.144	-5.139	-4.713
$C_{m_{\hat{q}}}$	-1.712	-1.733	-1.732	-1.576
$M_c = 0.2$	QUADPAN	S-NISFLOW	FD A-NISFLOW	VORLAX
$C_{\ell_{\hat{q}}}$	$-$	-5.236	-5.250	$-$
$C_{m_{\hat{q}}}$	$-$	-1.762	-1.766	$-$
$M_c = 0.5$	QUADPAN	S-NISFLOW	FD A-NISFLOW	VORLAX
$C_{\ell_{\hat{q}}}$	-5.657	-5.988	-5.991	-5.396
$C_{m_{\hat{q}}}$	-1.913	-2.006	-2.007	-1.806
$M_C = 0.8$	QUADPAN	S-NISFLOW	FD A-NISFLOW	VORLAX
$C_{\ell_{\hat{q}}}$	-7.857	-10.242	-10.541	-7.704
$C_{m_{\hat{q}}}$	-2.667	-3.925	-4.047	-2.584

Table 6.1: Computed Pitch-rate Derivatives

As we mentioned before, S-NISFLOW can be used to calculate the stability derivatives with respect to the pitch rate q even when $q \neq 0$. As example, we consider again the NACA 0012 airfoil at $M_c = 0.8$ at $\alpha = 0.0^o$. In Figures (4.12) (Section 4.14) we show the flow solutions corresponding to planar aerodynamically steady motions with $\hat{q} = 0.0$, 0.01, 0.03 and 0.05. Using S-NISFLOW we calculated the flow sensitivities around such flight conditions. The results are shown in Figures (6.4). Figures (6.4)-(a) and (6.4)-(b) correspond to the sensitivity solutions for the cases $\hat{q} = 0.0$ and $\hat{q} = 0.01$ shown in Figures (4.12)-(a) and (4.12)-(b), respectively. Figures (6.4)-(c) and (6.4)-(d) correspond to the sensitivity solutions for the cases $\hat{q} = 0.03$ and $\hat{q} = 0.05$ shown in Figures (4.12)-(c) and (4.12)-(d), respectively. The behavior shown by the pressure sensitivities of Figures (6.4) agrees with the real pressure variations shown in the flow solutions. Particularly, it is interesting to note that the pressure sensitivity solutions predict the slow vanishing of the shock on the airfoil's upper surface.

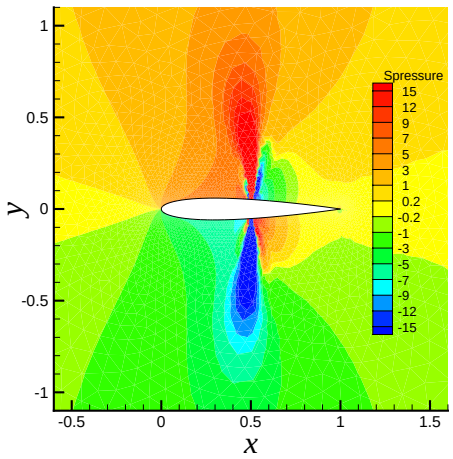

(a) Pitch-rate $\hat{q} = 0$

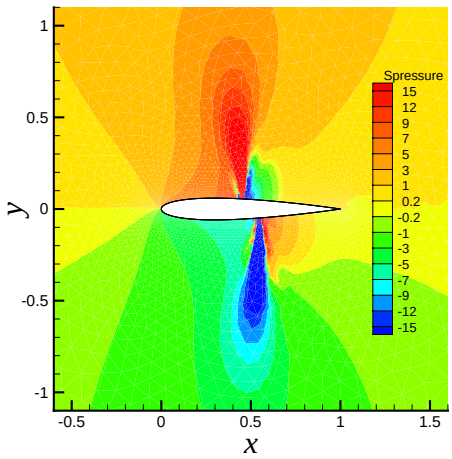

(b) Pitch-rate $\hat{q} = 0.01$

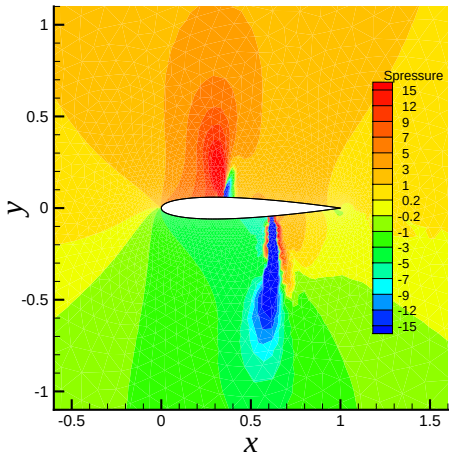

(c) Pitch-rate $\hat{q} = 0.03$

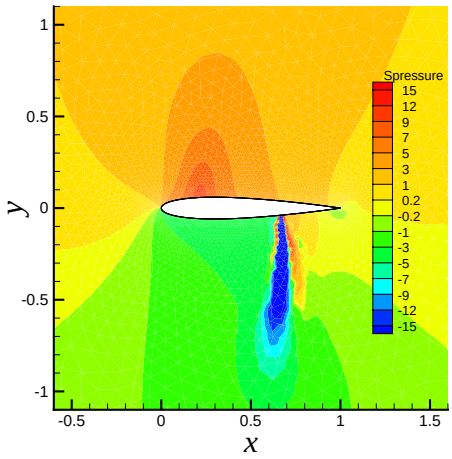

(d) Pitch-rate $\hat{q} = 0.05$

Figure 6.4: Pitch-rate pressure sensitivity contours for a NACA 0012 airfoil at $M_c = 0.8$ and $\alpha = 0.0^o$. For the sensitivities of Figure (a) the airfoil is moving in rectilinear motion, $\hat{q} = 0.0$. For the sensitivities of Figures (b), (c) and (d) the airfoil is moving in steady circular motions with pitch-rates $\hat{q} = 0.01$, 0.03 and 0.05, respectively.

Conclusions

A mathematical model for the determination of the aerodynamic forces and stability derivatives has been developed. The mathematical model is based on the idea aerodynamically steady motions and as part of this work a complete mathematical characterization and generalization of all possible aerodynamically steady motions was obtained. In particular, it was proved that in these generalized steady motions the aircraft moves in a class of helical trajectories. For the case of longitudinal motions the most general aerodynamically steady motions correspond to circular trajectories where the aircraft is moving at a constant translational velocity, at a constant angle of attack and at a constant pitch rate.

One important use of these results is the determination of time invariant aerodynamic forces and moments. While such forces could be determined experimentally, such experiments can be quite complex. An alternative approach is to determine these steady aerodynamic forces using computer simulation, and this was the approach used in this work. The idea is to determine numerically the flow around the aircraft and obtain the aerodynamic forces and moments by an appropriate integration of the pressure and shear forces acting along the aircraft surface. The best reference frame to determine these flow solutions is the body-fixed reference frame, since as seen from this reference frame the flow is steady, i.e. time-invariant. However, for general aerodynamically steady motions the body-fixed reference frame is non-inertial and standard (inertial) CFD formulations can not be used. The problem is solved by developing a CFD formulation for general non-inertial reference frames. This CFD formulation was presented in Chapter 3 and it differs from the non-inertial CFD formulations used in turbomachinery simulations by the fact the non-inertial frame is not only allowed to rotate but also to translate with a non-zero acceleration. The mathematical description of the aerodynamically steady motions was incorporated into the CFD formulation. As a consequence, the generalized Navier-Stokes equations and the generalized Euler equations were derived. These equations allow the determination of the flow around an aircraft moving in any aerodynamically steady motion. The formulation is valid for all ranges of Mach numbers including transonic flow.

The method was implemented for the planar case using the generalized Euler equations. The developed computer codes can be used to obtain numerical flow solutions for the flow around any airfoil moving in general steady motions (i.e. circular trajectories). To the best of our knowledge this type of numerical simulations have never been done. From these

numerical solutions it is possible to determine the variation of the lift, drag and pitching moment with respect to the pitch rate q at different Mach numbers. In particular, it is shown that for the case of a NACA 0012 airfoil at subsonic speeds there is a linear behavior of the lift and pitching moments with respect to q. This linear behavior would explain why linear aerodynamic models work so well in practice.

One of the advantages of the mathematical model developed here, is that the stability derivatives with respect to the six motion variables can be obtained in a straightforward manner. In particular, the model allows the determination of rotary stability derivatives in a decoupled way. Also, it is important to note that the model makes explicit the notion of the "stability derivatives" as "partial derivatives" of the aerodynamic forces. The stability derivatives can be obtained either by finite differences or by using the sensitivity equation method. In Chapter 5, the sensitivity equation method was applied to the mathematical formulation in order to handle the computation of stability derivatives. The method was implemented numerically for the case of planar motions. Pitch-rate derivatives $C_{\ell_{\hat{q}}}$ and $C_{m_{\hat{q}}}$ were computed for a NACA 0012 airfoil. The results were compared with two panel methods (`VORLAX` and `QUADPAN`) developed at Lockheed. Good agreement was shown for the subsonic cases where these panel methods are valid. The method presented here is able to obtain stability derivatives in transonic flows (where approximations based on the linearized potential flow equations do not work well). The main virtue of the sensitivity equation approach is that the stability derivatives can be obtained from a single solution of the nonlinear fluid mechanics (plus relatively cheap solutions of a linear partial differential equation).

The natural continuation of this work, would be the numerical implementations of the three-dimensional CFD formulation and of the Sensitivity formulation presented here. Based on the successful results obtained from the two-dimensional implementation, the three-dimensional implementation should give results of direct practical application for the evaluation of the aerodynamic forces and stability derivatives of arbitrary aircraft. The implementation of the three-dimensional Euler Equations seems to be straightforward. The implementation of the Navier-Stokes equations should also be direct as long as the turbulence models do not introduce problems.

Bibliography

[1] Allan, B. G., Holt, M. and Packard, A., "Simulation of a Controlled Airfoil with Jets," *Journal of Guidance, Control, and Dynamics* , Vol. 21, No. 2, March-April 1998, pp. 257-263.

[2] Anderson, W.K. and Bonhaus, D.L, "An Implicit Upwind Algorithm for Computing Turbulent Flows on Unstructured Grids," *Computers and Fluids*, Vol. 23, No. 1, 1994, pp. 1-21.

[3] Anderson, W.K., Rausch, R.D. and Bonhaus, D.L, "Implicit/Multigrid Algorithms for Incompressible Turbulent Flows on Unstructured Grids," *J. of Comp. Phys.*, Vol. 128, 1996, pp. 391-408.

[4] Arakawa, C., Samejima, M., Matsuo, Y., and Kubota, T., "Computational Simulation offrancis Water Runner with Pseudo-Compressibility," *Numerical Simulations in turbomachinery*, ASME-JSME Fluids Engineering Conference, ASME FED-Vol. 120, 1991, pp. 119-124.

[5] Atwood, C.A., "Computation of a Controlled Store Separation from a Cavity," *Journal of Aircraft* , Vol. 32, No. 4, July-August 1995, pp. 846-852.

[6] Borggaard, J., and Pelletier, D., "Optimal Shape Design in Forced Convection Using Adaptive Finite Elements," AIAA Paper 98-0908, Aerospace Sciences Meeting, January 1998.

[7] Brebbia, C.A., and Walker, S., *Boundary Element Techniques in Engineering*, Newnes-Butterworth, London, 1980.

[8] Brinker, J.S. and Wise, K.A., "Stability and Flying qualities Robustness of a Dynamic Inversion Control Law," *Journal of Guidance, Control and Dynamics*, Vol. 19, No. 6, November-December 1996, pp 1270-1277.

[9] Bryan, G.H., *Stability in Aviation*, Macmillan, New York, 1911.

[10] Bryson, Arthur, E., Jr., "Stability Derivatives for a Slender Missile with Application to a Wing-Body-Vertical-Tail Configuration," *Journal of the Aeronautical Sciences*, Vol. 20, No. 5, May 1953, pp. 297-308.

[11] Bussing, T.R. and Murman, E.M., "A Finite Volume method for the Calculation of Compressible Chemically Reacting Flows," AIAA Paper 85-0331, January 1985.

[12] Chambers, J.R. and Grafton, S.B., "Static and Dynamic Longitudinal Stability Derivatives of a Powered 1/9-scale Model of a Tilt-Wing V/STOL Transport," *NASA Technical Note*, NASA TN D-3591, Washington DC, September 1966.

[13] Etkin, B., *Dynamics of Atmospheric Flight*, J. Wiley, New York, 1972.

[14] Godfrey, A.G., and Cliff, E.M., "Direct Calculation of Aerodynamic Force Derivatives: A Sensitivity-Equation Approach," AIAA Paper 98-0393, Aerospace Sciences Meeting, January 1998.

[15] Godfrey, A.G., Eppard, W.M., and Cliff, E.M., "Using Sensitivity Equations for Chemically Reacting Flows," AIAA-98-4805, 7th AIAA/USAF/ NASA/ ISSMO Symposium on Multidisciplinary Analysis and Optimization, September 1998.

[16] Grafton, S.B. and Libbey, C.E., "Dynamic Stability Derivatives of a Twin-Jet Fighter Model for Angles of -10^o to 110^o. NASA TN D-6091, January 1971.

[17] Greenwell, D.I., "Frequency Effects on Dynamic Stability Derivatives Obtained from Small-Amplitude Oscillatory Testing," *Journal of Aircraft*, Vol. 35, No. 5, September-October 1998, pp. 776-783.

[18] Guglieri, G. and Quagliotti, F.B., "Dynamic Stability Derivatives in a Low-Speed Wind Tunnel," *Journal of Aircraft*, Vol. 30, No. 3, May/June 1993, pp 421-423.

[19] Guruswami, G.P. and Tu, E.L., "Euler/Navier Stokes Flow Computations on Flexible Configurations for Stability Analysis," *36th AIAA/ASME/ASCE/AHS/ASC Structures, Structural Dynamics and Materials Conference and AIAA/ASME Adaptive Structures Forum*, AIAA, New Orleans, April 1995, Part 2, pp. 1164-1171.

[20] Hanff, E.S., "Direct Forced-Oscillation Techniques for the Determination of Stability Derivatives in Wind Tunnels," *Dynamic Stability Parameters*, AGARD, Lecture Series No. 114, March 1981.

[21] Hemdan, H.T., "Oscillating Two-Dimensional Hypersonic Airfoils at Small Angles of Attack," *Journal of Aircraft*, Vol. 30, No. 3, March 1992, pp. 703-710.

[22] Herdman, T.L., and Turi, J., "A Natural State-Space Model for an Aeroelastic Control System," *Journal of Integral Equations*, Vol. 7, No. 4, Fall 1995, pp 413-424.

[23] Hirsch, C., *Numerical Computation of Internal and External Flows*, Vol. 1, J. Wiley, New York, 1988, Chapter 1.

[24] Hirsch, C., *Numerical Computation of Internal and External Flows*, Vol. 1 and 2, J. Wiley, New York, 1988.

[25] Holmes, D.G. and Tong, S.S. "A Three-Dimensional Euler Solver for Turbomachinery Blade Rows," *Transactions of the ASME*, Vol. 107, April 1985, pp. 258-264.

[26] Hutt, G.R., East, R.A. and Wilson, R.D., "Large amplitude oscillation effects on cone pitch stability in viscous hypersonic flows," *The Aeronautical Journal*, Vol. 93, No. 922, February 1989, pp. 50-57.

[27] Jones, R.T., "The Unsteady Lift of a Wing of Finite Aspect Ratio", NACA Report 681, 1940.

[28] Konstadinopoulos, P., Thrasher, D.F., Mook, D.T., Nayfeh, A.H., and Watson, L.T., "A Vortex-Lattice Method for General Unsteady Aerodynamics," *Journal of Aircraft*, Vol. 22, No. 2, 1985, pp 43-49.

[29] Lijewski, L. and Suhs, N.E., "Chimera-Eagle Store Separation," AIAA Paper 92-4569, August 1992

[30] Lutze, F.H. and Hreha, M.A., "Linear Analysis of Poststall Gyrations," *Journal of Aircraft*, Vol. 17, No. 10, October 1980, pp 727-733.

[31] Lutze, F.H., Chambers, J.R. and Grafton, S.B., "Curved-flow, Rolling-flow, and Oscillatory Pure-yawing Wind-tunnel Test Methods for Determination of Dynamic Stability Derivatives," *Dynamic Stability Parameters*, AGARD, Lecture Series No. 114, March 1981.

[32] Marcum, D.L., and Weatherill, N.P., "Unstructured Grid Generation Using Iterative Point Insertion and Local Reconnection," *AIAA Journal*, Vol. 33, No. 9, 1995, pp. 1619-1625.

[33] Marcum, D.L., "Generation of Unstructured Grids for Viscous Flow Applications," AIAA Paper 95-0212, 1995.

[34] Mavriplis, D.J., "Unstructured Grid Techniques," *Annual Review of Fluid Mechanics*, Vol. 29, 1997, pp. 472-514.

[35] Miele, A.,*Flight Performance*, Addison-Wesley, 1962.

[36] Miranda, L.R, Elliott, R.D., and Baker, W.M., "A Generalized Vortex Lattice Method for Subsonic and Supersonic Flow Applications," NASA Contractor Report 2865, December 1977.

[37] Morton, S.A., Melville, R.B , Visbal, M.R.,"Accuracy and Coupling Issues of Aeroelastic Navier-Stokes Solutions on Deformed Meshes," *Journal of Aircraft* , Vol. 35, No. 5, Sep.-Oct. 1998, pp. 798-805.

[38] Mracek, C.P., and Mook, D.T., "Numerical Simulation of Three-Dimensional Lifting Flows by a Vortex Panel Method," AIAA Paper 88-4336-CP, Atmospheric Flight Mechanics Conference, August 1988.

[39] Noack, R., and Bishop, D. "A Three-Dimensional Delaunay Unstructured Grid Generator and Flow Solver for Bodies in Relative Motion," AIAA Paper 93-3349, July 1993.

[40] Orlik-Ruckemann, K., "Review of Techniques for Determination of Dynamic Stability Parameters in Wind Tunnels," *Dynamic Stability Parameters*, AGARD, Lecture Series No. 114, March 1981.

[41] Owczarek, J.A. , *Fundamentals of Gas Dynamics*, International Textbook Company, Scranton, 1964.

[42] Queijo, M.J., "Methods for Obtaining Stability Derivatives," NASA SP-258, NASA Langley Research Center, 1971, pp. 71-101.

[43] Rajamurthy, M.S., "Generation of Comprehensive Longitudinal aerodynamic Data Using Dynamic Wind-Tunnel Simulation," *Journal of Aircraft*, Vol. 34, No. 1, January-February 1997, pp. 29-33.

[44] Roe, P.L., "Approximate Riemann Solvers, Parameter Vectors, and Difference Schemes," *Journal of Computational Physics*, **43**, 1981, pp 357-372.

[45] Srinivasan, G.R., Baeder, J.D., Obayashi, S., and McCroskey, W.J., "Flowfield of a Lifting Rotor in Hover: A Navier-stokes Simulation," *AIAA Journal*, Vol. 30, No. 10, October 1992, pp. 2371-2378.

[46] Stevens, B.L. and Lewis, F.L. *Aircraft Control and Simulation*, John Wiley & Sons, Inc., New York, 1992, Chapter 2.

[47] Suzuki, S. and Fukuda, K., "Calculation of Stability Derivatives for Slender Bodies Using Boundary Element Method," *Journal of Guidance, Control and Dynamics*, Vol. 13, No. 4, July-August 1990, pp 763-765.

[48] Tannehill, J.C., Anderson, D.A. and Pletcher, R.H., *Computational Fluid Mechanics and Heat Transfer*, Taylor & Francis, Washington DC, 1997.

[49] Theodorsen, T., "A General Theory of Aerodynamic Instability and the Mechanism of Flutter," NACA Report 496, 1935.

[50] Thompson, J.F., Soni, B.K. and Weatherill, N.P., editors, *Handbook of Grid Generation*, CRC Press, 1999.

[51] Tobak, M. and Pearson, W.E., "A Study of Nonlinear Longitudinal Dynamic Stability," NASA TR R-209, September 1964.

[52] Tobak, M., "On Nonlinear Longitudinal Dynamic Stability," AGARD-CP-17, Part 1, Stability and Control, 1966, pp. 161-175.

[53] Tobak, M. and Schiff, L. B., "Aerodynamic Mathematical Modelling-Basic Concepts," *Dynamic Stability Parameters*, AGARD, Lecture Series No. 114, March 1981 (Lecture 1).

[54] van Leer, B., "Flux-Vector Splitting for the Euler Equations," ICASE Report No. 82-30 in *Lecture Notes in Physics Vol. 170*, Springer-Verlag, New York, 1982, pp. 507-515.

[55] Vinokur, M., "Review Article: An Analysis of Finite-Difference and Finite-Volume Formulations of Conservation Laws," *Journal of Computational Physics*, **81**, 1989, pp. 1-52.

[56] von Mises, R., *Theory of Flight*, Dover Publishing, 1959.

[57] von Karman, T., and Burgers, J.M., "General Aerodynamic Theory of Perfect Fluids," in *Aerodynamic Theory - A General Review of Progress*, Division E, W.F. Durand *editor*, California Institute of Technology, Pasadena, CA, 1943. (originally published in 1934).

[58] Weinacht, P., Sturek, W.B. and Schiff, L.B., "Navier-Stokes Prediction of Pitch-Damping for Axisymmetric Projectiles," *Journal of Spacecraft and Rockets*, Vol. 34, No. 6, November-December 1997, pp. 753-761.

[59] Weinacht, P., "Prediction of Pitch-Damping of Projectiles At Low Supersonic and Transonic Velocities," *36th Aerospace sciences Meeting & Exhibit*, AIAA 98-0395 January 1998.

[60] Yen, G.W., Newmann, J., and Baysal, O., "Dynamic Overlapped Grid Simulation of Aerodynamically Determined Three-Dimensional Relative Motion," AIAA Paper 93-3018, July 1993.

[61] Youngren, H.H., Bouchard, E.E, Coopersmith, R.M., and Miranda, L.R, "Comparison of Panel Method Formulations and its Influence on the Development of QUADPAN, an Advanced Low Order Method," AIAA Paper 83-1827, AIAA Applied Aerodynamics Conference, July 1983.

[62] Johnston, C.E., Youngren, H.H., and Sikora, J.S., "Engineering Applications of an Advanced Low-Order Panel Method," SAE Technical Paper Series 851793, Aerospace Technology Conference & Exposition, October 1985.

Vita

Alejandro Cesar Limache was born on August 6, 1968, in Vila, Santa Fe, Argentina. In 1992, he graduated with a (equivalent) B.S and M.S. degree in physics from National University of Cordoba, Argentina. After graduation he worked as a researcher for the Secretary of Science and Technology. He came to the United States in 1996. He earned the M.S. degree in 1998 and the Ph.D. degree in aerospace engineering in 2000, both from Virginia Polytechnic Institute and State University in Blacksburg, Virginia. He will join NLX Corporation to work on flight simulators as a software engineer in Sterling, Virginia.